January 2012

Targeting α4 Integrin Containing Complexes in Multiple Myeloma Using Peptidomimetics

Michael Foster Emmons
University of South Florida, michael.emmons@moffitt.org

Targeting α4 Integrin Containing Complexes in Multiple Myeloma Using Peptidomimetics

by

Michael F. Emmons

A dissertation submitted in partial fulfillment
of the requirements for the degree of
Doctor of Philosophy
Department of Cell Biology, Microbiology and Molecular Biology
Cancer Biology Ph.D. Program
University of South Florida

Major Professor: Lori Hazlehurst, Ph.D.
Steven Eschrich, Ph.D.
John Koomen, Ph.D.
Mark McLaughlin, Ph.D.

Date of Approval:
August 16, 2012

Keywords: necrosis, integrins, CAM-DR, VLA-4, Ca^{2+}

Table of Contents

List of Tables

List of Figures

List of Abbreviations

3-MA	3-methyladenine
AGM	aorta gonad mesonephros
AIF	apoptosis inducing factor
AKT	protein kinase B
AML	acute myeloid leukemia
APC	antigen presenting cell
ATO	arsenic trioxide
ATP	adenosine triphosphate
B cell	bursa-derived cell
Bcl-2	b-cell lymphoma 2
Bcl-x	bcl-2-like protein 1
Bcl-xL	b-cell lymphoma extra large
BCR	b-cell receptor
BH3	bcl-2 homology 3
BM	bone marrow
BMSC	bone marrow stromal cell
BME	bone marrow microenvironment
CAM-DR	cell adhesion mediated-drug resistance
CaV	voltage gated calcium channel

CD138	syndecan 1
cFLIP	cellular FLICE-inhibitory protein
CLP	common lymphoid progenitor
CMP	common myeloid progenitor
CRAB	hypercalcemia, renal insufficiency, anemia, bone lesion
CRAC	calcium release activated calcium
CS-1	connecting segment-1
CXCL12	chemokine ligand 12
CXCR4	chemokine receptor 4
cyD	cyclophilin D
DISC	death inducing signaling complex
ECM	extracellular matrix
ELISA	enzyme-linked immunosorbent assay
ELP	early lymphoid progenitor
ER	endoplasmic reticulum
ERK	extracellular signal-regulated kinase
ETP	T-cell lineage progenitor
FACS	fluorescence activated cell sorting
FAK	focal adhesion kinase
FISH	fluorescence in situ hybridization
FN	fibronectin
GFP	green fluorescence protein
GPCR	g protein coupled receptor

gp130	glycoprotein 130
HSC	hematopoietic stem cell
IAP	inhibitor of apoptosis protein
IFN-α	interferon-alpha
IGF-1	insulin growth factor-1
IgH	immunoglobulin heavy chain
IgL	immunoglobulin light chain
IgM	immunoglobulin M
IL-6	interleukin-6
ip3	1,4,5-inositol triphosphate
ISS	international staging system
JNK	c-jun N-terminal kinase
LC3	light chain 3A
LFA-1	lymphocyte-associated function antigen 1
LMP	lysosomal membrane permeability
MadCAM-1	mucosal addressin cell adhesion molecule-1
Mcl-1	myeloid cell leukemia sequence 1
MEF	mouse embryonic fibroblast
MGUS	monoclonal gammopathy of undetermined significance
MIDAS	metal ion dependent adhesion site
MM	multiple myeloma
mmp	mitochondrial membrane potential
MPP	multipotential progenitor

mpT	mitochondrial permeability transition
MRD	minimal residual disease
MSC	mesenchymal stem cell
NAD	nicotinamide adenine dinucleotide
NAM	nicotinamide adenine mononucleotide
NK cell	natural killer cell
NO	nitric oxide
ORR	overall response rate
PARP	poly ADP-ribose polymerase
PBMC	peripheral blood mononuclear cell
PCR	polymerase chain reaction
PI3K	phosphoinositide 3-kinase
PIP2	phosphatidylinositol 4,5-bisphosphate
PLC	phospholipase c
PMCA	plasma membrane calcium ATPase
PML	polymorphonuclear leukocyte
RIPK	receptor interacting protein kinase
ROS	reactive oxygen species
RTK	receptor tyrosine kinase
RT-PCR	reverse transcriptase polymerase chain reaction
RyR	ryanodine receptor
SDF-1	soluble derived factor-1
SERCA	sarcoendoplasmic reticulum calcium ATPase

SOC	store operated channel
STIM1	stromal interaction molecule 1
T cell	thymus derived cell
TNF α	tumor necrosis factor alpha
TRAIL	TNF-related apoptosis-inducing ligand
VAD	vincristine, doxorubicin, dexamethasone
VCAM1	vascular cell adhesion molecule 1
VDJ	variable, diversity, joining segment
VEGF	vascular endothelial growth factor
VLA-4	very late antigen-4
VLA-5	very late antigen-5
XIAP	X-linked inhibitor of apoptosis protein

Abstract

In our previous work we demonstrated that the integrin antagonist, HYD1, induced necrotic cell death in myeloma cell lines *in vitro* and *in vivo* as a single agent. In order to further delineate biomarkers of response to HYD1 we developed an isogenic drug resistant variant named H929-60. We show that the acquisition of resistance towards HYD1 correlates with reduced expression of the cleaved α4 integrin subunit and beta 1 integrin. Moreover, we demonstrate that HYD1 interacts with α4 integrin in myeloma cells. Consistent with reduced VLA-4 expression, the resistant variant showed ablated functional binding to fibronectin, VCAM-1 and the bone marrow stroma cell line, HS-5. The reduction in binding to extracellular matrices of the resistant variant translated to sensitivity to melphalan and bortezomib induced cell death in the bone marrow stroma co-culture model of drug resistance. Moreover, CD138 positive myeloma cells were more sensitive to HYD1 induced cell death compared to the CD138 negative fraction, and potency of HYD1 induced cell death significantly correlated with α4 integrin expression. We were also able to show that reducing α4 or β1 integrin using shRNA strategies was sufficient to cause resistance in myeloma cell lines. In addition we investigated the effects of cyclized variants of HYD1 to improve potency of the agent. One such compound, named HM-27, was determined to be 30 fold more active in H929 cells when compared to HYD1. HM-27 and HYD1 were determined to have similar

mechanisms of action as H929-60 cells were shown to be resistant to both compounds when compared to H929 cells. We further characterized HM-27's mechanism of action by investigating what effects HM-27 induced Ca^{2+} oscillations had on HM-27 induced cell death. The increases in intracellular Ca^{2+} seen after treatment with HM-27 were determined to occur via release from ER stores and not through influx through plasma membrane channels. Inhibiting Ca^{2+} release from the ER also potentiated the effects of HM-27 in MM cells. Furthermore, inhibiting Ca^{2+} release from the ER was also shown to block the onset of autophagy after ER treatment. Treating cells with the lysosomotropic agent, chloroquine, was shown to potentiate the activity of HM-27 *in vitro* and *ex vivo*. HM-27 was also shown to have activity in an *in vivo* model with combination treatment containing bortezomib and HM-27 increasing mouse survival. Collectively our data indicate that VLA-4 expression is a critical determinant of response to HYD1 induced cell death. We also showed that increases in intracellular Ca^{2+} seen after treatment with HM-27 had a cytoprotective effect in MM cells. Moreover, neutralizing autophagy potentiates HM-27 induced cell death *in vitro* and *ex vivo* while combining bortezomib and HM-27 increased survival *in vivo*. These data continue to provide rationale for further pre-clinical development of HYD1 as a novel anticancer agent.

Chapter I: Introduction

Hematopoiesis

Because mature blood cells are predominately short lived, approximately 1 x 10^{10} red blood cells and 1 x 10^{9} white blood cells are produced per day to maintain normal levels in the peripheral circulation. This production of new cells is accomplished by the differentiation of hematopoietic stem cells (HSCs) through the highly regulated process termed hematopoiesis. In vertebrates, blood stem cells are produced in a variety of sites that change during development [1]. In mammals, these hematopoiesis sites include the yolk sac, the aorta-gonad mesonephros (AGM) region, the fetal liver and the bone marrow. After birth, hematopoiesis ceases in the yolk sac, AGM region and the fetal liver with the bone marrow becoming the predominant site for the production of new blood cells.

HSCs are self-renewing hematopoietic cells that reside in the bone marrow of adult humans. Operationally these cells are defined by their capacity to reconstitute the entire blood system of a recipient whose bone marrow has been destroyed by irradiation or treatment with toxic drugs [2]. In addition to their self renewing capacity, HSCs can also differentiate into multipotential progenitors (MPPs) which in turn can differentiate into either common myeloid progenitors (CMPs) or early lymphoid progenitors (ELPs) [3]. CMPs differentiate into megakaryocytes, myeloid cells or erythrocytes while ELPs differentiate into lymphocytes.

Cells derived from CMPs have a variety of different functions. Platelets are produced in the bone marrow via budding off from megakaryocytes and are involved in hemostasis, leading to the formation of blood clots. Erythrocytes are the most common type of blood cell and are responsible for delivering oxygen throughout the body. Myeloid cells can further differentiate into a category of leukocytes that include granulocytes and monocytes. Granulocytes, also known as polymorphonuclear leukocytes (PMLs) because of the abnormal shapes of their nuclei, are characterized by the presence of small particles named granules which reside in the cytoplasm. PMLs consist of neutrophils, eosinophils and basophils. Neutrophils are the most abundant granulocyte, constituting 50% of total circulating white blood cells, and aid in the innate immune response by releasing bacteria-killing enzymes or engulfing invading microorganisms or particles by phagocytosis. Eosinophils are important mediators of allergic responses and also play a role in fighting viral and parasitic infections. Basophils are the least common type of granulocyte and like eosinophils function in the immune response to allergens and parasites. Monocytes can differentiate into macrophages, which also act as phagocytes. Monocytes can also differentiate into dendritic cells, which capture antigens and function as antigen presenting cells (APCs), or cells that enable the recognition of the antigen by T-cells.

ELPs can differentiate into bursa-derived cells (B cells), thymus cells (T cells) or natural killer (NK) cells. B cells are an integral part of the adaptive immune response and function as APCs and also as antibody producing cells. There are several subsets of T cells which each have a distinct function. T helper cells are activated by APCs and

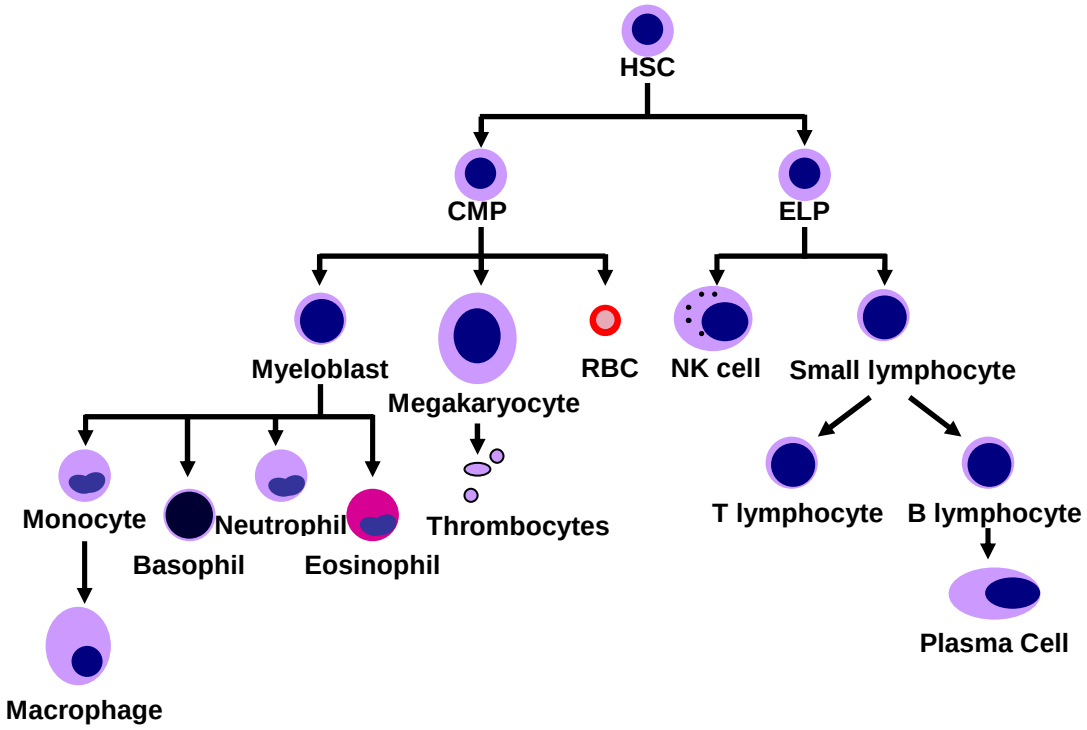

Figure 1: The process of hematopoiesis. The cellular components of the blood are all derived from hematopoietic stem cells. Myelocytes, megakaryocytes and red blood cells are derived from common myeloid progenitors and function in the innate and adaptive immune response, blood clotting and carrying oxygenated throughout the body respectively. Lymphocytes are derived from early lymphoid progenitor cells and constitute the backbone of the adaptive immune response while plasma cells are teminally differentiated B cells and are an integral part of the humoral immune response

function in the maturation of B cells and activation of cytotoxic T cells and macrophages. Cytotoxic T cells are responsible for the destruction of dysfunctional somatic cells and accomplish this by releasing the cytotoxins perforin, granzyme and granulysin. Regulatory T cells are imperative for the maintenance of immunological tolerance and Natural killer T cells which help in the innate immune response by recognizing glycolipid antigen. Natural Killer cells are a part of the innate immune response and need no

activation from t helper cells in order to release cytotoxins to destroy tumors and virally infected cells.

B cell Differentiation

Normal B-cell differentiation begins in the bone marrow. ELPs can differentiate into either early T-cell-lineage progenitors (ETPs) or into the bone marrow common lymphoid progenitors (CLP) which can generate B cells, NK cells and T cells [4]. As CLPs are pluripotent, it is the expression of a specific B cell marker B220 by a subset of the population, termed pro-B cells, that initiates the B cell differentiation pathway. Pro-B cells undergo a process known as VDJ recombination where the immunoglobulin heavy chains (IgH) are assembled from variable(V), diversity(D), and joining(J) gene segments [5]. The pre-B cell receptor (pre-BCR) formed from the VDJ recombination is then expressed on the surface of pre-B cells to act as a checkpoint to determine success of recombination. If recombination is successful, pre-b cells undergo substantial clonal proliferation and VJ recombination where the immunoglobulin light chain (IgL) of B cell receptors (BCR) are formed. In addition to the formation of the BCR IgL, pre-B cells also require the presence of immunoglobulin M (IgM) on the surface to proceed to negative selection [6]. Immature B220+IgM+ B cells are subsequently tested for autoreactivity. Some B cells that are autoreactive can be rescued by a secondary immunoglobulin gene rearrangement known as receptor editing while others that are autoreactive are eliminated by anergy [7]. B cells that pass these requirements are known as naïve B cells leave the bone marrow and circulate in the blood.

Naïve B cells that leave the bone marrow continue their development in the spleen. In the spleen naïve B cells pass through 2 transitional stages and another round of

negative selection. While a small percentage of transitional B cells home to the splenic marginal zone and become naïve marginal zone B cells, the vast majority of naïve B cells mature into follicular B cells. These follicular B cells circulate between the spleen, lymph nodes and bone marrow until they expire or encounter antigen and undergo further development. After antigen uptake and subsequent activation by T cells, B cells migrate into the center of the primary follicles forming the germinal center [8].

Germinal B cells comprise two distinct areas of the germinal center. In the dark zone, B cells are termed centroblasts. Centroblasts main function is to proliferate and undergo hypersomatic mutations of the immunoglobulin variable region resulting in an alteration of the affinity of the antibody produced by the cell. By this mechanism there is a marked increase in intraclonal diversity in a population of cells that are derived from a few precursors. In the light zone, B cells are termed centrocytes. Centrocytes are the result of hypersomatic mutations of the immunoglobulin variable region and are activated by selection from T cells or follicular dendritic cells that are also present in the region. Centrocytes and centroblasts are very sensitive to apoptosis as they switch off expression of Bcl-2-like protein 1 (Bcl-x) while in the germinal centers. Centrocytes that do not display increased affinity to antigen undergo apoptosis while centrocytes that do display increased affinity for antigen turn back on expression of Bcl-x [9]. Surviving centrocytes differentiate into either long-lived memory B cells which reside in the follicle marginal zones or long-lived plasma cells which primarily reside in the bone marrow.

Plasma Cells

Plasma cells are recognized as an integral part of the humoral immune response whose primary function is the production and secretion of antigen specific antibodies.

During B cell differentiation, two distinct types of plasma cells can be generated; short-lived or long-lived plasma cells. Short-lived plasma cells are generated from follicular B cells that do not undergo affinity maturation therefore secreting antibodies that possess a low affinity for antigen. Short-lived plasma cells serve in the early defense of immunogens during the primary immune response while higher affinity antibodies are produced in the germinal center. Long-lived plasma cells are generated from germinal center B cells that do undergo affinity maturation hence secreting antibodies that possess a high affinity for antigen. While a proportion of plasma cells generated from germinal center B cells are lost after antigenic challenge, some plasma cells that are able to access the bone marrow microenvironment niche are able to survive indefinitely [10].

Plasma cells are identified as having different expression of cell surface proteins than B cells and early plasmablasts. Plasma cells show decreased expression of proteins important during B cell differentiation like CD19, B220, MHC class II, and surface Igs. In contrast, there is increased expression of cell surface proteins like the chemokine receptor type 4 (CXCR4), interleukin-6 (IL-6) receptor, syndecan-1 (CD138) and CD44. These receptors have been shown to play a role in plasma cell homing and survival in the bone marrow microenvironment. Newly formed plasma cells have been shown to express high levels of the chemokine ligand 12 (CXCL12) receptor CXCR4 which enables plasma cells to migrate to bone marrow stromal cells (BMSCs) [11]. Once in the bone marrow microenvironment (BME), plasma cells need physical interaction with stromal cells in order to persist. CD138 has been shown to facilitate plasma cell adherence to BMSCs through an interaction with type 1 collagen [12]. Plasma cell interaction with stromal cells has also been shown to induce stromal cell production and

secretion of IL-6. IL-6 in turn binds to the IL-6 receptor on plasma cells and promotes plasma cell survival [13]. The interaction of CD44 with a ligand on the stromal cells has also been shown to induce production of IL-6 [14]. In addition to IL-6 and CXCL12, cytokines like interleukin-5 (IL-5) and tumor necrosis factor-alpha (TNF-alpha) have also been shown to mediate plasma cell longevity (Cassese 2003).

In an adult human, the percentage of plasma cells constitutes about 0.1-1 % of bone marrow (BM) cells [15]. This frequency of plasma cells is stably maintained over the years even though an individual generates around 10^4-10^5 new plasma cells every year [16]. With each new infection, there is competitive displacement of some established plasma cells by newly formed plasma cells in order to maintain the frequency of plasma cells in the BM and add new specificities to the plasma cell population. It has been shown that non-specific plasma cells appear in circulation after immunization indicating that some established plasma cells are removed from the BM microenvironment after each infection in order to maintain plasma cell numbers [17] When a plasma cell clone accumulates and disrupts the normal frequency of plasma cells in the bone marrow, it is characterized as a plasma cell disorder.

Several forms of plasma cell disorders can be distinguished. Plasma cell leukemia is the least common form of plasma cell neoplasms accounting for 2-3% of plasma cell disorders. It is one of the most aggressive neoplasms and is diagnosed when more than 20% of the peripheral blood contains plasma cells. Plasmacytomas are clonal proliferations of plasma cells that grow in soft tissue (extraosseous) or bone (osseous). These neoplasms are also rare and account for 5 % of plasma cell disorders. The most common plasma cell neoplasm is termed multiple myeloma (MM) which is a malignant

proliferation of a plasma cell clone which is dependent on the bone marrow microenvironment for survival and proliferation.

Chapter II: Multiple Myeloma

Characterization of Multiple Myeloma

MM is a neoplastic cell disorder that is characterized by clonal expansion of malignant plasma cells in the bone marrow microenvironment and increased levels of secreted paraprotein, which consists of either an immunoglobulin or an IgL, in the blood or urine [18]. It is the second most common hematologic malignancy, accounting for 13% of hematologic cancers and 1% of all cancers. The median age of diagnosis is approximately 65, with occurrence in men being more common. The symptoms associated with MM consist of hypercalcemia, renal insufficiency, anemia, and bone lesions (CRAB). With the continued discovery of newer and more effective therapies, the 5 year survival rate of patients diagnosed with MM has increased from 25% to 35%.

There are four stages of progression associated with MM that are categorized into 2 distinct groups, asymptomatic plasma cell dyscrasia and symptomatic plasma cell dyscrasia. The 2 asymptomatic disorders are multiple myeloma precursor diseases and are termed monoclonal gammopathy of unknown significance (MGUS) and smoldering multiple myeloma. MGUS is defined as the presence of serum M-protein < 3 g/dL with fewer than 10% monoclonal plasma cells in the bone marrow. MGUS is also characterized by lack of organ damage. MGUS is present in over 3% of the population over 50 years old with an annual progression risk to MM of 1% [19]. In addition to being more prevalent in older populations, MGUS is also 2 times higher in African Americans

compared with Whites [20]. It has also been demonstrated that most cases of MM are preceded by MGUS. In one study serum samples were collected from 77,000 healthy donors. Of the 71 patients who developed multiple myeloma at the 10 year follow up, the presence of MGUS was detected in 100 % of the cases in the years prior to the diagnosis of MM [21].

Smoldering myeloma is another asymptomatic plasma cell dyscrasia that has been shown to progress to MM. Smoldering myeloma is defined as the presence of serum protein > 3 g/dL with greater than 10 % monoclonal plasma cells in the bone marrow with lack of organ damage. Smoldering myeloma has a much higher risk of progression to multiple myeloma (10%) than MGUS [22]. Once patients with smoldering myeloma or MGUS start experiencing symptoms associated with MM they are diagnosed with either intermedullary myeloma or extramedullary myeloma. Intermedullary myeloma is defined as MM which can only exist within the confines of the bone marrow microenvironment while extramedullary myeloma is defined as MM which can exist outside of the bone marrow microenvironment and is often called primary plasma cell leukemia.

MM can also be characterized by the presence of genetic aberrations present in the tumor. Even though cytogenetic analysis can be difficult because of the low proliferative fraction of MM, techniques like fluorescence in situ hybridization (FISH) have been used to distinguish tumors with differing cytogenetics. Structural and numerical chromosomal abnormalities are found in 55-70% in newly diagnosed symptomatic patients. These abnormalities are usually hyperdiploid with multiple trisomies or nonhyperdiploid with IgH translocations. In one study using FISH, it was

shown that 42% of MGUS, 63% of smoldering myeloma and 57% of MM cases were hyperdiploid [23]. The hyperdiploid karyotype is usually characterized by trisomies of chromosomes 3,5,7,9,11,15,19 and 21 [24]. While the hyperdiploid group is regarded as neutral in terms of prognosis, the nonhyperdiploid group is associated with poorer overall survival.

The nonhyperdiploid classification consists of clones containing hypodiploid, pseudodiploid and tetraploid variants. The common nonhyperdiploid translocations t(4;14)(p16;q32) and t(14;16)(q32;q23) are usually associated with poor prognosis while the t(11;14)(q13;q32) are associated with a favorable prognosis [25]. For the two translocations with poor prognosis, the immunoglobulin switch region on chromosome 14 is juxtaposed to MAF on chromosome 16 and MMSET on chromosome 4 [26]. These translocations are usually a result of errors in IgH switch recombination or hypersomatic hypermutation during B cell differentiation [27]. The incidence of IgH translocations increases from 50% in MGUS to 80% in human MM cell lines. In addition to primary IgH translocations, virtually all MM and MGUS patients have cyclin D dysregulation as a primary event. As disease progresses MM becomes more proliferative and develops a number of secondary aberrations.

Four main secondary aberrations are most often reported. These include the deletion of chromosome 13, deletions and amplications in chromosome 1, the deletion of chromosome 17p13 and translocations of Myc [28]. Chromosome 13 aberrations are found in 50% of cases and are associated with an unfavorable prognosis [29]. Chromosome 1 aberrations are the most common type of aberration in MM and are also

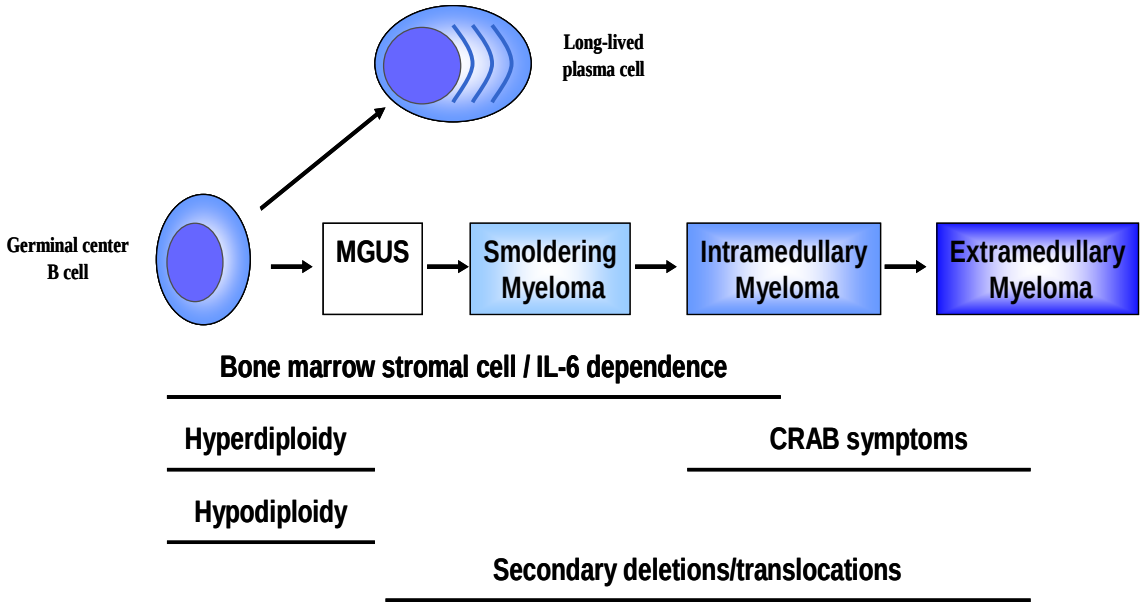

FIGURE 2: Key events in the progression of MM. There are four stages of myeloma categorized into 2 groups, asymptomatic (MGUS and SM) and symptomatic (intramedullary and extramedullary myeloma) plasma cell dyscrasias. Primary cytogenetic aberrations result in development of MGUS. Secondary cytogenetic aberrations result in progression to smoldering myeloma and finally advanced stages of the disease.

associated with poor prognosis [30]. The deletion of 17p13 leads to the loss of heterozygosity of the tumor suppressor gene TP53 and is sited as an important molecular cytogenetic factor and is an indicator of very poor prognosis [31]. Translocations of the oncogene Myc are involved in up to 45% of patients and are considered a late event in tumor progression when tumors are less dependent on stromal adhesion [32]. In addition to these secondary aberrations, the activation of NRAS and KRAS and the inactivation of cyclin-dependent kinase inhibitors have also been implicated in disease progression [33].

In addition to cytogenetic abnormalities multiple myeloma cells also have different surface markers compared to normal plasma cells. CD56 is an adhesion molecule that is expressed in 70-80% of MM cases but is not expressed in normal plasma

cells [34]. CD28 is another surface protein that increases expression as cells progress to MM. In one study, CD28+ plasma cells were detected in 19% of 31 monoclonal gammopathy of undetermined significance, 41% of 116 MM, and 100% of 13 human myeloma cell lines [35]. The CD44 variant CD44v9 has also been shown to be overexpressed on MM cells with expression inducing production of IL-6 by bone marrow stromal cells. Overexpression of the CD44v9 on MM cell lines has also been shown to have a poor prognosis.

Current Treatment Options

MM treatment is focused on decreasing the signs and symptoms of the disease. While asymptomatic myeloma requires only evaluation since treatment shows no added benefit, symptomatic disease should be treated immediately [36]. 73% of patients diagnosed with symptomatic myeloma have anemia, which is usually related to myeloma marrow infiltration [37]. Bone lesions develop in around 80% of patients while renal dysfunction occurs in 30% of newly diagnosed patients. For patients who meet the diagnostic criteria for myeloma, including clonal plasma cells >10% on a bone marrow biopsy and myeloma related organ impairment, the international staging system (ISS) is used. The ISS defines three risk groups based on serum β2-microglobulin and albumin levels [38]. Once the diagnostic testing is complete, initial treatment is administered which is based on a person's age and prognosis factors.

The treatment strategy for MM is mainly related to patient age. For patients 65 or younger who do not have substantial organ dysfunction autologous stem cell transplantation is administered in combination with high dose chemotherapy. The chemotherapy consists of either thalidomide or lenalidomide-doxorubicin treatment or

bortezomib induced treatment [39]. Older patients or patients with preexisting conditions have a hard time withstanding autologous stem cell transplantation. For these patients either 3 drug therapy or 2 drug therapy has been used. Three drug therapy consists of the use of melphalan, prednisone and one of lenolidomide, thalidomide or bortezomib. In a sample study using melphalan, prednisone and bortezomib the proportions of patients with a partial response or better were 71% in the bortezomib group and 35% in the control group; complete-response rates were 30% and 4%, respectively [40]. 2 drug induction consists of the combination of dexamethasone and either thalidomide or lenalidomide. In a sample study using lenalidomide and dexamethasone 31 of 34 patients achieved an objective response, including 6% achieving complete response and 32% achieving near complete response [41]. Sometimes after initial therapy an ongoing maintenance therapy is administered to prolong progression free survival.

The natural progression of patients with MM is for the occurrence of relapse after treatment. Patients who have progressive disease are classified as having either relapsed or refractory myeloma. Relapsed MM is defined where a patient who has achieved complete response through initial therapy experiences progressive disease, whereas refractory MM is defined as a scenario where a patient is unresponsive to current therapy or progresses within 2 months of last treatment [42]. In addition, some patients fail to achieve a response after induction therapy and then progress are considered patients with primary refractory myeloma. When these situations arise, new treatment regimens are administered to prolong survival. Some patients are given conventional chemotherapy which includes approaches containing high-dose dexamethasone; high-dose melphalan; and combinations of vincristine, doxorubicin, and dexamethasone (VAD). High-dose

dexamethasone is used for patients who are not candidates for more aggressive treatments and has shown response rates ranging from 18-27% with 4 day courses at 40 mg per day [43]. High-dose melphalan has been used for over 20 years and it was shown in one study that 61% of patients responded after treatment with 100 mg/m^2 with an autologous bone marrow infusion [44]. VAD is a widely used regimen for refractory myeloma with an increase in response in relapsed patients compared to dexamethasone treatment alone [45]. In addition to VAD, doxorubicin and dexamethasone have been combined with other chemotherapeutic agents including prednisone, carmustine, cyclophospamide and melphalan to achieve response in relapsed and refractory myeloma patients.

The novel therapeutic agents thalidomide, lenalidomide and bortezomib have also been used to treat relapsed and refractory patients. Thalidomide alone was shown to produce partial remission in 30% of relapsed patients with a 1 year survival rate of 60% [46]. Combination therapy with thalidomide and conventional drugs usually results in an overall response rate (ORR) of 60%-70% with complete response rates of 10-20% [47]. Lenalidomide has also been shown to have an effect in relapsed patients with a combination of lenalidomide and dexamethasone having an ORR of 60% compared to an ORR of 20% for dexamethasone alone [48]. The protease inhibitor bortezomib has also been shown to be an attractive therapy for targeting relapsed/refractory MM. As a single agent bortezomib was shown to elicit an ORR of 38% compared to 18% for high-dose dexamethasone [43]. Bortezomib is also used in combination studies since it has mild myelosuppression and lack of thrombogenecity seen with thalidomide and lenalidomide. For example, a recent study with bortezomib combined with prednisone and cyclophospamide produced an ORR of 85% with 50% of patients exhibiting a complete

response of over a year [49]. Even though new regimens have been utilized to prolong intervals of progressive disease and patient survival, MM is currently defined as an incurable disease, because of the ultimate development of drug resistance.

Drug Resistance in Multiple Myeloma

Because multiple myeloma ultimately develops drug resistance to treatment strategies, researchers have invested considerable amounts of research into delineating the mechanisms by which multiple myeloma cells develop resistance. Even after therapy in which complete response is achieved, small populations of myeloma cells are able to survive, a condition known as minimal residual disease (MRD). These cells have historically been able to evade detection as they do not secrete detectable amounts of serum or urine monoclonal proteins by established diagnostic tests [50]. However, techniques being developed including the use of a polymerase chain reaction (PCR) with patient specific primers have been able to detect MRD in patients that have been classified as having a complete response [51]. Subsequent expansion of these cells correlates with drug relapse, frequently with an acquired multidrug resistant phenotype making salvage therapy unsuccessful even with novel therapeutic agents. MRD is thought to escape drug treatment through two distinct methods of resistance, *de novo* resistance and acquired resistance. *De novo* resistance is defined as resistance that is present prior to drug selection and selection of drug resistance. Mechanisms associated with *de novo* resistance help contribute to the failure to eliminate MRD and contribute to the emergence of acquired drug resistance.

Soluble factors and direct MM cell contact both contribute to *de novo* drug resistance. Soluble factors that contribute to *de novo* drug resistance include both

chemokines and cytokines. The chemokine SDF-1 has been shown to be important for MM homing to the bone marrow via interactions with the CXC chemokine receptors CXCR4 and CXCR7. SDF-1 has been shown to induce motility and cytoskeletal rearrangement in MM cells while inhibition of the CXCR4 receptor with AMD3100 reduced motility [52]. Expression of the SDF-1 receptor CXCR7 has also been shown to increase tumor cell adhesion properties [53]. SDF-1 has also been shown to up-regulate the production of the cytokine IL-6 by stromal cells, therefore enhancing MM cell survival [54].

In addition to the chemokine SDF-1, cytokines have also been shown to contribute to *de novo* drug resistance in MM cells. The cytokine IL-6 has been identified as one of the main factors that contributes to the growth and survival of MM cells in the bone marrow microenvironment. IL-6 binds to IL-6Rα and leads to the dimerization and phosphorylation of gp130 [55]. Phosphorylation of gp130 leads to the initiation of 3 major signaling pathways in MM cells that contribute to drug resistance: the Ras/Raf-MEK-ERK pathway; the phosphatidylinositol 3-kinase (PI3K) pathway and the JAK/STAT pathway. Ras gene mutations have been shown to have an oncogenic effect and occur in 30% to 40% of patients with MM [56]. In addition to specific mutations, IL-6 has been shown to also activate Ras by the phosphorylation of Shc through cytokine stimulation [57]. This activation of Ras by IL-6 has been shown to trigger the ERK cascade and subsequent growth of MM cells [58]. IL-6 was also shown to activate AKT in MM cells and subsequently protecting the cells from dexamethasone induced apoptosis [59]. IL-6 has also been shown to activate the JAK/STAT pathway and in particular up-regulate the expression of the anti-apoptotic proteins B-cell lymphoma-extra large (BCL-

xL) and myeloid cell leukemia sequence 1 (Mcl-1) [60]. Expression of Mcl-1 in particular has been shown to correlate to an increase in dexamethasone resistance.

In addition to IL-6, other cytokines have been shown to play a role in de novo drug resistance. TNF-α has been shown to activate NF-κβ and up-regulate IL-6 secretion which contributes to mm growth and survival [61]. Insulin-like growth factor-1 (IGF-1) is also an important survival factor in multiple myeloma cells. For example, it has been shown that IGF-1 mediates the down regulation of the proapoptotic BH3-only protein Bim and protecting myeloma cells from bortezomib and melphalan induced cell death [62]. The vascular endothelial growth factor (VEGF) has also been shown to protect multiple myeloma cells against apoptosis by inducing the up-regulation of Mcl-1 [63]. Interferon-alpha (IFN-alpha) is a cytokine that has been shown to induce autocrine production of IL-6 in myeloma cell lines and protect myeloma cells from dexamethasone treatment [64].

Direct cell contact of MM cells to bone marrow stroma cells and extracellular matrix (ECM) proteins has also been shown to play a prominent role in MM pathogenesis and MDR. Multiple adhesion molecules have been shown to cause cell adhesion mediated-drug resistance (CAM-DR), including CD44, lymphocyte-associated function antigen-1 (LFA-1), Notch-1 and integrins. CD44 has been shown to adhere to hyaluronan and this engagement promotes dexamethasone resistance in myeloma cells [65]. LFA-1 binds to the intracellular adhesion molecule 1 (ICAM) and the blockage of this adhesion with an anti-LFA1 antibody has been shown to reverse CAM-DR to melphalan in myeloma cells [66]. Inhibition of notch with a gamma secretase inhibitor was shown to

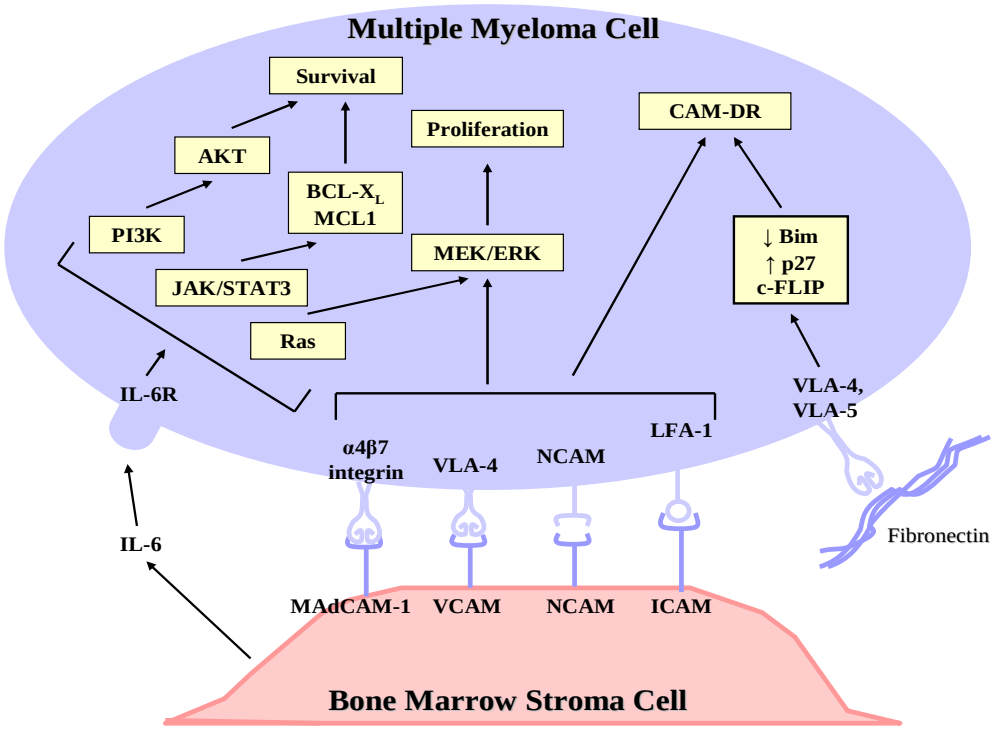

Figure 3: *de novo* resistance in MM. Soluble factors and direct MM cell contact both contribute to *de novo* drug resistance. IL-6 leads to the activation of major signaling pathways leading to increased cell survival and proliferation. Adhesion of MM cells to BM stroma cells and ECM proteins like FN lead to CAM-DR.

induce apoptosis and increase sensitivity to doxorubicin and melphalan [67]. In addition to adhesion molecules, it has been shown that genes associated with certain myeloma translocation gene products, specifically the MMSET gene and the t (4:14) translocation, are associated with increased myeloma cell adhesion and tumorigenicity [68].

β1 integrin specific CAM-DR was initially described in studies showing that β1 integrin mediated adhesion to fibronectin (FN) conferred resistance to melphalan and doxorubicin [69]. Adhesion by integrins has been shown to modify distinct cellular

processes leading to drug resistance. For example, β1 integrin-mediated adhesion to FN upregulates $p27^{kip1}$ and induces cell cycle arrest and resistance to the topoisomerase inhibitor etoposide [70]. MM cell adhesion to FN was also shown to control the localization of cFLIP, making it able to associate with FADD and block the extracellular apoptotic cascade [71]. Leukemic cells were also shown to downregulate the expression of the proapoptotic protein bim resulting in CAM-DR [72]. In addition to β1 integrin other integrins have been implicated in CAM-DR. Silencing of the β7 integrin reversed FN induced CAM-DR in myeloma cells to bortezomib and melphalan.

De novo resistance results in the acquisition of mechanisms that confer resistance to multiple classes of therapeutic agents, also known as acquired drug resistance. Mechanisms that result in acquired resistance include: reduction in intracellular drug accumulation; alterations in drug targets; inhibition of apoptosis; and enhanced DNA repair. An increase in the drug-efflux pump P-glycoprotein has been shown to reduce intracellular drug accumulation and increase resistance to therapy. Resistance to melphalan and thalidomide has been associated with reduced drug accumulation in multiple myeloma cells [73, 74]. Mutations in drug targets have also led to acquired resistance to therapy. Alterations in topoisomerase II have led to resistance from etoposide while alterations in the glucocorticoid receptor have led to resistance to dexamethasone [75]. An alteration in a specific subunit of the proteasome has also led to bortezomib resistance in MM cells [76]. Upregulation of proteins that inhibit apoptosis also confers acquired drug resistance. The upregulation of Bcl-2 has also been shown to confer drug resistance to dexamethasone and doxorubicin [77]. Elevated levels of the inhibitor of apoptotic protein XIAP has also been shown to correlate with poorer survival

in patients post chemotherapy [78]. Finally, alterations in DNA-repair pathways have been shown to contribute to acquired resistance in MM cells. Enhanced DNA repair via the Fanconi Anemia pathway has been shown to contribute to melphalan resistance in MM cells [79]. By understanding mechanisms of *de novo* and acquired resistance, new therapeutic targets are being identified to reduce MRD or target known markers of relapsed/refractory patients.

Chapter 3: Integrins

Structure and Function

Integrins are transmembrane heterodimeric proteins which consist of non-covalently bound alpha and beta subunits. In vertebrates, there are 18 alpha and 8 beta subunits that can assemble to form 24 distinct receptors with different binding properties and tissue distribution [80]. These distinct heterodimer combinations confer cell-cell and cell-ligand specificity relevant to the cell and the environment in which it functions. Through these interactions integrins trigger signaling pathways by clustering with other integrins and activating kinases via the formation of focal adhesion complexes. These functions of integrins play a role in cancer defining processes including tumor cell growth, survival, migration, homing, metastasis and environmental mediated-drug resistance.

The alpha and beta subunits form a non-covalently bound dimer, which consists of an ectodomain that contains multiple domains with flexible linkers, a transmembrane domain and a short cytoplasmic tail. The extracellular domain interacts with and binds to ligands of the extracellular matrix. The transmembrane domain traverses the cell membrane, linking the ectodomain and the cytoplasmic tail. The cytoplasmic tail acts as an adaptor protein for intracellular signaling and as part of the scaffold, along with the cytoskeleton, for the formation and growth of focal adhesions.

Integrins are structurally classified based on the presence or absence of an I domain in the α-subunit ectodomain. Within this domain is a five amino acid motif termed the metal ion dependent adhesion site (MIDAS) which acts to coordinate ligand binding [81]. Integrins lacking the I-like domain contain a similar domain within the β-subunit, termed the β I-like domain. Each individual integrin dimer generally recognizes one specific ECM protein. There is some overlap between integrins and their ligand recognition, as they recognize sequence motifs common among matrix proteins. For example, the αV integrins, two β1 integrins (α5, α8) and αIIbβ3 all share the ability to recognize ligands containing an RGD tripeptide active site contained by fibronectin and vitronectin. The RGD-binding site is located at the interface between the β-propeller domain and the β I-like domain and amino-acid residues from the two domains interact directly with the RGD peptide [82]. α4β1, α4β7 and α9β1, on the other hand, bind to the CS1 region of fibronectin through a LDV motif that is functionally related to RGD [83].

Integrins are known to exist in two major conformational states. They can exist in an inactive or low affinity state or an active or high affinity state. Two models have been proposed for the activation of integrins from a low affinity state to a high affinity state. One model of integrin activation is the switchblade model in which the inactive state corresponds to a bent conformation and the active state corresponds to a straight conformation [84]. The other model is the deadbolt model in which the bent conformation is maintained when integrins are activated but movements of the transmembrane regions cause sliding of the extracellular stalks of the α and β subunits [85].

Integrins can also be activated bidirectionally, meaning both extracellular and intracellular events can regulate activation. One way in which integrins can be activated is by inside-out signaling. In inside-out signaling, adaptor proteins, like talin, bind to the integrin β cytoplasmic tail and induce a conformational change in the ectodomain that increases the integrins affinity for ligand [86]. Integrins can also be activated by outside-in signalling. In outside in signalling, binding of ligand to the integrins induces a conformational change, including the separation of α and β stalk domains, transmembrane domains which lead to the interaction of the β integrin cytoplasmic tail with intracellular adaptor proteins like talin.

The integrin tails have no intrinsic kinase domain but rather serve as a site for adaptor proteins to bind and help recruit various kinases that activate downstream signaling. Talin and paxillin bind to β-integrin tails and recruit focal adhesion kinase (FAK) and vinculin to the focal adhesions. α –actinin serves to crosslink both talin and actin, which help to strengthen focal adhesions and promote focal adhesion growth [87]. Although some myeloma cells lack FAK, the tyrosine kinase pyk2 has been shown to serve a similar function in cells lacking FAK expression [88]. The recruited kinases are then able to govern many downstream kinases including AKT, ERK, and Jnk which are important in multiple myeloma cell cycle progression, growth, survival, and migration.

Integrin Expression in Multiple Myeloma

Of the 18 alpha and 8 beta integrin subunits that have been identified very few have been shown to have significant expression in MM cells. Different studies have been done to try to identify the important integrin subunits in MM cells. In one study, it was shown that MM cells extracted from bone marrow express no alpha 2 integrin, and

almost no alpha 6 integrin, although they have variable expression of alpha 4, alpha 5, and beta 1 integrins [89]. Another study showed that in the cell lines studied, there was high expression of alpha 4 and beta 1 integrin expressed with minimal expression of alpha 3 integrin and no expression of alpha 2 integrin and alpha 6 integrin [90]. Yet another study focused on other cell lines showed high levels of alpha 4 integrin, alpha 5 integrin, beta 1 integrin and beta 7 integrin [69]. Consistent in these studies is the high expression of alpha 4 integrin, beta 1 integrin and beta 7 integrin with some myeloma cell lines expressing alpha 5 integrin. In addition to these integrins the alphaLbeta2 integrin and the alphavbeta3 have also been shown to be expressed on MM cell lines.

The α4β1 (very late antigen 4 or VLA-4), α5β1 (VLA-5), and α4β7 heterodimers are major integrin heterodimers associated with MM cells. VLA-5 has been shown to mediate cell adhesion to the ECM protein FN while the α4β7 integrin has been shown to mediate cell adhesion to the MAdCAM-1 receptor of bone marrow stroma cells. VLA-4 is unique among integrins as it has been shown to be the only heterodimer that mediates cell-ECM as well as cell-cell interactions [91]. VLA-4 has been shown to bind to the CS-1 region of FN as well as to VCAM-1 via a separate binding site. The α4 integrin is also unique in it is the only integrin to be expressed on the plasma membrane in two distinct forms, the intact (150 kDa) alpha 4 subunit and a cleaved form which consists of two noncovalently associated fragments (80 and 70 kDa). Even though cleavage of α4 has been shown to be increased after T cell activation, previous binding studies using the intact and cleaved subunits showed no alteration in VLA-4 binding function [92]. In addition to existing in two distinct isoforms on the cell surface of myeloma cell lines, there was shown to be a difference in VLA-4 expression in relapsed MM patients

compared to newly diagnosed patients. In a study done by Schmidmaier, it was shown that VLA-4 and VCAM expression was higher in pre-treated patients than in chemo-naive patients and the expression levels increased with the number of chemotherapy regimens [93].

In addition to patient samples α4, α5, β1, and β7 integrin levels have been studied in sensitive and drug resistant MM cell lines. In sensitive 8226/s cell lines, there was minimal expression of α4 and β7 integrins with high expression of α5 and β1. 8226/s was then chronically treated with melphalan and doxorubicin to develop the isogenic drug resistant cell lines 8226/LR5 and 8226/dox6 cell lines respectively. As the cell lines are selected for resistance the surface expression of the integrins are changed. In the drug resistant cell lines α4 and β7 integrin expression is increased while α5 integrin expression is decreased, indicating that an increase in α4 integrin expression is correlative for drug resistance in MM cells [69]. In addition to increased integrin expression being a determinant for drug resistance to therapeutic agents, integrin function associated with VLA-4 was also shown to be changed in drug resistant cell lines. In the melphalan resistant MM cell line U226/LR7 there were similar levels of α4 integrin in the resistant line compared to the U226 sensitive line. However, U266/LR7 cells adhere to FN at a significantly higher rate than U266 cells in a VLA-4 dependent fashion and correlated with CAM-DR to melphalan [94]. β7 integrin mRNA expression was also screened in a panel of MM cell lines. Results showed that cells with a t(4;14)(H929,OPM2) or t(14;16)(MM1S) that correlates with poorer prognosis expressed the highest levels of β7 integrins [95].

As VLA-4 is shown to have higher expression on drug resistant cell lines and relapsed/refractory patients, therapeutics that target or lower VLA-4 levels have been investigated in MM cell lines. For example, a study showed that the highly successful MM therapeutic bortezomib reverses CAM-DR and sensitizes cells to dexamethasone in the coculture environment in part by downregulating the expression of VLA-4 [96]. Antibodies against α4 integrin have also shown to have decrease myeloma growth *in vitro* and *in vivo*. The monoclonal antibody PS/2 was shown to inhibit the growth of GFP-expressing 5TGM1 cells in C57Bl/KaLwRij mice [97]. The humanized monoclonal antibody natalizumab was also shown to disrupt the binding of MM cells to FN and chemosensitize cells to bortezomib [98]. Micellular nanoparticles targeting α4 integrins have also been developed and have been shown to overcome CAM-DR [99]. In addition to targeting VLA-4, other integrins have been an attractive target for developing new therapeutics to target MM as well as other cancers.

Integrin Targeted Therapeutics

Targeting integrins is of great interest in the treatment and prevention of cancer. Antibodies, peptidomimetics, and small molecule antagonists have all been utilized in order to target integrins. Each type has its own advantages and disadvantages. Antibodies are the most widely used strategy in developing integrin targeting drugs. Antibodies are advantageous as they have very high target specificity and affinity, leading to a decrease in off target effects. Antibodies also have high circulation times compared to small molecule inhibitors and peptides. The disadvantages for antibodies include the need for intravenous administration and the propensity for host immunogenicity. Peptide-based drugs have high target affinity and specificity but have

limited stability. Techniques can be utilized to increase stability and decrease proteolytic cleavage such as cyclization of peptides or the use of D-amino acids. Small molecule inhibitors have high stability and can be administered orally but have low selectivity in integrins. There have been promising results utilizing antibodies, peptidomimetics and small molecular inhibitors in targeting integrin heterodimers shown to be expressed in MM cells like VLA-4, VLA-5 and αVβ3.

Antibodies that target α4, α5 and αVβ3 integrins have been shown to have success in decreasing tumor burden and decrease integrin mediated CAM-DR. The anti-α4 integrin antibody, natalizumab, has been shown to prevent the adhesion of leukocytes to the receptors VCAM-1 and MAdCAM-1 and is currently used in the treatment of multiple sclerosis and Crohn's disease. As MM cells have been shown to express high levels of α4 integrin, newer studies have looked into the effect that Natalizumab has on MM cell growth in the bone marrow microenvironment. It was shown that Natalizumab blocked VEGF and IGF-1 induced MM cell migration and also chemosensitized MM cells to bortezomib [98]. Volociximab, a monoclonal antibody against VLA-5, has also been shown to inhibit angiogenesis and impede solid tumor growth. It is currently in a phase II clinical trial in solid renal cell carcinoma and is also being investigated in the treatment of macular degeneration [100]. In addition several therapeutic antibodies are currently being investigated that target the αVβ3 integrin. Vitaxin is a humanized mouse monoclonal antibody that blocks angiogenesis and induces apoptosis in advanced solid tumors and is currently in phase I clinical trials. CNTO 95 has also been shown to inhibit melanoma cell adhesion and inhibit tumor growth in mouse xenografts. In a phase I

clinical trial an analysis of a post-treatment biopsy showed decreased expression of bcl-2 after treatment and it is being investigated in phase II clinical trials [101].

Peptidomimetics targeting integrins are also being looked at as a means to block tumor growth and progression. One of the first peptide sequences shown to block the interaction between integrins and FN was the sequence RGD. In addition to mediating the interaction between the cell and FN, cyclized RGD containing peptides were also shown to directly induce apoptosis in breast cancer cells by directly binding to and activating caspase-3 [102]. Other peptides have been developed with the RGD sequence and have been shown to have anti-tumor effect on cancer cells. Cilengitide is a cyclic pentapeptide containing the RGD sequence and was selected for its capacity to specifically inhibit the αVβ3 and αVβ5 integrins [103]. Cilengitide is currently being tested in phase II clinical trials for patients with lung and prostate cancer. It has been shown to have anti-tumor effect in newly diagnosed glioblastomas with 69% of patients being progression free after 6 months [104]. Cilengitide is currently in a phase III clinical trial for the treatment of glioblastoma. ATN-161 is a non-RGD-based peptide that has been shown to block the growth of breast cancer cells *in vivo* [105]. ATN-161 was tested in a phase I clinical trial of patients with advanced solid tumors with 1/3 of patients treated showed prolonged stable disease [106]. In MM cells a VLA-4 antagonist peptide has been developed that when conjugated to doxorubicin and nanoparticles blocks MM cell adhesion and induces apoptosis in a xenograft model.

Small molecule antagonists targeting integrins have also been shown to inhibit integrin signaling and decrease cancer metastasis. The VLA-5 small molecule inhibitor JSM6427 was shown to reduce FN-induce ERK phosphorylation which has been shown

to be a signal associated with CAM-DR and further studies are ongoing for its effects on cancer cells [107]. The αVβ3 integrin small molecule antagonist S247 has been shown to inhibit breast cancer bone metastasis and decreased colon cancer metastasis. In addition, it was shown to inhibit the development of colon cancer metastases and growth to the liver in an *in vivo* model [108]. A different αVβ3 integrin small molecule antagonist, PSK1404, was also shown to inhibit breast and ovarian bone metastases in a murine mouse model. In addition, PSK1404 was shown to inhibit osteoclastic activity in the bone marrow microenvironment which substantially decreased tumor initiated bone destruction [109].

Chapter 4: Cell Death Pathways

Apoptosis

Different kinds of cell death are distinguished by distinct morphological criteria, and are classified into distinct modes of cell death. Three of the most commonly classified modes are defined as apoptosis, autophagy and necrosis. Apoptosis has been determined to be an important mode of programmed cell death in cells with activation of caspases leading to cell shrinkage, chromatin condensation and cell blebbing. Autophagy is defined as a process in which the cell degrades its own components through the merging of the autophagosome and lysosome and is known to occur via cell starvation or extreme cell stress. Necrosis is usually defined as a passive and energy-independent form of cell death which results in swelling of cellular organelles and loss of plasma membrane integrity but there are some forms of necrosis, like necroptosis, which are now classified as a form of programmed cell death. In apoptosis, two classes of proteins play a distinct role; the Bcl-2 family of proteins which are responsible for mitochondrial integrity and the cysteinyl aspartate-specific proteases or caspases, which are responsible for the direct execution of cells.

Caspases are divided into initiator caspases (caspase-2, -8, -9, -10) and executioner caspases (caspase-3,-6, -7). These caspases can be activated by either the intrinsic or extrinsic cell death pathways. The intrinsic cell death pathway is activated by internal cell stimuli such as DNA damage or internalized cytotoxic drugs and acts

through release of proteins from the mitochondria which are controlled by the Bcl-2 family of proteins. Under normal conditions, anti-apoptotic Bcl-2 family members sequester the pro-apoptotic proteins Bax and Bak from dimerizng. During cellular stress, Bcl-2-homology 3 (BH3)-only proteins, like Bim, are activated and bind the antiapoptotic Bcl-2 family members, leading to the dimerization of Bax and Bak and subsequent formation of a channel on the mitochondrial membrane where cytochrome c is released. Cytochrome c associates with Apaf-1 and helps with the recruitment and activation of procaspase-9 [110]. Other proteins like Smac/DIABLO and Omi are released from the mitochondria and help promote caspase 9 activation by inhibiting inhibitors of apoptosis protein (IAP) activity [111]. Activated caspase 9 cleaves and activates executioner caspases like caspase-3 which causes chromatin condensation and apoptotic cell death.

The extrinsic pathway of apoptosis is activated by external stimuli and involves the stimulation of death receptors belonging to the tumor necrosis factor receptor (TNFR) family, such as itself, Fas and TRAIL-R. The binding of Fas ligand to Fas receptor results in the association of the adaptor protein FADD while the binding of TNF ligand to TNFR results in the association of the adaptor protein TRADD and subsequent recruitment of FADD [112]. FADD associates with procaspase 8, resulting in the formation of a death-inducing signaling complex (DISC). Caspase 8 is then activated which triggers the execution phase of apoptosis. Like IAP inhibition of procaspase 9 the extrinsic apoptotic pathway can also be inhibited. The protein c-FLIP has been shown to bind to FADD and procaspase 8, rendering the cell death pathway useless [113].

Many drugs used in treating MM induce apoptosis. The DNA alkylating drug, melphalan, for example, has been shown to disrupt the interaction of Mcl-1 and Bim,

thereby releasing Bim which leads to Bax activation and cytochrome c release [114]. The glucocorticoid, dexamethasone, has also been shown to induce apoptosis in multiple myeloma cell lines. As the MM1R cells gain resistance to dexamethasone, they lose expression of the glucocorticoid receptor which binds dexamethasone. Reexpression of the glucocorticoid receptor in dexamethasone resistant MM1R cells induced Bim expression and dexamethasone apoptosis, indicating that dexamethasone also induces apoptosis in MM cells in a Bim dependent manner [115]. The proteasome inhibitor bortezomib has been shown to trigger caspase activation in retinoblastoma and chronic lymphocytic leukemia as a primary agent. In addition to directly causing activation of caspases, bortezomib has also been shown to sensitize MM to apoptosis inducing drugs like dexamethasone and melphalan [116]. In addition to sensitizing agents that induce apoptosis by the intrinsic apoptotic pathway, bortezomib has also been shown to sensitize MM cells to cell death by the extrinsic pathway drugs like TRAIL by decreasing the protein expression of the antiapoptotic protein c-FLIP [117]. New classes of compounds are being developed and tested that induce apoptosis in MM cells in addition to established therapeutics. For example, arsenic trioxide has been shown to activate caspases in MM cells [118]. Utilization of different compounds that target the apoptotic pathway via different mechanisms could potentially reverse drug resistance in MM that occurs because of the microenvironment like the upregulation of antiapoptotic proteins Mcl-1, Bcl-2, c-FLIP and XIAP or downregulation of proapoptotic proteins like Bim. Utilizing drugs that target the other cell death pathways like autophagy and necrosis could also prove to be useful in treating MM patients in combination with apoptotic inducing drugs.

Autophagy

Autophagy is a catabolic pathway that allows cells to degrade and recycle cellular components. Autophagy is unique among cell death pathways as induction of autophagy has been shown to correlate with both cell survival and cell death. The presence of autophagic vacuoles is commonly seen in dying cells, often accompanying apoptotic and necrotic cell death. In fact, there have been shown to be interconnections that exist between autophagy and apoptotic and necrotic cell death. For example, the anti-apoptotic protein Bcl-2 has been shown to repress autophagy by binding to the autophagy stimulating protein Beclin-1 [119]. Active caspase 8 has also been shown to cleave Beclin-1 into 2 fragments, with one of the fragments translocating to the mitochondria and facilitates release of cytochrome c [120]. Even though the outcome of autophagy usually reflects a pro-survival function, autophagy can induce cell death under certain conditions. RNA interference (RNAi) directed against 2 autophagy genes, atg7 and beclin 1, blocked cell death in mouse L929 cells treated with the caspase inhibitor zVAD [121]. Further, RNAi against atg5 and beclin 1 blocked death of $bax^{-/-}$, $bak^{-/-}$ murine embryonic fibroblasts (MEFs) treated with etoposide [122]. Notably, in both of these studies RNAi blocked the death of cells whose apoptotic pathway had been crippled, implicating autophagy as a cell death mechanism when apoptosis is inhibited.

Three types of autophagy have been described; chaperone-mediated autophagy, microautophagy and macroautophagy. Macroautophagy has been the best described autophagic process and is usually referred to as just autophagy. Autophagic signaling has been shown to be regulated by mTOR, a protein kinase that is important in controlling translation and cell-cycle progression. When mTOR is inhibited by stimuli such as

nutrient starvation or rapamycin, the ULK-Atg13-FIP200 complex is formed, with the formation of this complex leading to the induction of the formation of the autophagosome. The synthesis of the autophagosome also requires vesicle nucleation, which is initiated by the formation of the PI3KC3 (Vps34)-complex, of which Beclin-1 is a member. Once this complex is activated, phosphatidylinositol 3-phosphate (PI3P) is generated and helps to recruit other proteins that elongate the autophagosome. The Atg12-Atg5-Atg16 complex is recruited which plays a role in vesicle curvature while the autophagic marker LC3 is lipidated and specifically binds to the autophagosome membrane. After all of these events occur, the autophagosome fuses with a lysosome, releasing its content into the lysosome to be degraded by hydrolases.

Autophagy is shown to be important in diseases where protein production is instrumental in characterizing the disease, like MM. It is believed that the ongoing induction of autophagy seen in some cell lines protects cells from the accumulation of misfolded proteins and is shown to be a survival mechanism in MM. Many drugs that induce apoptosis in MM cells are also shown to induce autophagy. For example, the apoptosis inducing DNA-damaging drugs doxorubicin and melphalan are also able to trigger Beclin 1-regulated autophagy in the human MM cell lines H929 and RPMI 8226 with the silencing of beclin-1 or Atg5 augmenting their proapoptotic activity [123]. Bortezomib was also shown to induce autophagy in MM cells but inhibiting autophagy with the lysosomotrophic agent chloroquine did not increase bortezomib induced cell death [124]. However, bortezomib is shown to exhibit synergistic effects in combination with agents that uncouple the aggresome, a proteinaceous inclusion body that forms when cellular degradation machinery is impaired, and autophagy pathways. Tipifarnib, a

farnesyl transferase inhibitor that also inhibits the oncogene Ras, has been shown to synergize with bortezomib in 8226 MM cells in this manner [125]. From most reports, it is shown that induction of autophagy produces a survival effect in MM cells and inhibiting this pathway either in conjunction with uncoupling the aggresome in the case of bortezomib or without uncoupling the aggresome in the case of doxorubicin and melphalan sensitizes the cells to established therapies.

Necrosis

Necrosis is predominantly described as an accidental or uncontrolled form of cell death and is characterized by organelle swelling, followed by loss of cell membrane integrity and release of cellular components from the cell. As necrosis is not thought of as being tightly regulated, key cellular processes are characterized as being important for the induction of necrosis instead of activation of executioner proteins. The key bioenergetic events that are usually implicated in necrosis are; increased mitochondrial dysfunction, adenosine triphosphate (ATP) depletion, depletion of intracellular nicotinamide adenine dinucleotide (NAD^+), increased levels of intracellular calcium, and increased generation of reactive oxygen species (ROS). Evidence is beginning to show that in addition to these key processes, some modes of necrosis can also be a tightly regulated event, with forms of necrosis such as necroptosis appearing to be programmed modes of cellular death. There also have been shown to be interconnections with necrosis and apoptosis and autophagy, as some of the key mediators of necrosis have been shown to disrupt the mitochondria, extracellular death receptors such as TNFR and lysosomes important in autophagy.

Mitochondrial dysfunction is a key event that occurs during necrosis. In normal cells, a membrane potential is generated across the mitochondrial inner membrane as protons are pumped across the inner membrane. This process is responsible for the generation of ATP by oxidative phosphorylation. Certain stimuli such as an increase in intracellular calcium or an increase in intracellular ROS have been shown to open the mitochondrial permeability transition (mPT) pore on the mitochondria inner membrane. Opening of the mPT pore causes a cell to stop the generation of ATP by oxidative phosphorylation. Experiments have shown that a transient opening of the mPT pore induces apoptosis by release of apoptotic factors such as cytochrome c or apoptosis inducing factor (AIF) but persistent opening of the mPT has been shown to induce necrosis [126]. MPT induced necrosis is regulated by the protein cyclophilin D (cyD) and inhibiting cyD with cyclosporin A has been shown to inhibit the MPT and inhibit calcium induced necrosis [127].

In addition to disrupting key metabolic events that produce ATP through oxidative phosphorylation, necrosis has also been shown to occur through disruption of ATP that is produced during glycolysis. Poly (ADP-ribose) polymerase (PARP) is a nuclear protein known to be activated following single-strand DNA breaks and is a signal to recruit other DNA-repair enzymes such as DNA ligase III to repair the DNA. In order to generate ADP-ribose monomers integral to the DNA repair process, activated PARP depletes intracellular stores of NAD^+ by converting NAD^+ into nicotinamide adenine mononucleotide (NAM). Overexpression of PARP has been shown to induce necrosis by depleting cellular NAD^+ levels in cells that depend on glucose metabolism. Activated PARP converts NAD^+ into NAM. Since NAD^+ cannot cross the mitochondrial

membrane activated PARP selectively inhibits glucose metabolism, which has been shown to induce necrosis [128].

Increases in intracellular Ca^{2+} have also been shown to initiate necrosis. As Ca^{2+} is a secondary messenger for many integral cell processes, levels of Ca^{2+} in the cell are tightly regulated. Under normal physiological conditions the concentration of Ca^{2+} is determined to be around 1.2 mM in the extracellular matrix and around 0.1 μM in the cytosol with most of the excess intracellular Ca^{2+} stored in the endoplasmic reticulum (ER). In order to maintain Ca^{2+} homeostasis, Ca^{2+} is either able to enter or leave the cell through distinct Ca^{2+} channels on the plasma membrane. Ca^{2+} levels in the cell are also maintained by storage or release of intracellular Ca^{2+} stores located in the endoplasmic reticulum(ER). If intracellular stores of Ca^{2+} are increased too quickly, the mitochondria will also store excess Ca^{2+}. If the concentration of Ca^{2+} is increased to too high a level (>1μM), the mitochondria becomes overloaded with Ca^{2+} [129]. Mitochondrial Ca^{2+} overload has been shown to lead to opening of the mPT pore and ATP depletion, which in turn leads to necrosis [130]. Ca^{2+} is also responsible for activation of the Ca^{2+} dependent proteases calpains. Calpains have been shown to induce lysomal membrane permeability (LMP) of lysosomes, thereby releasing lysosomal enzymes into the cytoplasm and inducing necrotic cell death [131].

During oxidative phosphorylation in the mitochondria, electrons frequently escape from the electron transport chain. The reaction of the escaped electron and oxygen produces oxygen radicals, which are converted into ROS. These ROS consist of molecules including superoxide, hydrogen peroxide (H_2O_2), and nitric oxide (NO). ROS are usually neutralized by enzymes such as superoxide dismutase and glutathione

peroxidase or by reacting with a scavenger such as glutathione. When the balance between ROS and their scavengers is disturbed, an excess of ROS has been shown to damage cellular biomolecules including DNA, proteins and lipids. For example, it was shown that excess mitochondrial ROS have been shown to cause cleavage of DNA strands, cross-linking and oxidation of purines resulting in necrosis [132]. In addition to causing necrotic cell death through double stranded DNA damage, mitochondria-produced ROS have also been shown to cause necrotic cell death of fibrosarcoma cells by TNFα [133].

In addition to studying key bioenergetic events that initiate necrosis, studies are also being done to determine instances of regulated necrotic cell death. One such form of programmed necrosis, necroptosis, has been shown to be activated by ligation of cell death receptors such as FAS, TNFR and TRAILR. Upon binding of ligands such as TNFα, the TNFR forms trimers and recruits several death domain-containing proteins to form the DISC. Key proteins present in this complex are FADD, RIP1, RIP3, and caspase 8 [134]. If caspase 8 is not inhibited by proteins such as IAPs, caspase 8 cleaves RIP1 and RIP3 and induces caspase dependent apoptosis. If caspase 8 is inhibited, as has been previously shown with RNAi, RIP1 and RIP3 become phosphorylated and induce necroptosis [135]. Phosphorylated RIP1 causes PARP activation, ATP depletion, activation of ROS and an increase in intracellular calcium, all considered to be hallmarks of necrosis.

Necrosis inducing drugs are not currently heavily used in MM treatment as most of the drugs used are shown to target the apoptotic pathway in MM cells. Some drugs, however, induce a multimodal mechanism of cell death in MM cells. Doxorubicin has

been shown to induce the formation of ROS in addition to inducing autophagy and apoptosis. In fact, at low doses of doxorubicin, it was shown that the primary mode of cell death was determined to be necrosis instead of apoptosis [136]. ATO has also been shown to induce mediators of necrotic cell death as well as apoptosis by increasing ROS production and loss of mitochondrial membrane potential [118]. A novel antibiotic active against nutrient-starved oncogenesis, kigamicin, is one compound that has been shown to induce necrosis in MM cells. One interesting note of this study was that kigamicin produced higher levels of cell death in melphalan resistant cell lines compared to the parental lines, indicating that agents that cause necrosis may be useful in causing cell death in cells that have become resistant to apoptosis inducing drugs [137]. As the ability of tumor cells to evade apoptosis has been well classified as a cause of drug resistance in MM cells, drugs that target other cell death pathways may become more useful in treating MM.

Chapter 5: Ca^{2+} Signaling

Ca^{2+} Homeostasis

Positively charged calcium ions (Ca^{2+}) along with negatively charged phosphate ions are considered two of the most important secondary messengers that regulate signaling in cells. As Ca^{2+} binds to thousands of proteins in order to mediate these signaling events, such as protein association, function and localization, Ca^{2+} needs to be tightly regulated inside the cell. As such, channels are present on the plasma membrane, ER and mitochondria whose function is to control the uptake and release of Ca^{2+} in order to ensure that the ideal cytoplasmic concentration (~100 μM) is maintained in resting cells. The plasma membrane contains 3 distinct types of Ca^{2+} influx channels, voltage-gated, ligand-gated and store operated channels (SOC), which are responsible for Ca^{2+} intake into the cell. In addition, the plasma membrane also contains the plasma membrane Ca^{2+} ATPase (PMCA) pump and a Na^{2+}/Ca^{2+} exchanger that are responsible for the efflux of Ca^{2+} out of the cell. The sarcoendoplasmic reticular Ca^{2+} ATPase (SERCA) causes an influx of Ca^{2+} into the ER while the 1,4,5- inositol triphosphate (ip3) receptor and ryanodine receptor (RyR) are responsible for release of intracellular ER stores into the cytoplasm. Finally, the Ca^{2+} uniporter is responsible for Ca^{2+} influx into the mitochondria while the mPT pore is responsible for efflux of Ca^{2+} into the cytoplasm.

Voltage-gated Ca^{2+}-selective channels (CaVs) are common in many different types of cells but their activity has mainly been studied in excitable cells; like neurons,

cardiocytes, muscle tissues and endocrine cells. CaVs are the fastest family of Ca^{2+} channels with a million Ca^{2+} ions per seconds crossing the channel gradient. The channel's receptor contains a helix-turn-helix loops containing positively charged arginine residues, which are opened following a change in voltage [138]. Ligand-gated Ca^{2+} channels are opened or closed by the direct binding of a ligand to the channel itself. Binding of the ligand opens the channel which allows influx of Ca^{2+} ions into the cell. These channels are present on most cells and there is a belief that these channels play a role in cell-cell communication between cells but most of the studies done on these channels have been performed in sensory cells with neurotransmitter ligands. SOCs represent the last family of plasma membrane Ca^{2+} influx channels. In many nonexcitable cells, there is little Ca^{2+} influx across the plasma membrane. As Ca^{2+} is constantly seeping out of the ER into the cytoplasm and is frequently released from the ER to mediate Ca^{2+} signaling pathways, ER calcium stores are frequently found to be depleted. Upon ER Ca^{2+} depletion, stromal interaction molecule 1 (STIM1) senses the depletion and aggregates in the ER just below Orai1 on the plasma membrane [139]. Orai1 is an essential pore subunit of the calcium-release-activated calcium (CRAC) channel and is responsible for the influx of Ca^{2+} by SOCs [140].

An important mechanism of Ca^{2+} signaling is the release of Ca^{2+} from the ER reticulum through two distinct receptors, the ip3 receptor and the RyR. G protein-coupled receptors (GPCR) and receptor tyrosine kinases (RTK) are both located at the plasma membrane of eukaryotic cells and serve a primary function of transducing extracellular stimuli into intracellular signals. 2 specific subtypes (Gq/11) of GPCR have been shown to activate phospholipase Cβ while RTKs have been shown to activate

phospholipase Cγ. Both isoforms of phospholipase c (PLC) cleave phosphatidylinositol 4,5 biphosphate (PIP2) into ip3 and diacylglycerol. Ip3 binds to the ip3 receptor on the ER membrane and allows diffusion of Ca^{2+} from the ER to the cytosol. Calcium release from the ER has been shown to occur by periodic discharges of Ca^{2+} from the ER [141]. RyR are different from ip3 receptors as the primary agonist of RyRs is Ca^{2+} itself. When cytoplasmic levels of Ca^{2+} are determined to be low, RyRs are opened to allow efflux of Ca^{2+} from the ER. When cytoplasmic levels of Ca^{2+} are increased to high levels (>1mM) the channel is completely inhibited.

Like the ER, mitochondria can store Ca^{2+} but the mechanism in how the mitochondrion regulates the influx of Ca^{2+} is different. While Ca^{2+} diffuses through the uniporter into the outer mitochondrial membrane, it crosses into the inner mitochondrial membrane from ion exchange channels, where Na^{2+} and H^{+} created by oxidation of NADH are exchanged for Ca^{2+} ions. An increase in Ca^{2+} levels in the mitochondria stimulates several dehydrogenases in the Krebs cycle and boosts ATP production along with ROS formation. An increase in matrix Ca^{2+} also activates the mPT pore, which causes release of calcium back into the cytoplasm.

Calcium Interaction with Apoptosis and Autophagy

Ca^{2+} has long been shown to play a role in necrotic cell death. As discussed earlier, high concentrations of intracellular Ca^{2+} can overload the mitochondria, causing an increase in ROS, ATP depletion and mitochondrial dysfunction. Ca^{2+} has also been shown to activate proteases like calpains which induce necrotic cell death. In addition to playing a role in mediating cellular necrosis, Ca^{2+} has also been shown to play a role in interacting with proteins that mediate apoptotic and autophagic cell death. Early studies

showed that different concentrations of intracellular calcium can activate either apoptosis or necrosis. Lower levels of Ca^{2+} (200-400 nM) have been shown to trigger apoptosis while higher levels of Ca^{2+} (>1 μM) have been shown to induce necrosis [129]. The ip3 receptor has been shown to bind to Bcl-2 on the ER membrane, with Bcl-2 levels determining whether Ca^{2+} oscillations will lead to cell survival or cell death. Ca^{2+} has also been shown to be regulated by the proapoptotic proteins, Bax and Bak. Recent evidence has also shown the ability of Ca^{2+} to help regulate autophagy via ip3r forming a complex with beclin-1 on the ER.

Bcl-2 has been shown to localize to the ER membrane in addition to localizing to the mitochondria. Bcl-2 has been shown to directly interact with the ip3 receptor on the ER membrane and this interaction inhibits ip3 dependent calcium efflux [142]. Further analysis indicated that the BH4 domain of Bcl-2 associates with a region within domain s of the ip3r [143]. A result of this interaction is that ER-targeted Bcl-2 (Bcl-cb5) was able to inhibit apoptosis to agents that deplete the mitochondrial membrane like ceramide [144]. Bcl-2 has also been shown to bind to the Ca^{2+} dependent phosphatase calcineurin which has been shown to phosphorylate the ip3 receptor. It is speculated that bcl-2 facilitates dephosphorylation of ip3 receptor by interacting with calcineurin as ip3 receptor phosphorylation is decreased in Bcl-2 overexpressing cells [142]. Although Bcl-2 can inhibit ip3 induced calcium oscillations that promote apoptosis, it can also enhance ip3 induced Ca^{2+} oscillations that promote survival. In B cell lymphocytes, Bcl-2 enhances Ca^{2+} oscillations by sensitizing the cells to lower levels of ip3, which leads to increased mitochondria metabolism and cell survival [145].

Ca^{2+} is also shown to be regulated by proapoptotic Bcl-2 family members. Like Bcl-2, Bax and Bak have also been shown to localize to the ER membrane where they have been shown to have a role in Ca^{2+} release from the ER. When Bax/Bak is knocked out in cells, ER luminal Ca^{2+} levels are decreased compared to wild type cells. This decrease in ER calcium compromises ER Ca^{2+} release as well as mitochondrial uptake [146]. In another study, the use of a Bax inhibitor facilitated the release of Ca^{2+} from the ER, depleting the ER pool [147]. These studies infer Bax/Bak prevents Bcl-2 mediated leaking of Ca^{2+} from the ER. When Bax/Bak are overexpressed, however, they induce an increase in Ca^{2+} levels followed by cytochrome c release and apoptosis [148]. There is also evidence that other BH-3 only proteins, such as Bim and Noxa, may have a role in mediating Ca^{2+} function. T-cells deficient in Bim have been shown to have impaired Ca^{2+} release following activation, which is associated with increased binding of Bcl-2 to ip3 receptor on the ER membrane, indicating a role of Bim in enhancing Ca^{2+} release from the ER by sequestering Bcl-2 [149]. The mitochondrial targeting region of Noxa was shown to increase mitochondrial permeability and release Ca^{2+}, while a peptide developed to correspond to the same region was shown to initiate necrotic Ca^{2+} dependent cell death [150].

Ca^{2+} signaling also plays a role in regulating the induction of autophagy. Previous studies showed that Ca^{2+} was mobilized after stimulated with agents such as thapsagargin and ionomycin and that the Ca^{2+} mobilization induced autophagy. The intracellular calcium chelater BAPTA-AM was also shown to inhibit the aggregation of GFP-LC3 aggregates, indicating that autophagosome formation was autophagy dependent [151]. The ip3 receptor has also been shown to play a role in regulating

autophagy. Beclin-1 has also shown to be in a complex with Bcl-2 and ip3 receptor, with the disruption of this complex with the ip3 receptor inhibitor Xestospongin B sufficient for the induction of autophagy [152]. Knocking down of the ip3 receptor was also sufficient to induce conversion of LC3I to LC3II [153]. In addition to inhibiting the ip3 receptor, direct inhibition of ip3 by L-690,330 was enough to induce autophagy [154].

Multiple cytotoxic agents have been identified that function to disrupt Ca^{2+} homeostasis leading to cell death. One such drug is cisplatin, a DNA crosslinking drug used to treat several different kinds of cancer including MM. Cisplatin has been shown to cause an ip3 receptor-dependent increase in cystolic Ca^{2+} prior to induction of apoptosis. Knocking down of the ip3 receptor in cancer cell lines also mediates resistance to cisplatin induced cell death [155]. In MM, cisplatin is used in combination with dexamethasone and etoposide as an effective regimen to treat relapsed/refractory patients. Staurosporine, a protein kinase inhibitor, also promotes Ca^{2+} leak from the ER by the cleavage of ip3 receptor. Inhibiting cleavage of the ip3 receptor by transfection of mutant ip3 receptors in B cells lacking ip3 receptors was shown to inhibit apoptotic induction by staurosporine [156]. Staurosporine is a precursor to PKC412 which is in phase III trials for AML and exhibits activity in MM cells. Thapsigargin is another cytotoxic agent that decreases the ER calcium pool by directly inhibiting SERCA pumps. Thapsigargin has been studied in MM cells alongside bortezomib has they have both been such to cause ER stress and induce autophagy. Thapsigargin produced a synergistic effect in MM cells when used in combination with an inhibitor of autophagosome formation, 3-methyladenine (3-MA), while bortezomib showed an antagonistic effect

with 3-MA [124]. Bortezomib and thapsigargin also have a synergistic effect in inducing cell death in pancreatic cancer cell lines when used in combination [157].

Chapter 6: HYD1

Development of HYD1 in Prostate Cancer Cells

HYD1 was first identified as a peptide that could support tumor cell adhesion and inhibit tumor cell adhesion to immobilized ECM proteins. In order to identify peptides, they used a 'one-bead one-compound' combinatorial screening method. In this method, coupling cycles were used to attach amino acids to beads. Because each bead only encountered one amino acid at each coupling cycle, when the reaction was driven to completion only one distinct peptide was displayed on each bead [158]. Utilizing this approach, several L-amino acid containing peptides were selected based upon the ability of prostate tumor cells to bind to the immobilized peptide [159]. As D-amino acid containing peptides are able to resist being degraded by proteases, screening with a D-amino acid containing peptide library was also done. Following this screening, two peptides, RZ-3 and HYD1 (kikmviswkg), were discovered to be biologically active peptides that can themselves inhibit tumor cell adhesion to immobilized ECM proteins [160].

HYD1 and it's scrambled derivative HYD1s (wiksmkivkg) were further tested on their ability to be able to inhibit tumor cell motility on laminin-5. HYD1 was shown to block migration of prostate cancer cells on laminin-5 while HYD1s did not. HYD1 was also to inhibit adhesion to immobilized laminin-5 to the same extent as integrin blocking antibodies to α3, α6, and β1. It was also shown to interact with α6 and α3 integrin

subunits, but not α2 integrins in prostate cancer cells, while HYD1s did not interact with any of the integrins tested. Depletion of β1 integrin containing integrins from membrane lysates of DU-145 cells removed the ability for HYD1 to bind with the α6 integrin, indicating that the peptide interacts with the α6β1 dimer. Incubation with HYD1 also increased the activation of FAK and phosphorylation of MEK, with the greatest signal occurring at 15 minutes after incubation. Lastly, treatment with HYD1 was shown to display increased filamentous actin and an accumulation of actin at the cell membrane [161]. In a different report, alanine substitution analysis and a peptide deletion strategy were used to determine the minimal element of HYD1 necessary for bioactivity in a prostate cancer cell lines. Bioactivity was measured by assays of cell adhesion, migration and ERK signaling. The sequence of HYD1 necessary to support cell adhesion was kmvixw, the block to migration required xkmviswxx and activation of ERK signaling required ikmviswxx, where x is a placeholder peptide [162].

HYD1 activity in MM cells

As HYD1 was shown to block cell adhesion to laminin 5 in a β1 integrin dependent manner, studies were done to see if HYD1 could block adhesion of MM cells to the ECM protein, FN [163]. HYD1 indeed blocked adhesion of MM cells to FN at a concentration of 50 μg/ml. Similar inhibition of adhesion to FN was seen when MM cells were treated with a blocking α4 integrin antibody. In contrast, HYD1 did not block MM cell adhesion to bone marrow stromal cells, a finding that was consistent with a β1 blocking antibody, suggesting that multiple cell adhesion molecules may be necessary to regulate adhesion of MM cells to bone marrow stroma. Even though HYD1 did not block

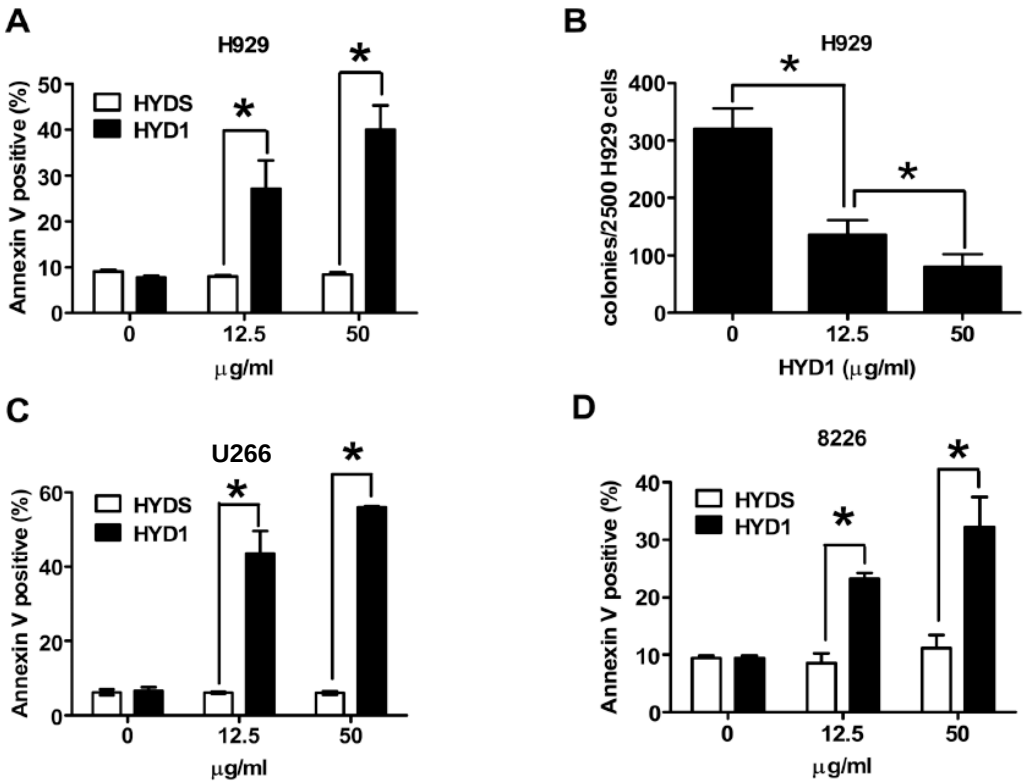

Figure 4: HYD1 induces cell death as a single agent in MM cells. (A,C,D) H929, U266 and 8226 cells were treated with varying concentrations of HYD1 for 6 hrs and Annexin V positivity was measured. (B) H929 cells were treated with HYD1 for 2 hrs and placed in soft agar for 12 days after which cell colonies were counted.

MM cell adhesion to bone marrow stroma cells, HYD1 treatment did reduce the level of resistance to melphalan in the bone marrow stroma co-culture model system. Upon testing HYD1 in the co-culture model system, an unanticipated observation was that HYD1 treatment induced cell death in suspension culture as a single agent. Furthermore, MM cells were not resistant to HYD1 treatment in the presence of bone marrow stroma cells.

Due to the finding that HYD1 induced equivalent cell death in MM cells as a single agent the mechanism of action of HYD1 induced cell death in suspension cultures

was investigated. MM cells were treated with 12.5 or 50 µg/ml of HYD1, or the scrambled peptide control HYDS, for 6 hours followed by measurement of annexin V positive cells, used as a marker for cell death. HYD1 treatment increased annexin V positive cell staining compared to cells treated with the scrambled variant HYDS in H929, 8226 and U266 cells. HYD1 also inhibited in a dose dependent manner the ability of H929 cells to form colonies in soft agar (figure 4).

In order to examine if HYD1-induced cell death was dependent on the apoptotic pathway involving caspases, the processing and activation of caspases was examined. 6 hours treatment with 50 µg/ml of HYD1 did not result in the activation of caspase-8 and only a minimal activation of caspase-3. Also, HYD1 treatment did not give rise to cleaved active form of caspase−3, −9 and −8 as shown by western blot analysis in H929 and 8226 cells (figure 5). It was next determined if HYD1 induced a latent induction of caspases. The pan caspase inhibitor zVAD-fmk was utilized to determine whether caspases contributed to HYD1 induced cell death following 24 hours of HYD1 treatment. Pretreatment of H929 cells with zVAD-fmk did not inhibit cell death induced by HYD1. In contrast, zVAD-fmk treatment blocked the majority of the melphalan-treated annexin V positive cells. These data were consistent with caspase activity assays which demonstrated that neither caspase 3 or 8 activity was induced following 24 hours of HYD1 treatment.

Endonuclease G (Endo G) and AIF have been reported to be released from the mitochondria in caspase independent manner. After mitochondrial damage, the

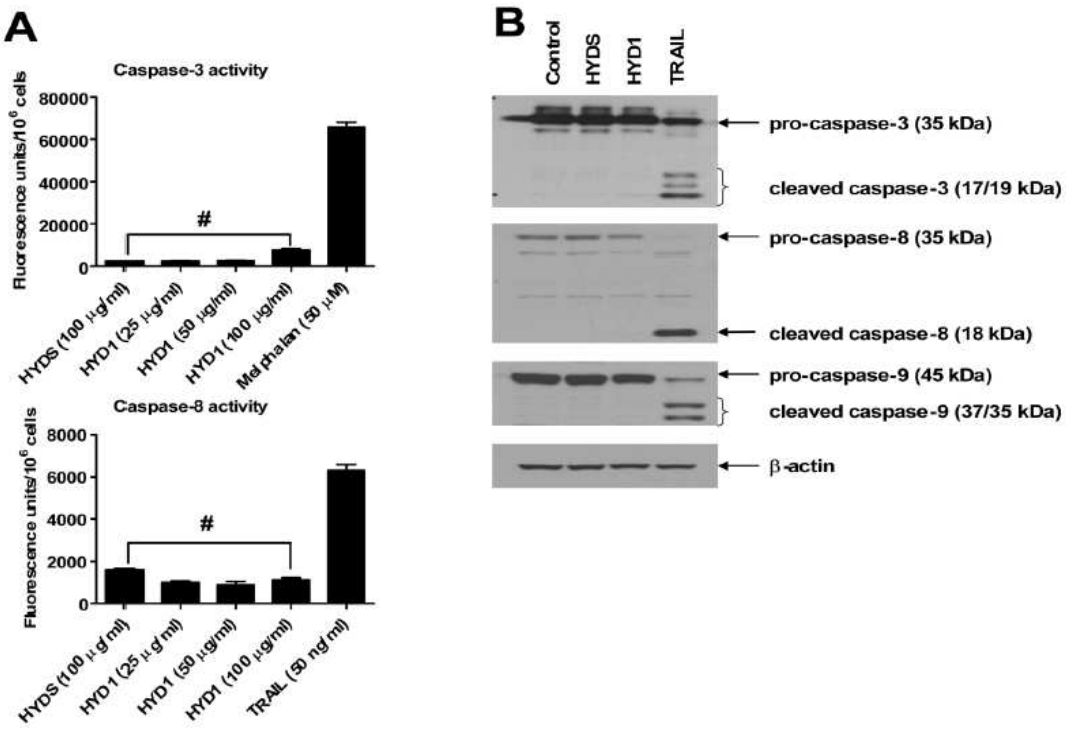

Figure 5: HYD1 did not induce apoptotic cell death. (A). H929 cells were treated with the indicated concentrations of drugs for 6 hrs before activated caspase-3 and caspase-8 were measured. (B). H929 cells were treated with 50 μg/ml of HYD1 and HYD1s or 50 ng/ml of TRAIL for 6 hrs and cleaved caspases were measured by western blot.

proapoptotic protein Bax is activated and functions in the formation of outer membrane mitochondrial pore, causing the release of AIF and Endo G from the mitochondria. This is followed by translocation of AIF and Endo G to the nucleus, leading to DNA fragmentation and nuclear condensation [164]. HYD1 treatment failed to increase the proportion of active Bax, as the levels were comparable to those seen in HYDS treated and control cells. There was also no translocation of AIF or Endo G from the cytoplasm to the nucleus after 6 hour treatment with HYD1. Finally, double-stranded DNA breaks resulting from the internucleasomal DNA cleavage by endonucleases (mediated

predominately by caspase activated DNAse, lysosomal DNAse II and Endo G) is an important biochemical marker for apoptotic cell death [165].TRAIL treatment lead to a significant increase in comet moments. However, HYD1, HYDS and control cells showed equivalent comet moments indicating the absence of activation of endonucleases and double stranded DNA breaks in HYD1 treated cells. Taken together, these data demonstrate that HYD1-induced cell death occurs independent of caspase and endonuclease activity. This data also indicates that HYD1 does not induce apoptosis in MM cells.

Electron microscopy of HYD1 treated cells showed that 4 hours treatment with HYD1 in H929 cells revealed the presence of several autophagosomes, observed as extensive double-membrane vacuolar structure containing cytoplasmic contents. Such autophagosomes were absent in HYDS treated cells. Another hallmark of autophagy is the lipidation of LC3 protein, which can be detected by western blot analysis [166]. Thus, western blot analysis was utilized to determine whether HYD1 treatment caused the conversion of cytoplasmic form of LC3 (LC3-I, 18 k Da) to the autophagosomal membrane-bound form of LC3 (LC3-II, 16 k Da). 4 hour treatment with HYD1 and tunicamycin, a known inducer of autophagy, resulted in increased conversion of LC3-I to LC3-II. HYD1 treatment also caused an increase in the number and size of acidic vesicles as shown by lysosensor staining.

Depending on the context, the induction of autophagy has been shown to be associated with cell survival or cell death. To determine whether autophagy induced by HYD1 plays a role in cell survival or cell death, the autophagic pathway was inhibited by two independent methods. siRNA targeting Beclin1, whose expression is required for the

formation of pre-autophagosomal structures, was used as well as a pharmacological approach using 3-methyladenine (3-MA), a nucleotide derivative and class III PI-3 kinase inhibitor shown to inhibit the earliest stages of autophagosome formation. Both strategies significantly sensitized H929 cells to HYD1-induced cell death, indicating that autophagy is an adaptive response and contributes to survival of MM cells following HYD1 treatment. There is a mutual crosstalk between autophagy and apoptosis. It has been reported that certain stimuli can induce cells to undergo autophagic cell death, and upon inhibition of autophagy, under the same stimuli the cells revert to apoptotic cell death [167]. To determine whether the increase in cell death observed upon HYD1 treatment under the inhibition of autophagy was due to a switch to apoptotic cell death, cells were pretreated with 3-MA followed by HYD1 and then examined for cleaved caspase−3, −8 and −9 in cell lysates by western blot analysis. Neither 3-MA, HYD1 alone nor their combination caused cleavage of caspases. These results suggest that the inhibition of HYD1-induced autophagy does not sensitize MM cells to undergo caspase-dependent cell death (figure 6).

Major bioenergetic markers associated with necrotic cell death are the loss of mitochondrial membrane potential ($\Delta\psi_m$) accompanied by loss of total ATP and a rise in ROS production in cells. It was determined that HYD1 (50 μg/ml) treatment caused a significant loss of $\Delta\psi_m$ in H929 and 8226 cells and a 62% decrease in ATP levels. Additionally, HYD1 treatment resulted in a significant increase in ROS production when compared to control cells. All these events occurred rapidly during treatment with HYD1, suggesting that in MM cells HYD1 induces cell death through the necrotic cell death pathway.

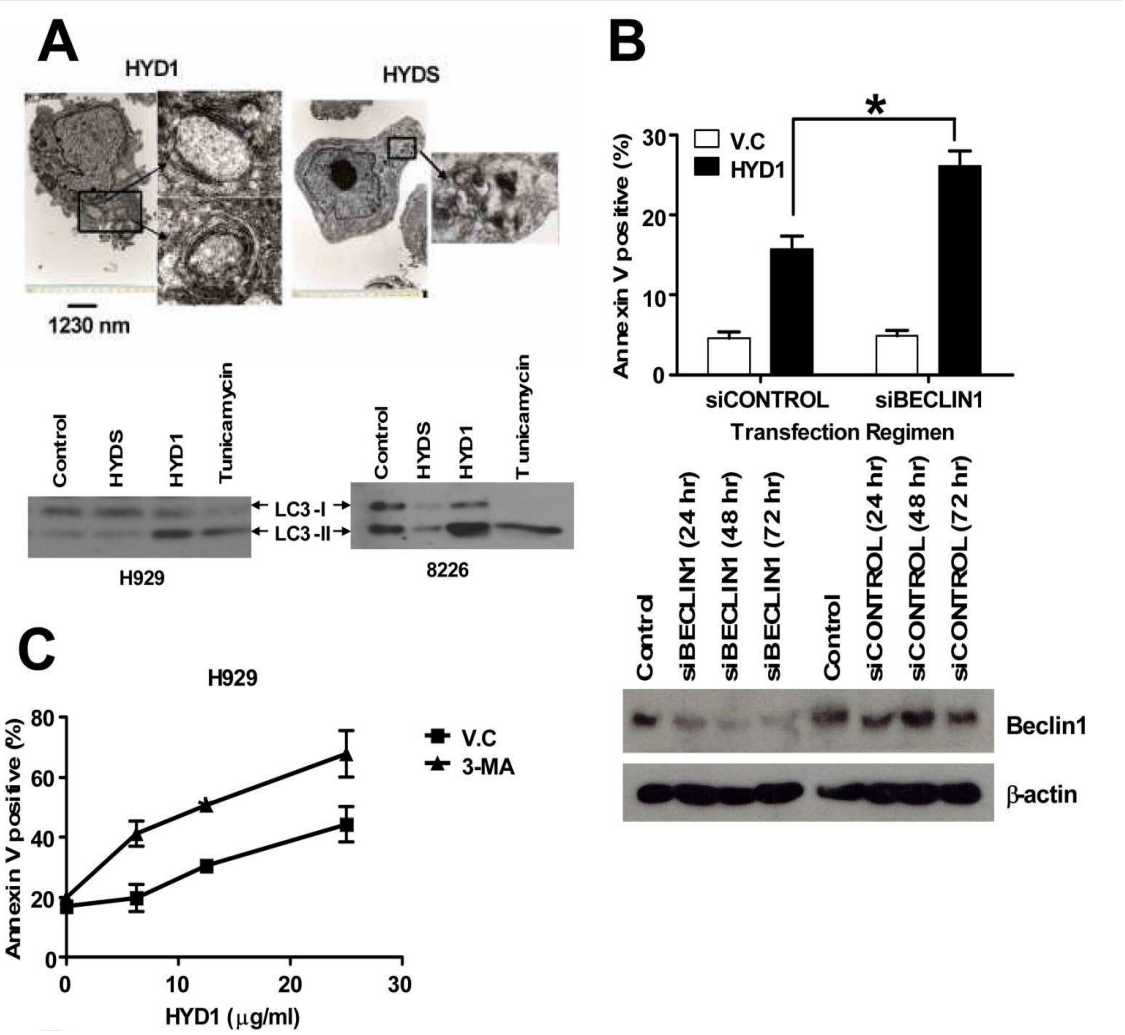

Figure 6: HYD1 induces autophagy which had a cytoprotective effect in MM cells. (A) H929 cells were treated with either 50 μg/ml HYD1 or HYDS or 100 μM tunicamycin for 4 hrs and then processed for electron microscopy or LC3-1 to LC3-II conversion. (B) H929 cells where transfected with a pool of 4 siRNA, targeting Beclin1 (siBECLIN1) or a control off Target siRNA (siCONTROL) using electroporation. 72 hrs post-transfection the cells where treated for 6 hrs with HYD1 (50 μg/ml) and cell death was determined by FACS analysis. (C) H929 cells were pretreated with 3-MA (10 mM) for 45 min before the addition of varying concentrations of HYD1. Cell death was determined by FACS analysis of annexin V positive cells after 6 hours of treatment.

ROS has been shown to be an important mediator involved in propagation and execution of necrotic cell death (figure 7).

To investigate whether an increase in ROS is the cause of cell death in HYD1 treated cells, cells were pretreated with 10 mM N-acetyl-cysteine (NAC), a thiol containing free radical scavenger. NAC partially protects H929 from HYD1 induced cell death. At the highest HYD1 concentration, NAC protected cells from death by 32% in H929 and U266 cells when compared to cells treated with HYD1 only. These data indicate that ROS plays an important role in inducing necrotic cell death in HYD1 treated MM cells.

As discussed earlier, mitochondria are considered the major organelle capable of generating ROS within cells. In order to determine whether ROS was the cause or the product of loss of $\Delta\psi_m$, cells were pretreated with NAC followed by treatment with HYD1. Loss in $\Delta\psi_m$ was not reversed by pretreatment with NAC, indicating that ROS production lies downstream of disruption of $\Delta\psi_m$.

Finally, oxidative stress has been shown to induce autophagy. In order to investigate whether autophagy observed in HYD1-treated cells was due to the induction of ROS, cells were pretreated with NAC followed by HYD1 treatment. HYD1 caused a substantial increase in LC3-II formation when compared to control cells. The increase in LC3-II was completely reversed by pretreating cells with NAC. Moreover, the addition of NAC reversed basal levels of LC3-II, suggesting that autophagy is driven by endogenous ROS levels in MM cells and may be a general mechanism whereby cancer cells can tolerate high basal levels of ROS typically associated with transformation. Taken

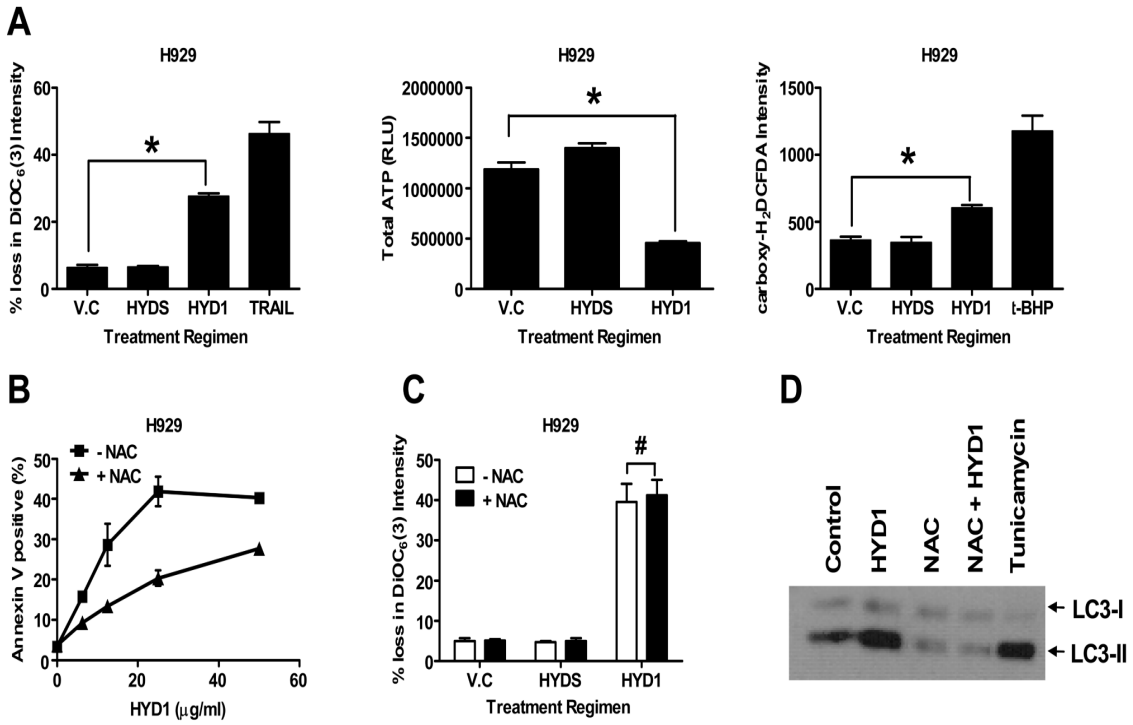

Figure 7: HYD1 induces necrotic cell death in MM cells. (A) H929 cells were treated for 2 hrs with HYD1 (50 µg/ml). Following treatment cells were analyzed for loss of $\Delta\psi_m$, loss of total cellular ATP and increase in ROS production. (B) H929 cells were pretreated with NAC (10 mM) for 30 min followed by addition of varying concentrations of HYD1 for 6 hrs followed by cell death analysis. (C) H929 cells were pretreated with NAC (10 mM) for 30 min before addition of HYD1 (50 µg/ml) for an additional 4 hrs. Following treatment cells were analyzed for loss in $\Delta\psi_{m.}$ (D) H929 cells (4×10^5 cells/ml) were pretreated with NAC (10 mM) for 30 min before the addition of HYD-1 (50 µg/ml) for an additional 4 hrs. Following treatment, the LC3-1 to LC3-II conversion was monitored by western blot analysis.

together, these data show that HYD1 induces ROS downstream of disruption of mitochondria membrane potential. Additionally HYD1 induction of ROS can paradoxically contribute to both cell survival by inducing autophagy and cell death by inducing necrosis in MM cells.

A colony forming assay was used to determine whether HYD1 induced cell death in normal hematopoietic cells. HYD1 did not inhibit colony formation of normal $CD34^+$

cells. Six hours treatment with increasing concentration of HYD1 did not induce cell death up to doses of 50 µg/ml in PBMC. Finally, the SCID-hu model was used to determine whether HYD1 demonstrates anti-tumor activity *in vivo*. The SCID-hu model consists of implanting human fetal bone into the mammary mouse fat pad of SCID mice. Mice treated with HYD1 showed a modest but significant reduction in tumor burden compared to control mice (figure 8). In these experiments no overt toxicity or weight loss was noted in HYD1 treated animals. Based on these results further studies are warranted to determine the upstream targets causative for HYD1 induced depolarization of the mitochondria membrane potential.

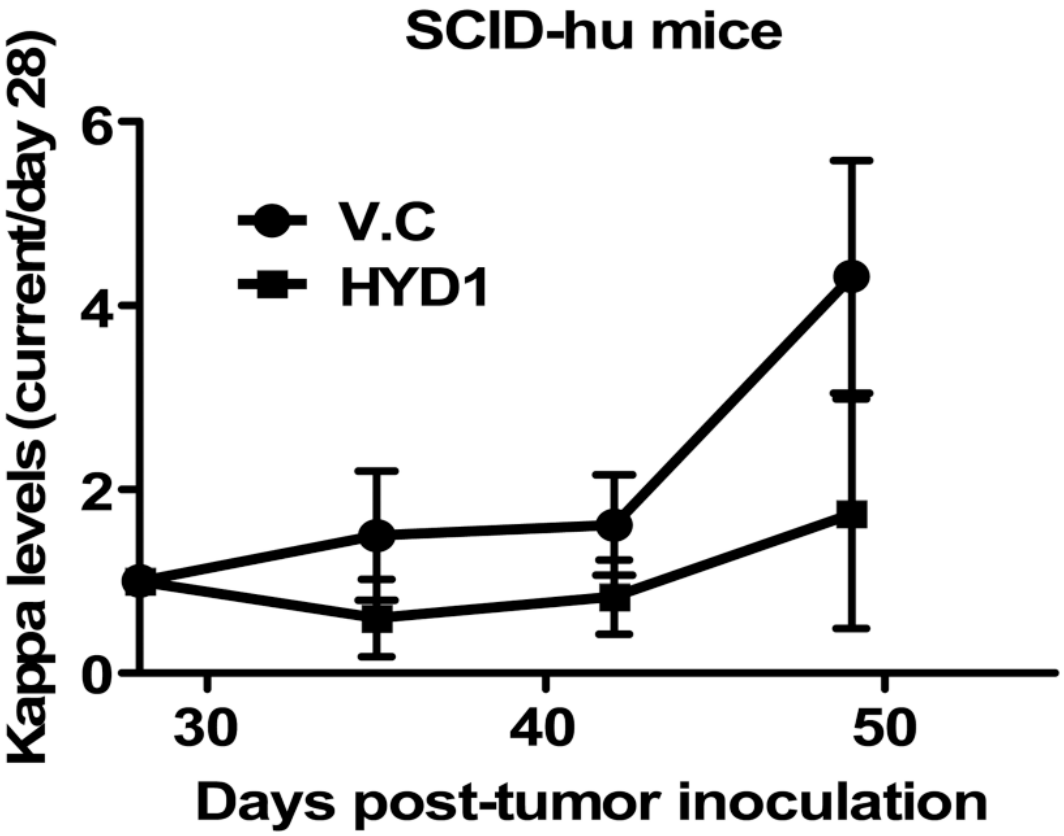

Figure 8: HYD1 displayed *in vivo* activity in the SCID-hu mouse model. Tumor burden in the SCID-Hu model was measured by quantification of circulating kappa levels using ELISA. On day 28 (before drug treatment) measurements were recorded for each individual mouse and subsequent values obtained weekly are represented as a ratio of day 28 (day X/day28). HYD1 was administered i.p. at 8 mg/kg daily for 21 days (starting day 28^{th}). n=5 for vehicle control (VC) and 4 for HYD1 treated mice ($P<0.05$, ANOVA).

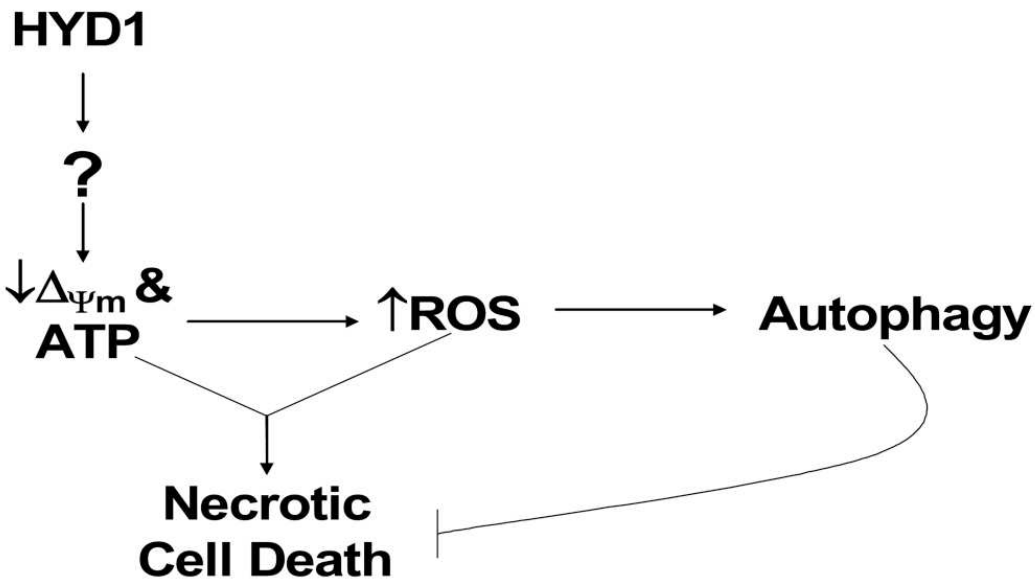

Figure 9: Proposed mechanism of HYD1 induced cell death. HYD1 induces mitochondrial dysfunction and a subsequent increase in ROS. The increase in ROS leads to the induction of autophagy which results in cell survival or the induction of necrotic cell death.

Chapter 7: Objectives

Even though MM is a treatable disease, it is still deemed to be incurable. Novel therapeutics, such as bortezomib, thalidomide and lenalidomide, have been shown to prolong intervals of progression free disease and patient survival, but MM patients ultimately relapse. Because MM develops resistance to treatment strategies, researchers have invested considerable amounts of effort into delineating the mechanisms by which multiple myeloma cells develop resistance. One mechanism in which myeloma cells develop resistance is via cell adhesion to bone marrow stroma cells and ECM proteins which is mediated by β1 integrin. Our laboratory has previously investigating the effects of blocking the integrin interaction with the ECM using a β1 inhibitory peptide (HYD1). In addition to blocking the adhesion of MM cells to bound FN, HYD1 was also unexpectedly shown to have a cytotoxic effect as a single agent *in vitro* and *in vivo*. HYD1 induced cell death displayed the same hallmarks as programmed necrosis; increased loss of mitochondrial membrane potential, ROS generation and ATP depletion. The primary goal of this project was to further delineate the mechanism of action that causes HYD1 induced cell death in myeloma cells. To further characterize the mechanism of HYD1 induced cell death an isogenic HYD1 resistant variant (H929-60) was developed. Gene expression profiling (GEP) was used as an unbiased approach to identify changes that may contribute to HYD1 resistance during the development of H929-60 cells. After analysis of the GEP data, expression of integrins was determined to

be significantly changed in H929-60 cells. Expression of key genes that induce Ca^{2+} release from ER stores was also changed. H929-60 cells also showed decreased surface expression of α4 and β1 integrin and displayed decreased adhesion to fibronectin. After analysis of the preliminary data the following hypothesis was proposed:

HYD1 binds the α4β1 integrin receptor in MM cells and leads to Ca^{2+} mediated necrotic cell death.

In order to refute or support this hypothesis, the following objectives were formulated:

1. Determine if a loss of integrin expression is causative for resistance to HYD1 induced cell death.
2. Determine if changes in intracellular Ca^{2+} levels effect HYD1 induced cell death.
3. Determine if blocking pathways that lead to cell survival, like autophagy, potentiates HYD1 induced cell death *ex vivo* and *in vivo*.

Chapter 8: Materials and Methods:

Cell Culture:

NCI-H929, RPMI-8226 and HS-5 cells were obtained from the American Type Culture Collection (Rockfield, MD). 293FT cells were obtained from Invitrogen and grown in Iscove's DMEM (Cellgro, VA) supplemented with 10 % FBS. Normal bone marrow aspirate was purchased from Lonza, Inc (Allentown, NJ). Mesenchymal stroma cells (MSC) were generated by plastic adherence of the bone marrow aspirate. MSC were confirmed by CD105, Stro-1, CD29 and CD73 positivity and CD34, CD33 and CD45 negativity (data not shown). MSCs were grown in MEMα/GlutaMAX^{TM} supplemented with 10% fetal bovine serum-qualified (FBS-Q) and 1% 100x penicillin-streptomycin-glutamine (Invitrogen). 5TGM1 myeloma cells were derived from murine myeloma 5T33.

Chemical Reagents, Antibodies, and Peptides:

5-Chloromethylfluorescein diacetate was purchased from Invitrogen (Carlsbad CA). Melphalan, bortezomib, and N-acetyl-L-cysteine were purchased from Sigma-Aldrich (St. Louis MO). Anti-α4 integrin (clone P4G9) antibody was purchased from Abcam (San Francisco CA). Anti-CD29 (4B7R) antibody was purchased from Novus Biologicals (Littleton, CO). FITC-conjugated anti-integrin β7 (FIB504) was purchased from Biolegend (San Diego CA). HYD1 (kikmviswkg) was synthesized by Bachem (San

Diego CA) and FAM conjugated HYD1 (FAM-kikmviswkg) were synthesized by Global Peptides (Fort Collins, CO).

Selection of a Drug-resistant Cell Line:

A HYD1 resistant cell line was developed as tool for delineating determinants of resistance and sensitivity to HYD1 induced cell death. NCI-H929 cells were exposed to increasing concentrations of HYD1 for 24 weeks. From weeks 1-8, cells were exposed to 10 μg/ml of HYD1 once a week for 24 hours. From weeks 9-16, cells were exposed to 20 μg/ml of HYD1 once a week for 24 hours. From weeks 17-24, cells were exposed to 30 μg/ml of HYD1 once a week for 24 hours. After week 24, the cells were exposed and maintained in media containing 60 μg/ml HYD1 and subsequently named H929-60 cells.

Cell Death Analysis:

After treatment with HYD1, cells were washed with PBS and incubated with 2 nM TO-PRO-3 iodide for 45 minutes. The cells were analyzed for fluorescence with the use of a FACSCalibur instrument (BD Biosciences, San Jose, CA).

Measurement of Δψm:

After treatment, cells were incubated for 15 minutes with 15 nM of 3,3'-dihexyloxacarbocyanine iodide (Invitrogen). Cells were washed and resuspended in PBS, and the loss of mitochondrial membrane potential was measured using FACScan.

ATP Measurement:

Treated cells were lysed in radioimmunoprecipitation assay buffer (Millipore, Billerica, MD), and ATP concentrations were measured using the ENLITEN ATP bioluminescence detection kit per manufacturer's instructions (Promega, Madison, WI). Samples were later normalized to the protein content of the lysates.

Confocal Microscopy:

To assess whether (a) HYD1 bound the cell surface and (b) whether binding of HYD1 was reduced in the resistant cell line FAM-HYD1 was used to image peptide binding in the parental and resistant cell line by confocal microscopy. A 35 mm glass bottom microwell dishes (Mattek cultureware, Ashland, MA) were plated with 10 µL Cell-tak (BD biosciences) per manufacturer's instructions. Media containing 1 µM Alexa Fluor 594 wheat germ agglutinin (WGA) (Invitrogen) and 20 µM Hoechst 33342 (Invitrogen) was placed back in the plates and the samples were incubated for 30 minutes. After 30 minutes, the cells were washed and treated with media containing 6.25 µg/ml FAM conjugated HYD1 for 10 minutes. Samples were immediately viewed with a Leica DMI6000 confocal microscope (Leica Microsystems, Germany). Gain, offset, and pinhole setting were identical for all samples within the treatment group.

Gene Expression Profiling:

One hundred nanograms of total RNA was isolated by a RNeasy mini kit (Qiagen) and served as the mRNA source for microarray analysis. The poly(A) RNA was specifically converted to cDNA and then amplified and labeled with biotin using the Ambion Message Amp Premier RNA Amplification Kit (Life Technologies, Grand Island, NY) following the manufacturer's protocol. Hybridization with the biotin-labeled RNA, staining, and scanning of the chips followed the prescribed procedure outlined in the Affymetrix technical manual. The oligonucleotide probe arrays used were the Human Genome U133 Plus 2.0 Arrays. This array contains over 54,000 probe sets representing over 47,000 transcripts that were designed from GenBank, dbEST, and RefSeq sequences

that were clustered based on builds 133 and 159 of the UniGene database. Each gene is represented by a series of oligonucleotides that are identical to the sequence in the gene as well as oligonucleotides that contain a homomeric (base transversion) mismatch at the central base position of the oligomer, which is used to measure cross-hybridization.

Scanned output files were visually inspected for hybridization artifacts and then analyzed using Affymetrix GeneChip Operating Software (GCOS) using the MAS 5.0 algorithm. Signal intensity was scaled to an average intensity of 500 prior to comparison analysis. Using the default settings, the GCOS software identifies the increased and decreased genes between any two samples with a statistical algorithm that assesses the behavior of 11 different oligonucleotide probes designed to detect the same gene (3). Probe sets that yielded a change *p*-value less than 0.002 were identified as changed (increased or decreased) and those that yielded a *p*-value between 0.002 and 0.002667 were identified as marginally changed. A gene was identified as consistently changed if it was identified as changed in all 3 replicate experiments performed by the software.

Surface Expression of Integrins:

To determine cell surface expression of integrins**,** cells were treated with a primary antibody for 45 minutes on ice. Cells were then washed and treated with a FITC conjugated secondary antibody for 45 minutes on ice. Cells were washed again and the fluorescence analyzed using a FACScan (BD Biosciences).

Cell adhesion to ECM proteins and Stroma:

Cell adhesion assays were performed to determine whether the resistant cell line demonstrated reduced adhesive capacity. Briefly, cells were pre-incubated with various

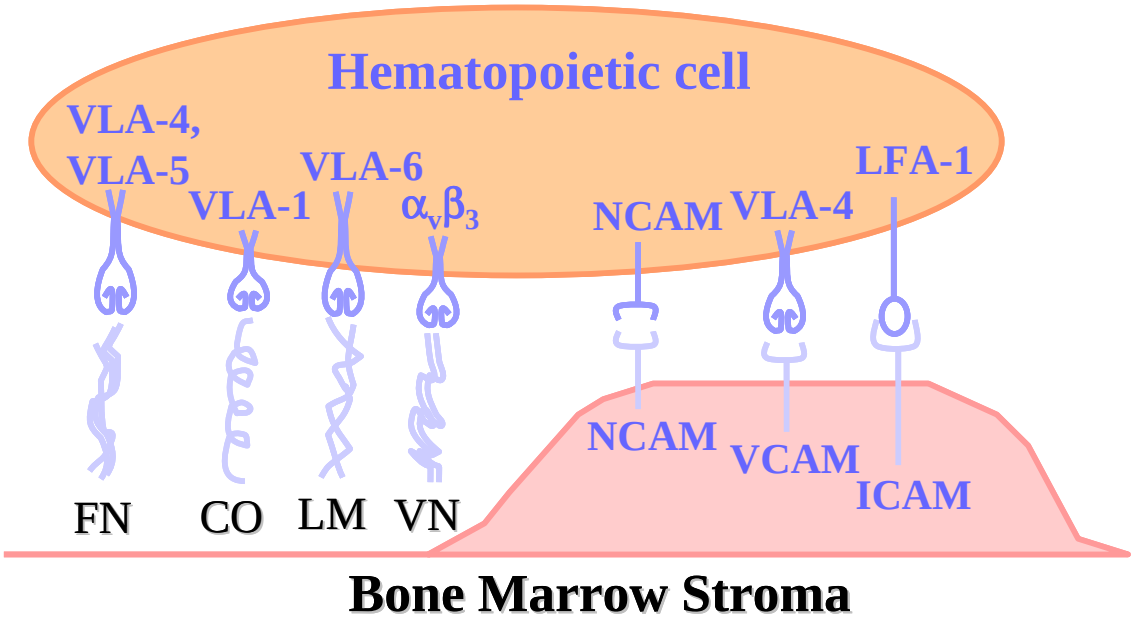

Figure 10: Hematopoietic cells can adhere to BMSCs and ECM proteins by various receptors. For adhesion assays, MM cells were allowed to attach to FN, VCAM-1 or HS-5 stromal cells for 2 hours. After 2 hours, unadhered cells were removed and cell adhesion was read using a fluorescence plate reader.

antibodies for 30 minutes. Cells were then allowed to attach to 50 µL of 40 µg/mL FN (Roche, Indianapolis, IN) or 10 µg/mL VCAM-1(Fisher Scientific, Pittsburgh, PA) for two hours. After 2 hours, cell adhesion was detected by crystal violet staining as previously described [168].

For stromal adhesion, 10,000 HS-5 or MSC cells were incubated overnight on immunosorb 96 well plates (Nunc, Denmark). H929 and H929-60 cells were incubated with 1uM of chloromethylfluorescein diacetate, or CMFDA (Invitrogen) for 30 minutes, washed and incubated for 45 minutes to allow unbound dye to diffuse out of the cells. Intensity was read on a fluorescence plate reader[169].

Reverse transcriptase Polymerase Chain Reaction (Rt-PCR):

Rt-PCR was used to determine whether the decrease in α4 integrin protein levels in the resistant cell line was due to decreased transcription. RNA was extracted from log growth cells with RNeasy columns (Qiagen, Valencia, CA) per manufacturer's instructions. First–strand cDNA synthesis was carried out with the Quantitect Probe RT-PCR kit (Qiagen, Valencia, Ca) per manufacturer's instructions. Real time PCR primers for alpha 4 integrin were obtained from Applied Biosystems (Carlsbad, Ca). The gene-expression level was normalized using the endogenous control gene GAPDH. Real-time PCR reactions were performed using ABI 7900 Sequence Detection System (Applied Biosystems).

Transfection of shRNAs:

ShRNA targeting strategies were used to determine whether α4 integrin expression was causally related to HYD1 induced cell death. α4 (TRCN0000029656) and β1 (TRCN0000029645) shRNA and non-silencing clone sets were purchased from Open Biosystems, Huntsville, AL and transfected into a lentivirus using the BLOCK-IT Lentiviral Pol II miR RNAi expression system (Invitrogen). After the viral supernatant was collected, 500,000 myeloma cells were infected with a 250 µL viral supernatant/750 µL media solution and 5 µg/mL polybrene (Sigma) for 24 hours. After 24 hours, the solution was removed and replaced with fresh media. At 72 hours of infection, 1µg/mL puromycin (Invitrogen) was added to 8226 cells to allow for the selection of a stable population of cells. For the H929 cell line, transient infections were used to reduce integrin expression.

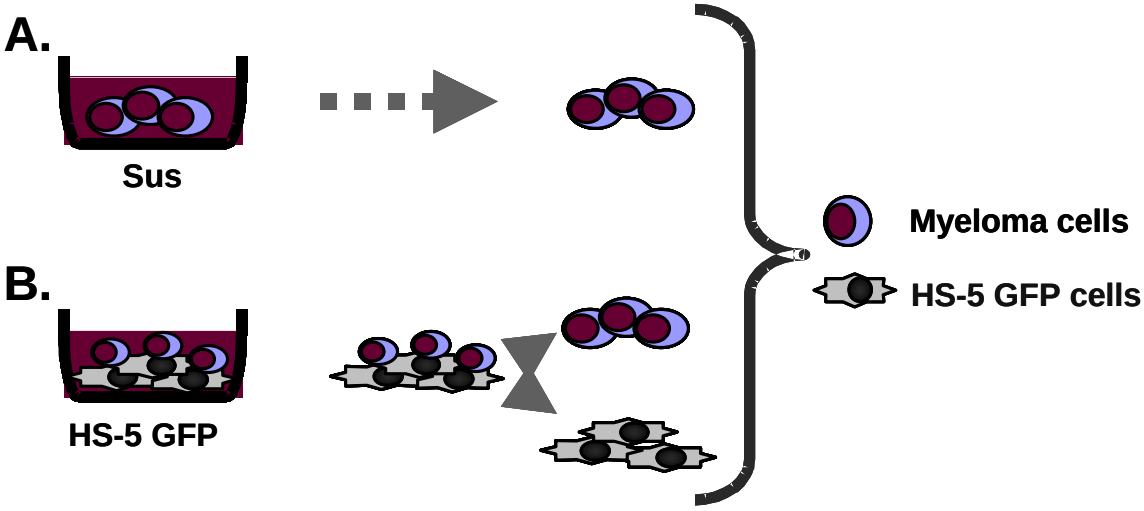

Figure 11: The coculture model is used to determine EM-DR of MM cells in the presence of stromal cells. MM cells are incubated in the presence or absence of HS-5 GFP stromal cells for 24 hours. After 24 hours, cells are treated with melphalan or bortezomib for 24 hours. After treatment, MM cells are unattached to stromal cells using Cellstripper and cell death is measured using a FACSCalibur instrument

Biotin-HYD1 pull-down assay:

To identify HYD1 interacting proteins biotin conjugated HYD1 was used as bait as previously described [170]. Briefly, 100 million H929 or the resistant variant H929-60 were washed once in PBS and then in alkaline phosphatase (ALP) buffer. Samples were spun at 15000xg for minutes at 4 degrees and the supernatant was removed and membranes were pelleted at 100,000xg for 15 minutes. Membrane pellets were solubilized in AP buffer containing 0.2% NP40 and protein was quantified using BCA reagents (Pierce, Rockford, IL). Five hundred μg of Biotin-HYD1 was bound to 30 μL of Ultra Link Neutral Avid in Plus beads (Pierce) for one hour in a buffer containing 0.5 mM Bcl, 0.3 mM KH_2PO4, 27.6 mM Nail and 1,6 mM Na_2HPO_4, pH 7.4. After one hour, the beads were washed twice in AP buffer and 50 μg of membrane extracts were

added to a total volume of 500 μL and incubated with beads overnight at 4 degrees. The beads were washed five times in AP buffer containing 0.2% NP40 and samples were suspended in SDS-PAGE sample buffer and bound proteins were resolved by SDS-PAGE.

Isolation of CD138 positive and negative populations derived from MM specimens:

To determine whether HYD1 was active in primary patient specimens 7 newly diagnosed and 7 relapsed specimens were obtained. Myeloma patients were consented through the Total Cancer Care tissue banking protocol per IRB regulations. Mononuclear cells were separated from human blood through the use of Ficoll-Paque PLUS (GE Healthcare, UK). After separation, CD 138 positive cells were sorted using 25 MS MACS Separation Columns (Miltenyi Biotec, Germany) and CD 138 microbeads (Miltenyi) per manufacturer's instructions. For each specimen obtained α4 integrin surface expression was determined by FACS analysis and HYD1 induced cell death was determined by Topro-3 staining and FACS analysis in the CD138 positive and negative fraction.

Measurement of Intracellular Ca^{2+}Concentrations:

Intracellular free-calcium was measured using the Ca2+ sensitive dye, fura-2. 35 mm glass bottom microwell dishes (Mattek cultureware, Ashland, MA) were plated with 10 μL Cell-tak (BD biosciences) per manufacture's instructions. Fura-2 loading was carried out incubating the plated cells for 1 hour at room temperature in either physiological saline solution (PSS) consisting of (in mM): 140 NaCl, 3 KCl, 2.5 CaCl2, 1.2 MgCl2, 7.7 glucose and 10 HEPES (pH to 7.2 with NaOH), which also contained 1 μM of the membrane permeable ester form of fura-2, acetoxymethylester (fura-2 AM)

and 0.1% dimethyl sulfoxide (DMSO) or in PSS which did not contain $CaCl_2$. All drugs were bath applied in PSS.

A DG-4 high speed wavelength switcher (Sutter Instruments Co., Novato, CA) was used to apply alternating excitation with 340- and 380-nm UV light. Fluorescent emission at 510 nm was captured using a Sensicam digital CCD camera (Cooke Corp., Auburn Hills, MI) and recorded with Slidebook Version 3.0 software (Intelligent Imaging Innovations, Denver, CO). Changes in $[Ca^{2+}]_i$ were calculated using the Slidebook 3 software (Intelligent Imaging Innovations, Denver, CO) from the intensity of the emitted fluorescence following excitation with 340- and 380-nm light, respectively, using the equation, $[\mathrm{Ca}^{2+}]_i = K_d Q(R - R_{\min})/(R_{\max} - R)$ where R represents the fluorescence intensity ratio (F_{340}/F_{380}) as determined during experiments, Q is the ratio of $F_{\min}$ to $F_{\max}$ at 380 nm, and K_d is the Ca^{2+} dissociation constant for fura-2. Calibration of the system was performed using a fura-2 calcium imaging calibration kit (Molecular Probes, Inc., Eugene, OR) and values were determined to be as follows: $F_{\min}/F_{\max}$ = 23.04; $R_{\min}$ = 0.31; $R_{\max}$ = 8.87.

Murine 5TGM1 Myeloma Model:

Animal studies were conducted using 6- to 8-week-old female C57BL/KaLwRijHsd mice (Harlan) in accordance with the NIH Guide for the Care and Use of Laboratory Animals. C57BL/KaLwRijHsd mice are used as the murine MM cell line 5TGM1 was established from these mice. 5TGM1 cells were induced in mice by i.v. inoculation through tail veins. Establishment of myeloma tumor in inoculated mice was followed by assaying immunoglobulin G2b (IgG2b) monoclonal paraprotein in sera prepared from whole blood obtained by sub-mandibular bleed. Mouse IgG2b levels were

assayed by ELISA (Bethyl Laboratories, Montgomery, Texas) on days 7,14,21, and 28 per manufacturer's instructions.

On day 10 after inoculation, the mice are treated with indicated doses of treatment: 10 mg/kg and 25 mg/kg for cHYD1, 0.5 mg/kg for bortezomib, and 10 mg/kg for chloroquine. Mice are treated 3 times weekly on Monday, Wednesday and Friday for 21 days for a total of nine treatments. For the chloroquine studies, mice were treated with 10 mg/kg chloroquine on days 9, 16, and 23 while mice were treated with 10 mg/kg HM-27 on days 10, 13, 15, 17, 20, 22, 24, 27 and 29.Following treatment, mice are examined until they need to be euthanized. Euthanization occurs when mice display hind leg paralysis or tumors grow in excess of 2 cm in diameter. On day 100, all remaining mice are euthanized.

Statistical Analysis:

For microarray data using the Mas 5.0 platform, significant genes were determined by comparing changes in expression across 3 individual experiments. If expression levels were increased across all 3 experiments or decreased in each experiment the gene was deemed to be significant. For microarray data using RMA, genes that were increased or decreased 2 fold between the two cells lines were determined to be significant. For all other experiments, either a student's t-test or analysis of variance (ANOVA) test were used as indicated by each figure legend.

Chapter 9: Results

H929-60 cells are resistant to HYD1 induced cell death but do not show cross-resistance to other active myeloma agents:

To identify determinants of resistance towards HYD1, we developed an isogenic resistant H929 cell line variant by chronically exposing H929 cells to increasing concentrations of HYD1 until a drug resistant variant emerged. As shown in figure 10, the H929-60 cell line is significantly resistant to HYD1 induced cell death ($p<0.05$ ANOVA) when compared to the parental H929 cells as measured by TOP-RO 3 positivity and FACS analysis. HYD1 induced cell death was previously characterized by the loss of mitochondrial membrane potential, ATP depletion, and an increase in reactive oxygen species (ROS). To determine whether the acquisition of resistance occurred upstream or downstream of mitochondria dysfunction the mitochondria membrane potential, ATP levels and ROS levels were compared following HYD1 treatment in the resistant (H929-60) and sensitive parental cell line (H929). H929-60 cells were shown to be resistant to the loss of mitochondrial membrane potential (figure 11) and failed to show a reduction in ATP levels following HYD1 treatment (figure 12). Finally ROS levels were reduced following HYD1 treatment in the resistant cell line compared to the parental cell line (figure 13). We utilized a FAM conjugated HYD1 peptide to determine whether the H929 resistant variant demonstrated a reduction in binding of FAM-HYD1 to

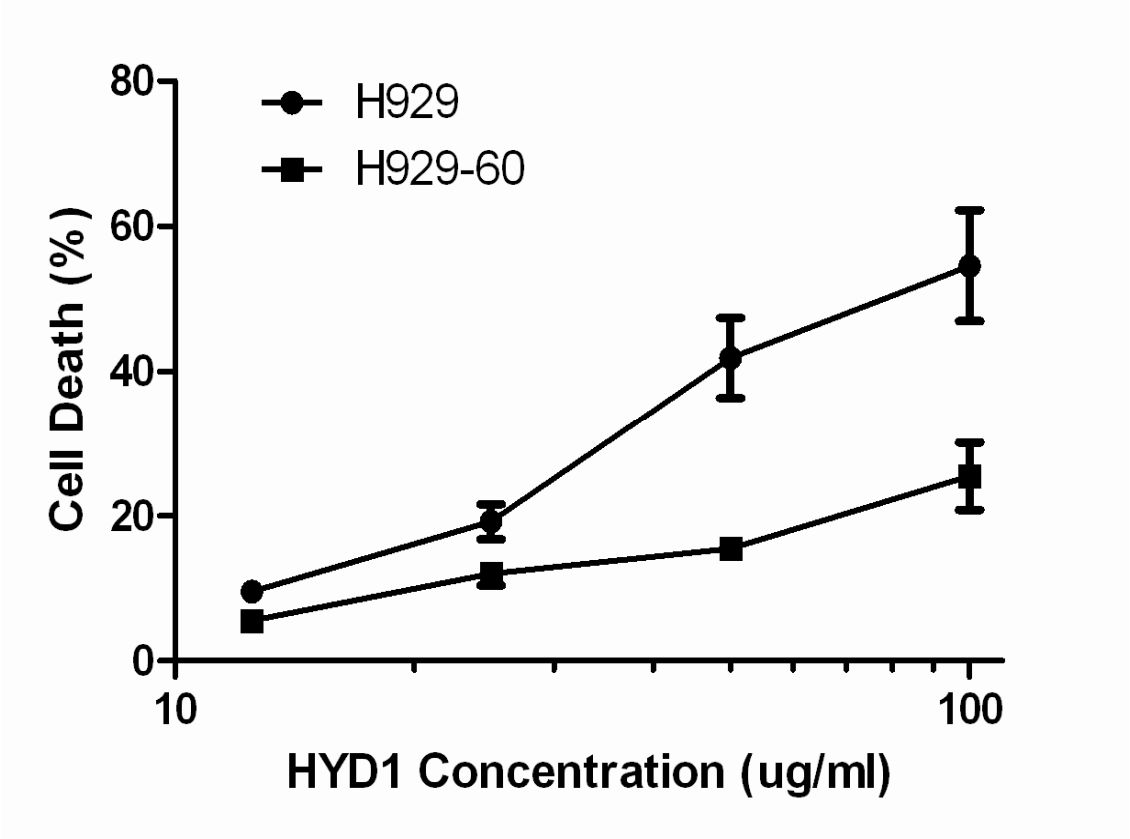

Figure 12: H929-60 cells are resistant to HYD1 induced cell death. H929 and H929-60 cells were incubated with varying concentrations of HYD1 for 6 hours and HYD1 induced cell death was determined by Topro-3 staining and FACS analysis (ANOVA test $p<0.05$ $n=9$). The experiment was repeated 3 independent times and a representative experiment is shown.

the cell membrane As shown in figure 14, FAM-HYD1 localizes to the plasma membrane in the parental cell line. Furthermore, the localization of FAM-HYD1 was not evenly distributed across the cell membrane, but rather FAM-HYD1 demonstrated punctuated staining in the parental cell line, suggesting potential clustering of the binding target. H929-60 cells treated with 6.25 μg/ml FAM-HYD1 demonstrated a 2.7-fold reduction in FAM-HYD1 binding relative to the parental cell line as determined by FACS analysis (data not shown). Collectively, these data indicate that the mechanism causative for

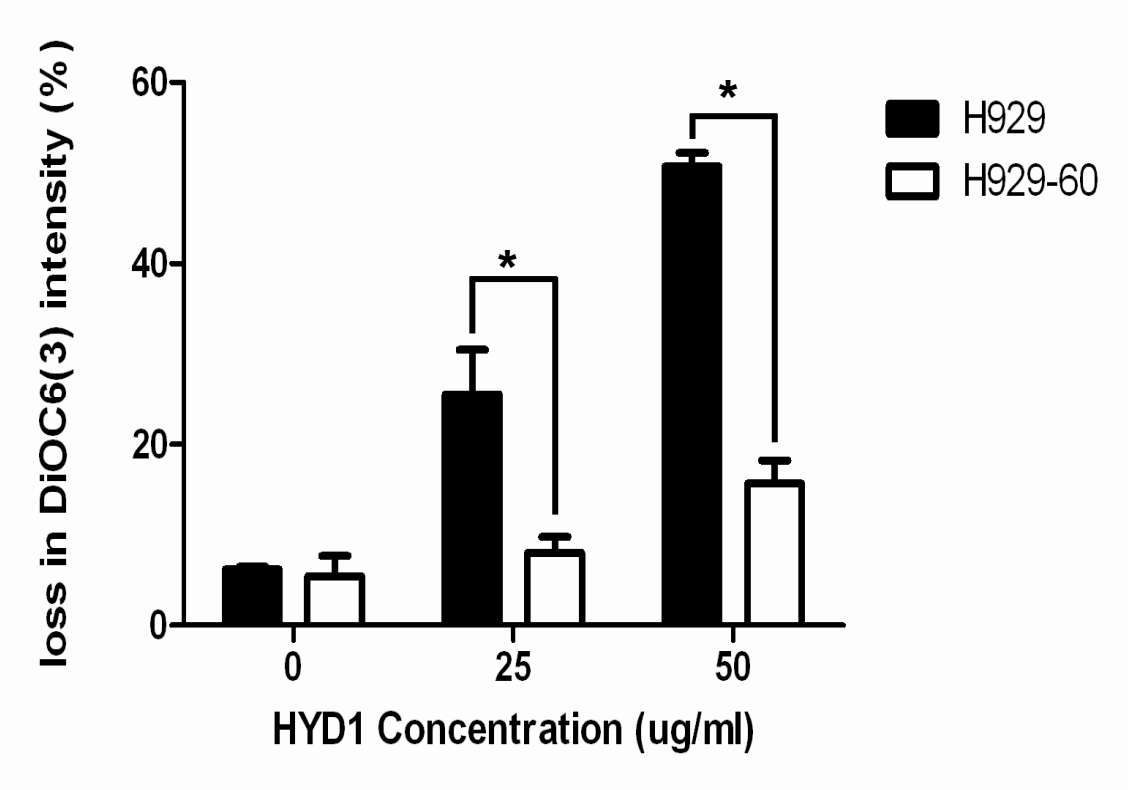

Figure 13: H929-60 cells display decreased HYD1 induced mitochondrial dysfunction. Loss of mitochondrial membrane permeability was determined using $DiOC_6$ staining following 2 hours of HYD1 treatment in H929 and H929-60 (* denotes $p<0.05$ n=9, Student's t-test). The experiment was repeated 3 independent times and shown is a representative experiment.

resistance towards HYD1 occurs upstream of mitochondrial dysfunction and generation of ROS and that the resistant mechanism is likely the result of qualitative or quantitative changes in the HYD1 binding complex located on the cell membrane.

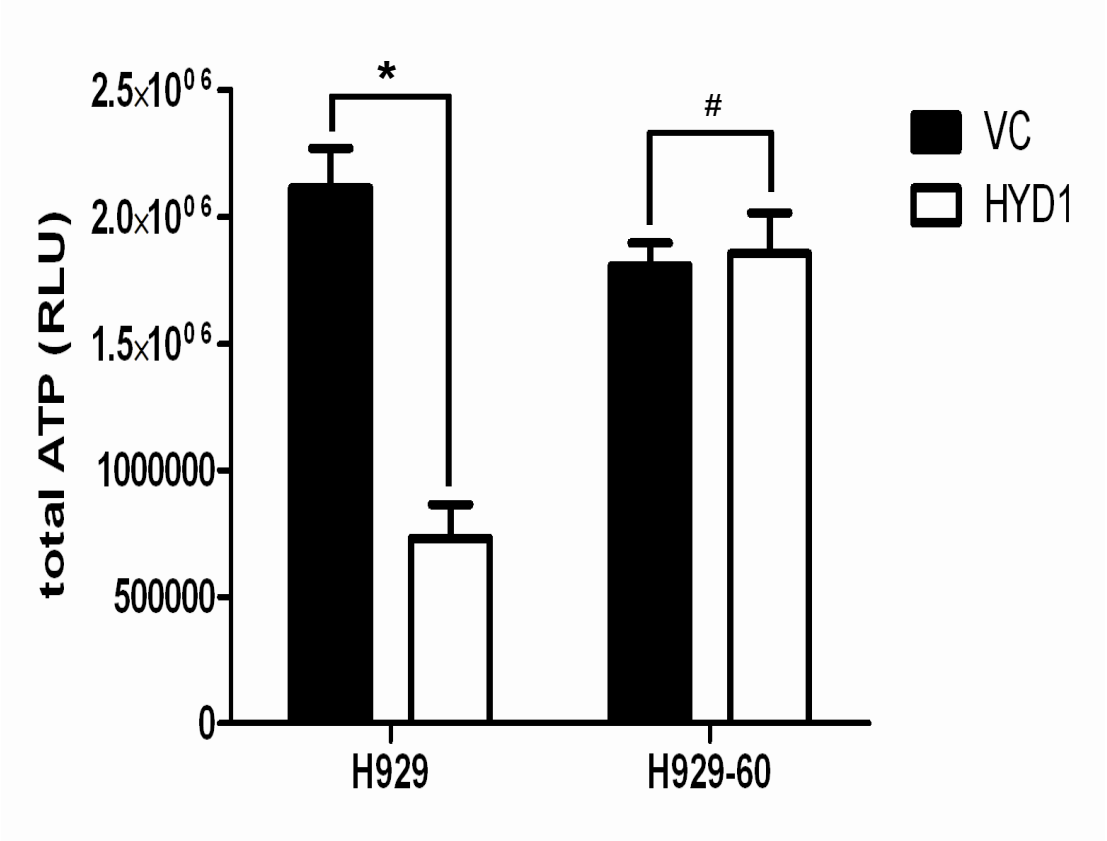

Figure 14: H929-60 cells do not display HYD1 induced ATP depletion. ATP levels were determined in the H929 and H929-60 cell lines following 6 hours of HYD1 (50 ug/ml) treatment. (* denotes $p<0.05$ and # denotes $p>0.05$, n=9, Student's t-test). The experiment was repeated 3 independent times and shown is a representative experiment.

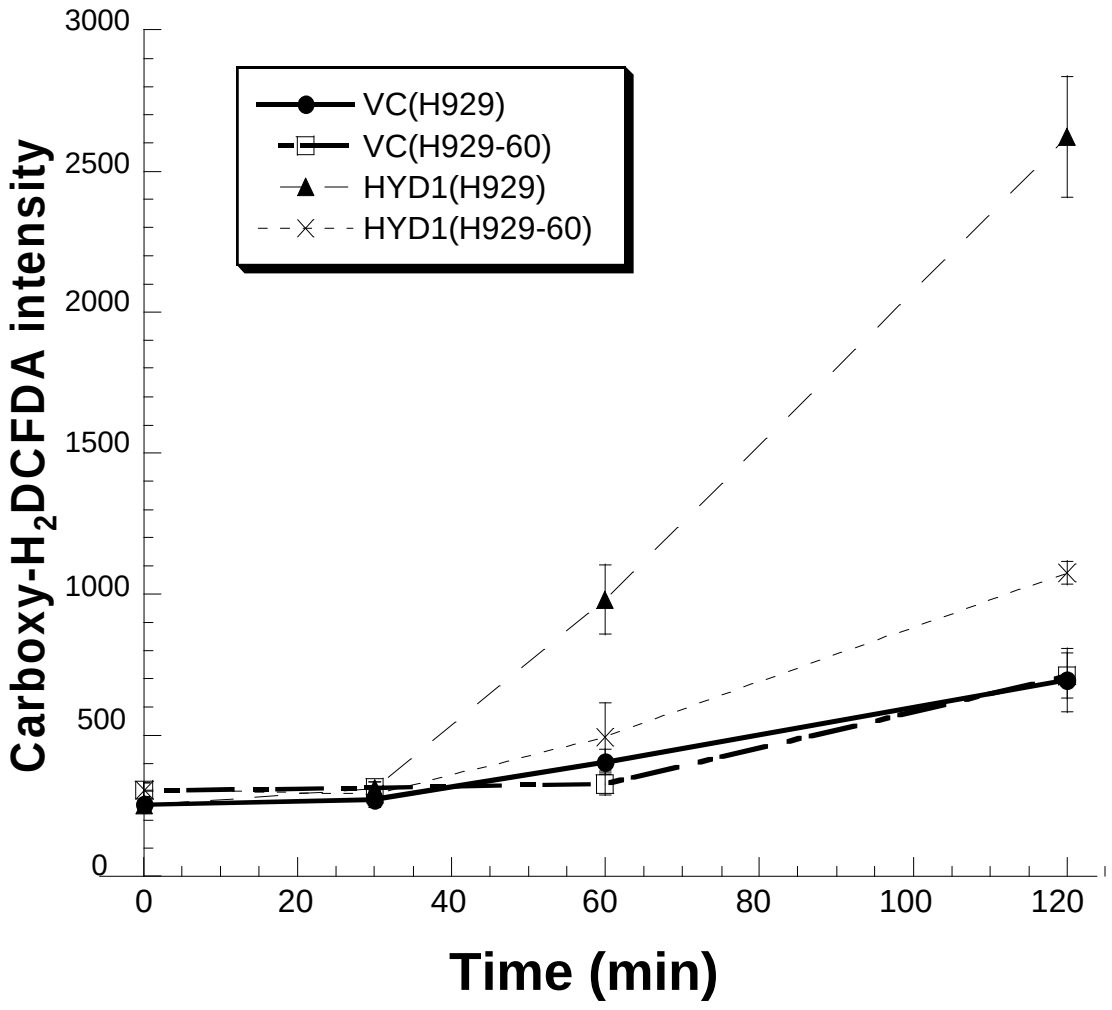

Figure 15: HYD1 induced levels of ROS are decreased in H929-60 cells compared to H929 cells. ROS production was measured using the dye 5-(and-6)-carboxy-2',7'-dichlorodihydro-fluorescein diacetate. H929 and H929-60 cells (4×105 cells/ml) were treated for various time points (0, 30, 60 and 120 minutes) with 50 μg/ml HYD1 or VC(H20). Dye fluorescence intensity was analyzed using Wallac VICTOR2 1420 multilabel counter (EG&G Wallac, Turku, Finland) (excitation: 485 nm, emission: 535 nm). A representative of three independent experiments is shown.

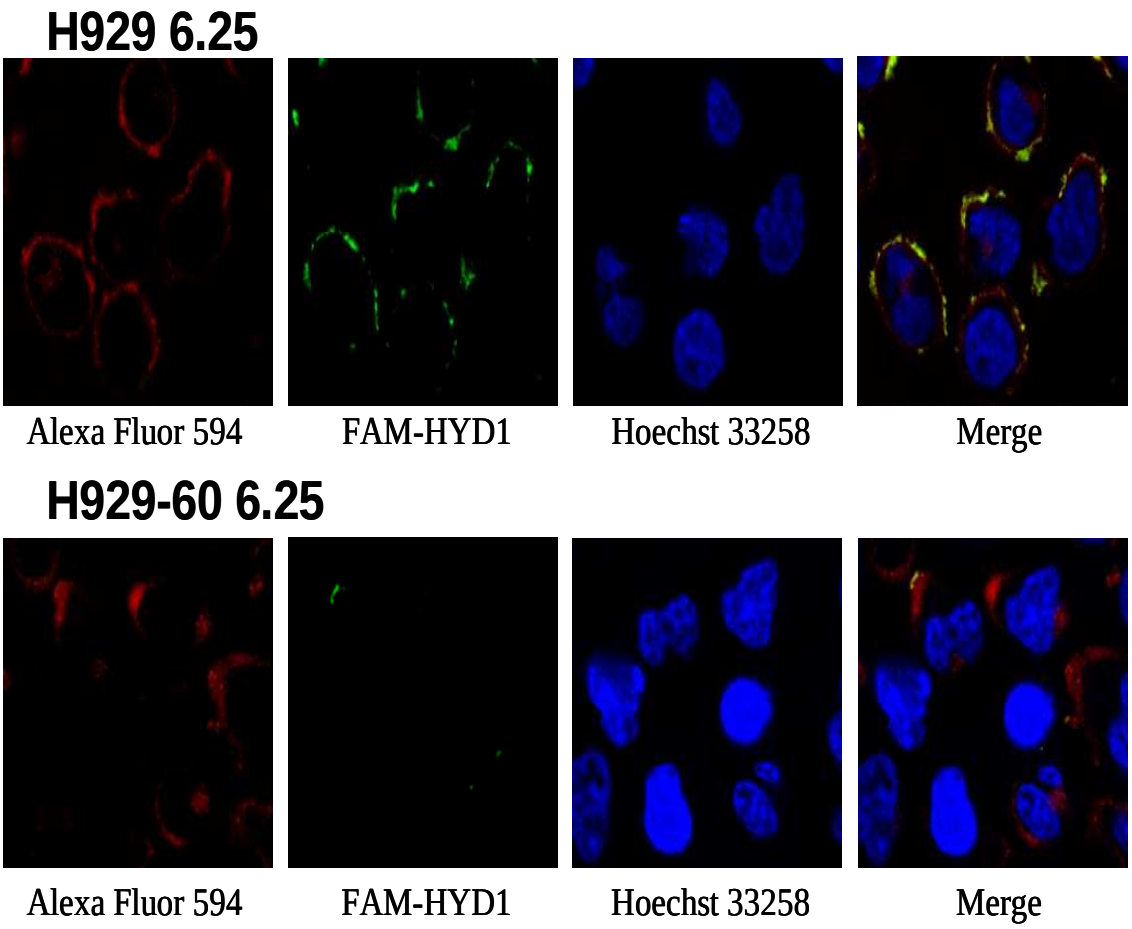

Figure 16: H929-60 cells demonstrated reduced binding of FAM-HYD1 to the cell surface. H929 and H929-60 cells were stained with Alexa Fluor 594 wheat germ agglutinin (WGA) and Hoechst 33342 for 30 minutes. 6.25 μg/ml FAM-HYD1 was added 10 minutes prior to analysis by confocal microscopy. The experiment was repeated 3 independent times and shown is a representative experiment.

Table 1: H929-60 cells are not resistant to standard myeloma therapies.

Compound	**H929 cells** IC_{50} (n=3)	**H929-60 cells** IC_{50} (n=3)
melphalan	11.3 +/- 2.5 μM	13.1 +/- 3.7 μM
mitoxantrone	1.42 +/- .4 μM	1.05 +/- .7 μM
bortezomib	11.3 +/- 5.1 nM	12.2 +/- 3.9 nM

H929 and H929-60 cells were treated with increasing concentrations of melphalan (100, 50, 25, 12.5, 6.25, 3.25 and 0 uM), mitoxantrone (8, 4, 2, 1, 0.5, 0.25, 0.125 and 0 uM) and bortezomib (256, 128, 64, 32, 16, 8, 4 and 0 nM) for 24 hours. After 24 hours, cells were stained with annexin V FITC/PI and acquired on FACScan. IC50 values were determined by linear regressions. Comparisons between H929 and H929-60 were not deemed to be significant using a students t-test ($p>0.05$ n=9).

Selection of acquired resistance in a population of cells (rather then clonal selection) often leads to multiple mechanisms of resistance and a phenotype that confers resistance to multiple agents [171]. However, we hypothesized that since HYD1 induces necrotic cell death, selection with HYD1 would not result in a phenotype which conferred resistance to other agents commonly used to treat myeloma. To address this question, we compared the IC_{50} values of H929-60 and the parental H929 cells to the alkylating agent, melphalan, the topoisomerase II inhibitor, mitoxantrone, and the proteasome inhibitor, Bortezomib. As predicted, H929-60 cells were not resistant to other classes of agents commonly used to treat multiple myeloma and known to induce apoptosis (Table 1). These data further support the potential advantage of targeting necrosis in combination with inducers of apoptosis for the treatment of multiple myeloma, as cross-resistance between these two agents is unlikely to occur during the course of drug treatment.

Expression of integrin genes are significantly changed in H929-60 cells when compared to H929 cells.

Gene expression profiling (GEP) of H929 and H929-60 cells was utilized as an unbiased way of analyzing expression of genes that are significantly changed between the H929 and H929-60 cell lines. Scanned output files were visually inspected for hybridization artifacts and then analyzed by Affymetrix Microarray Suite 5.0 and robust multi-array average (RMA) software. 5700 genes were deemed to be significantly changed when Mas 5.0 software was utilized. Significance was determined when gene expression was increased or expression was decreased in all 3 of the samples tested. While Mas 5.0 is good at predicting true fold change between comparison groups, it also produces more false positive genes. In order to more precisely determine what genes were changed, RMA software was also used to determine significance between groups. 2200 genes were deemed to be significantly changed when RMA software was utilized. Significance was determined when there was more than a two fold difference in gene expression between H929 and H929-60 cell lines. Each set of significantly changed genes was put into the pathway analysis programs GeneGO and Ingenuity to determine key pathways and gene families are significantly. As shown in table 2, the integrin family of genes were significantly changed in H929-60 cells compared to H929 cells.

Table 2: Genes expressing integrins were significantly changed in H929-60 cells compared to H929 cells.

Integrin	H929	H929-60	Fold change	Adheres to
Alpha 1	absent	absent		Collagen
Alpha 2	absent	absent		Collagen
Alpha 3	166.3	135.5	-1.24	Laminin
Alpha 4	4367.6	5169.1	1.18	FN, VCAM1, MadCAM-1
Alpha 5	absent	absent		FN
Alpha 6	530.5	99.5	-5.33 (*) #	Laminin
Alpha 7	80.1	191.9	2.40 (*)	Laminin
Alpha 8	2144.6	1791.4	-1.20	FN
Alpha L	580.6	4771	8.22 (*) #	ICAM 1-3
Alpha V	620.5	381.3	-1.63 (*) #	FN, VN
Beta 1	6713.6	6127.8	-1.39 (*)	Collagen, FN, Laminin, VN
Beta 3	absent	absent		FN, VN
Beta 5	1038.6	2387.0	2.30 (*) #	FN
Beta 7	15047.3	18940.8	1.26 (*)	MadCAM-1
Beta 8	169.3	28.2	-6.00 (*) #	VN

Probe sets that express integrins were tested for significance between H929 and H929-60 cells. 8 out of 11 genes that were expressed in H929 and H929-60 cells were determined to be significantly changed using Mas 5.0 software while 5 out of 11 genes were significantly changed using RMA. Significance using Mas 5.0 was determined if expression levels were either increased across 3 individual experiments or decreased across 3 individual experiments. Significance using RMA was determined if there was a 2 fold difference in gene expression between H929 and H929-60 cells. (*=significance using Mas 5.0, #=significance using RMA)

Acquisition towards resistance to HYD1 results in reduced expression of α4, β1 integrin and ablated functional binding to FN and VCAM-1:

To determine whether the acquisition of resistance correlated with quantitative changes in integrin expression we screened multiple α integrin sub-units (α3, α5, αV and α6 integrin data not shown) that are commonly expressed in hematopoietic cells and determined that α4 integrin was the most abundant integrin expressed on the parental cell line and expression was reduced in the resistant cell line (figure 15). Using FACS analysis we determined that α4 integrin was found to be reduced by 1.8 fold. As shown in figure 16, the reduction at the cell surface corresponded to reduced protein expression using a whole cell whole cell lysate preparation. Interestingly, when examining the whole cell lysate the most dramatic decrease was the cleaved form of α4 integrin. In some cell types, the mature 150 kD α4 integrin is cleaved into a non-disulfide linked 80 and 70 kD fragment. For example, activation of T-cells was previously reported to correlate with increased cleavage of the mature α4 integrin[172]. However, the cleavage of α4 integrin was found to not alter the adhesive properties of VLA-4 integrin to fibronectin or VCAM1[173]. The attenuation of protein expression is post-transcriptionally regulated as the parental and resistant cell line demonstrated equal levels of α4 mRNA (Figure 16). Further studies are warranted to delineate the post-transcriptional regulation of α4 integrins in the resistant cell line.

Since β1 integrins require inside-out activation in order to be competent to bind ligand, expression does not necessarily directly correlate with functional adhesion. Thus, we next sought to determine whether a reduction in the expression of VLA-4 integrin resulted in a functional reduction in adhesion to extracellular matrices. To this end, we

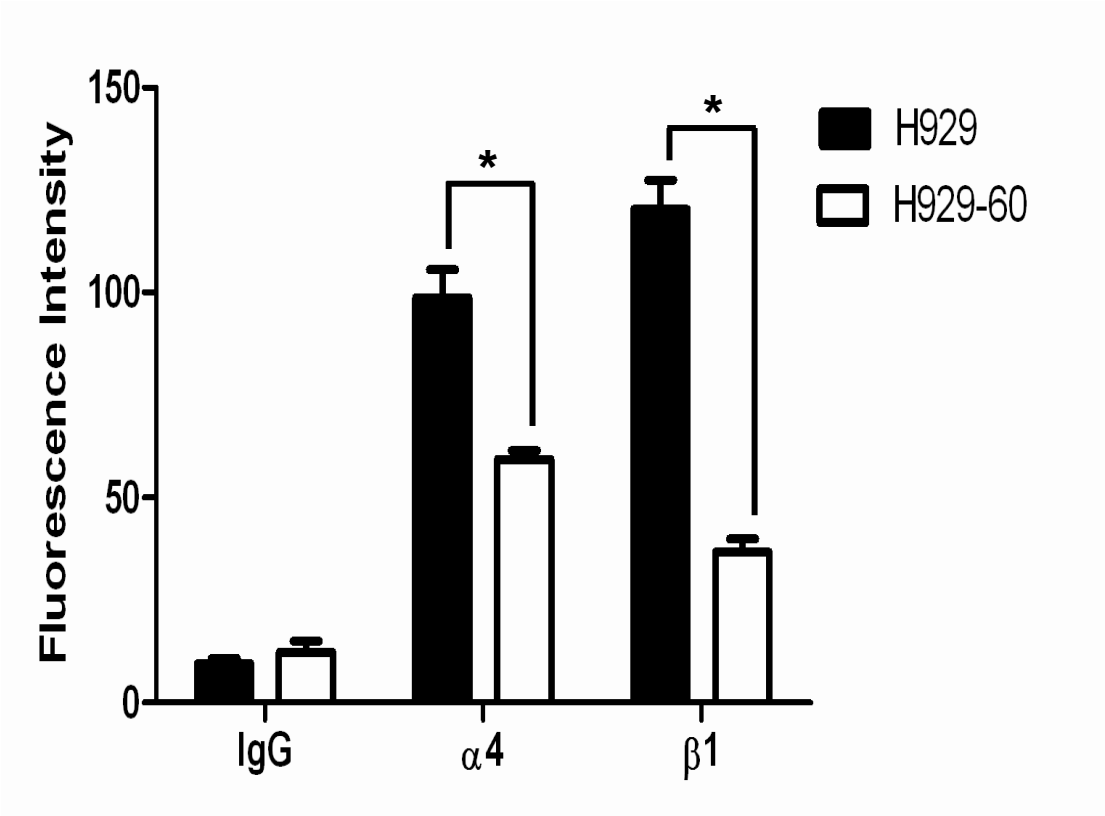

Figure 17: α4 and β1 integrin surface expression are reduced in H929-60 cells. Surface expression of α4 and β1 integrin on H929 and H929-60 cells was determined by FACS analysis (* denotes $p<0.05$ n=9, Student's t-test). A representative of each experiment is shown.

compared the levels of adhesion of the sensitive and resistant cell line to fibronectin and the more specific ligand for α4 integrin, VCAM-1. In figure 17, H929-60 cells demonstrated a dramatic reduction in the binding to FN and VCAM-1. An α4 integrin blocking antibody was used as a positive control for blocking the parental cell line to FN and VCAM-1.

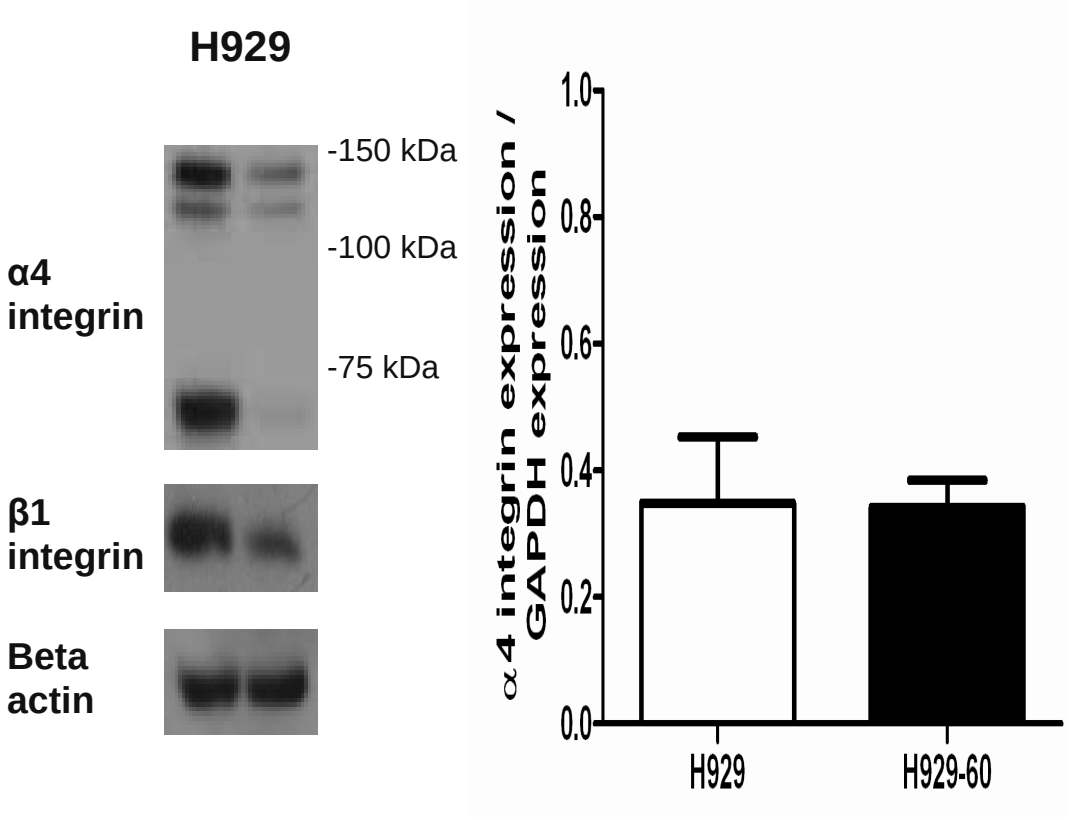

Figure 18: H929-60 cells have decreased α4 integrin protein but not mRNA levels. Whole cell lysates of H929 and H929-60 cells were probed for α4 integrin, β1 integrin and beta actin by Western blot analysis. α4 integrin mRNA levels were determined using real time rt-PCR. α4 integrin mRNA expression levels were normalized by dividing by GAPDH levels ($p>0.05$ $n=3$). A representative of each experiment is shown.

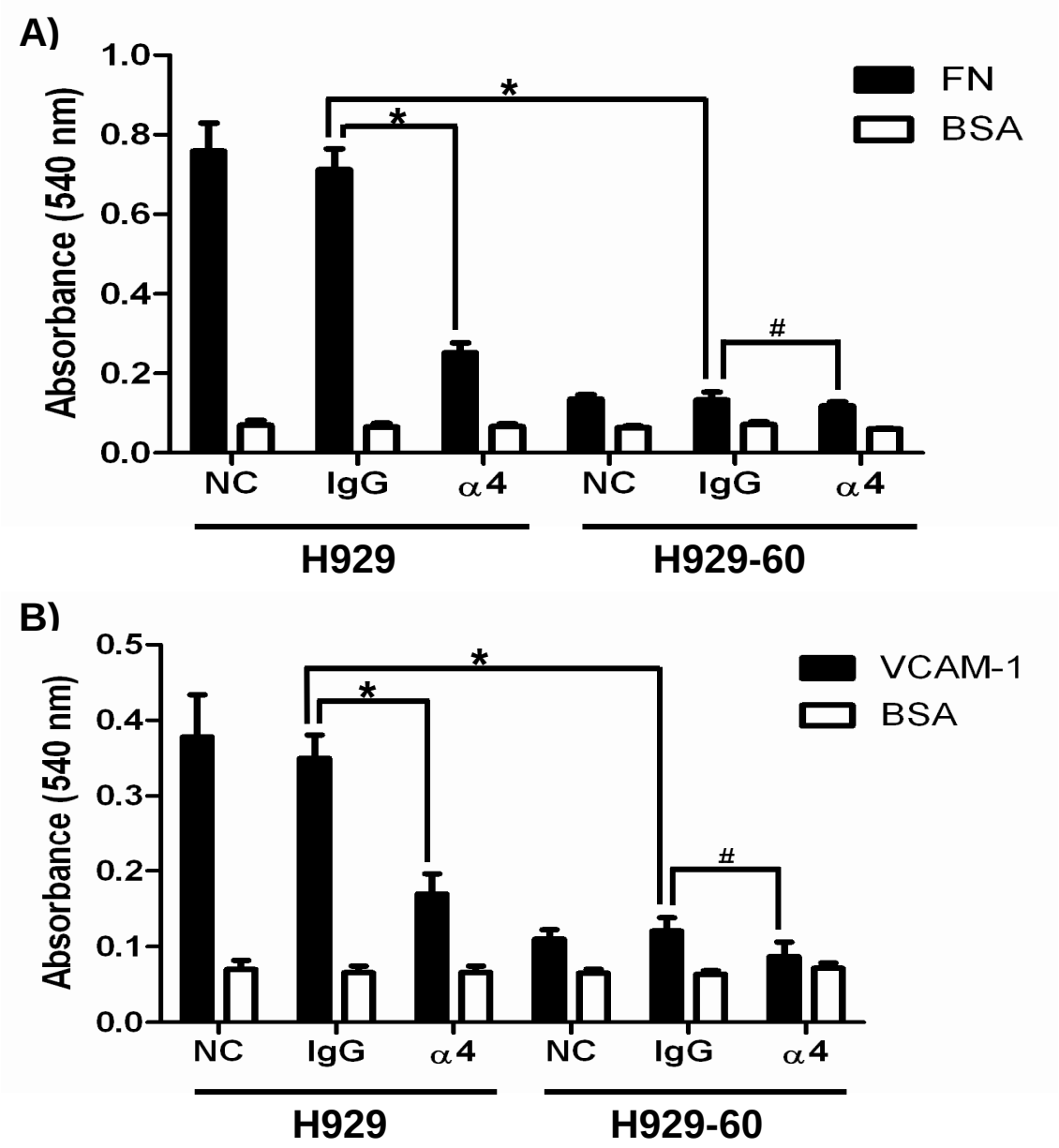

Figure 19: H929-60 cells have reduced α4 integrin protein levels and reduced adhesion to FN and VCAM-1. H929 and H929-60 cells were incubated with α4 blocking antibody or IgG control antibody for 30 minutes and subsequently adhered to (A) FN (40 μg/ml) or (B) VCAM-1 (10 μg/ml) coated plates for 2 hours. A representative of each experiment is shown (* denotes $p<0.05$ or # denotes $p>0.05$ Student's t-test).

Reducing the expression α4 and β1 integrins causes resistance to HYD1 induced cell death in H929 and 8226 MM cells.

Considering H929-60 cells were resistant to HYD1 induced cell death and demonstrate reduced surface expression of the α4 integrin subunit, we next determined whether reducing the expression of α4 integrins using shRNA targeting strategies in myeloma cell lines was sufficient to induce resistance towards HYD1 induced cell death. As shown in figure 18, reducing the expression of α4 integrin conferred resistance to HYD1 ($p<0.05$, Student's t-test) in both 8226 and H929 cells.

Since α4 integrin can heterodimerize with either β1 or β7 integrin, we tested whether reducing β1 integrin was sufficient to induce resistance to myeloma cell lines. As shown in figure 19, reducing β1 integrins rendered H929 and 8226 cells resistant to HYD1 induced cell death ($p<0.05$, student's t-test). β1 integrin can heterodimerize with 11 different α sub-units. The observation that reducing α4 or β1 integrin gave similar levels of protection indicates that the α4β1 integrin is the predominant β1 integrin partner associated with HYD1 induced cell death in myeloma cells. The observation that reducing integrin expression afforded only partial resistance may be due to (a) residual levels of α4β1 integrin remaining on the cell surface or (b) α4β1 represents only one component of the binding complex required for HYD1 induced cell death.

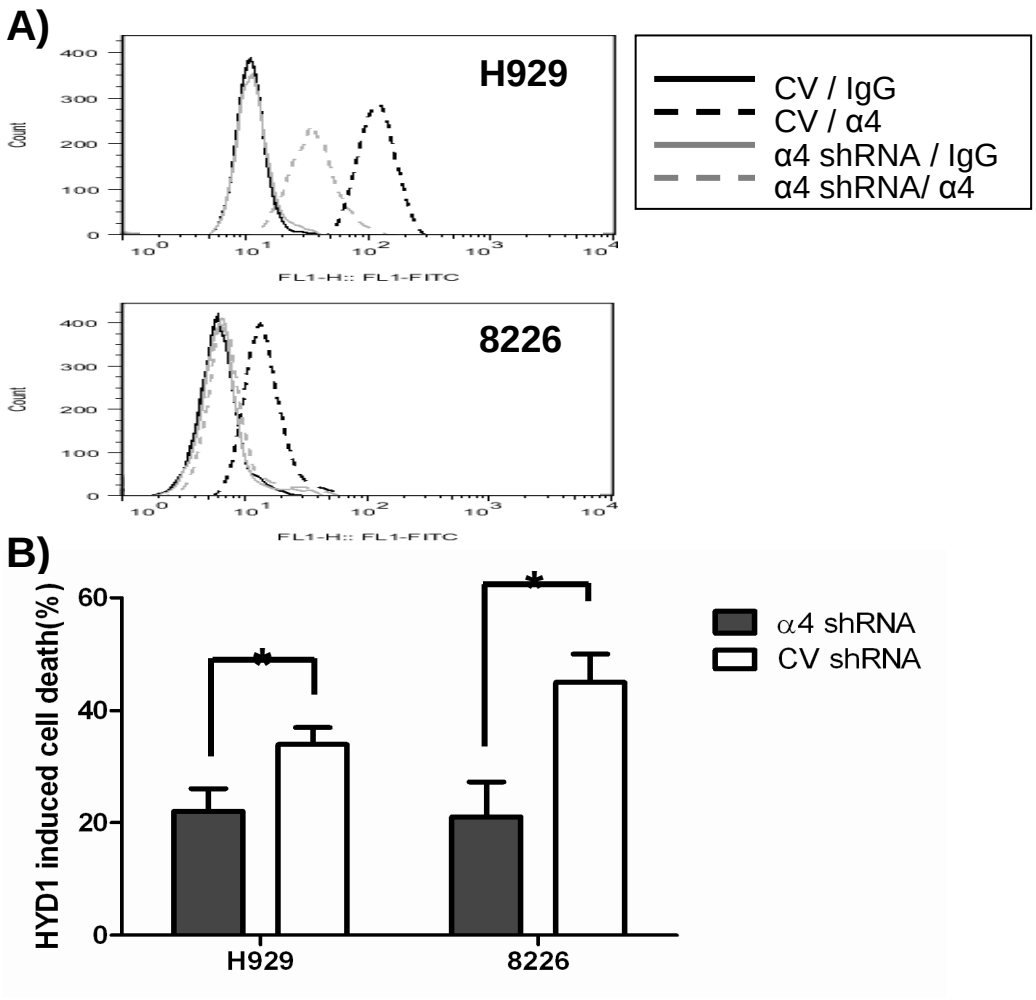

Figure 20: Reducing the expression of α4 integrin caused partial resistance to HYD1 induced cell death in H929 and 8226 cells. A) In H929 cells α4 integrin expression was reduced via transient infection. A: At 72 hours post infection of shRNA, α4 integrin expression was determined by FACS analysis. 8226 cells were stably infected with α4 integrin shRNA or control vector shRNA. Shown is a representative histogram from one experiment. B) H929 and 8226 cells were treated with 50 μg/ml and 100ug/ml of HYD1 respectively for 6 hours. After 6 hours, cell death was analyzed by Topro-3 staining and FACS analysis. (* denotes $p<0.05$ n=9, Student's t-test).

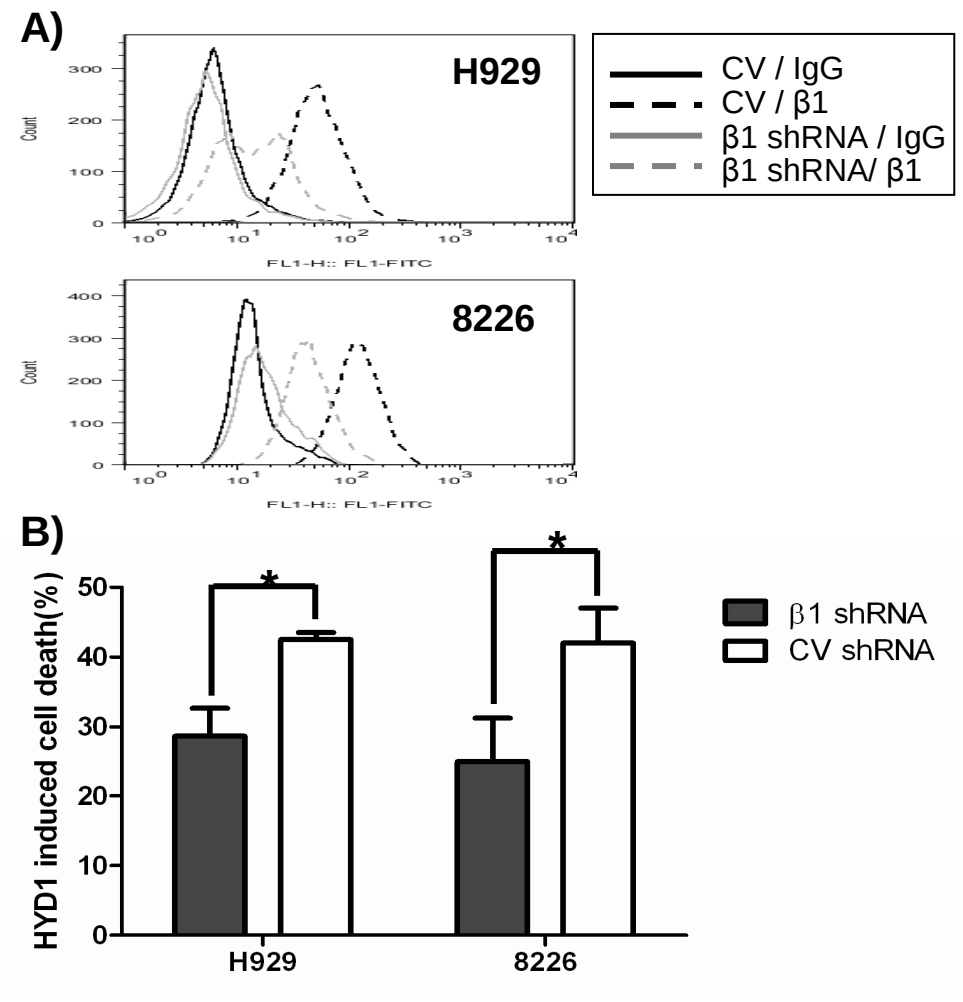

Figure 21: Reducing the expression of β1 integrin caused partial resistance to HYD1 induced cell death in H929 and 8226 cells. A) In H929 cells β1 integrin expression was reduced via transient infection. A) At 72 hours post infection of shRNA, β1 integrin expression was determined by FACS analysis. 8226 cells were stably infected with β1 integrin shRNA or control vector shRNA. Shown is a representative histogram from one experiment. B) H929 and 8226 cells were treated with 50 μg/ml and 100ug/ml of HYD1 respectively for 6 hours. After 6 hours, cell death was analyzed by Topro-3 staining and FACS analysis. (* denotes $p<0.05$ n=9, Student's t-test).

Biotin-HYD1 interacts with α4 integrin and reduced binding was observed in the cell line with acquired drug resistance.

Previous data indicated that biotin-HYD1 associated with α3 and α6 integrins but not α2 integrins on prostate cancer cell lines[170]. We utilized a similar strategy to determine whether biotin-HYD1 interacted with an α4 integrin containing complex and whether that interaction was attenuated in the resistant cell line. The total membrane lysate was used as a control for detection of α4 integrin. Again the reduction in the cleaved α4 integrin subunit in membrane extracts (although not as dramatic as the whole cell lysate), was most prominent in the resistant cell line compared to the mature α4 integrin subunit. Additionally, as shown in Figure 20, using biotin-HYD1 we demonstrate that the resistant cell line shows decreased binding for the cleaved α4 sub-unit. Further studies are warranted to fully understand the significance of the cleaved α4 integrin sub-unit in mediating HYD1 induced cell death and the CAM-DR phenotype.

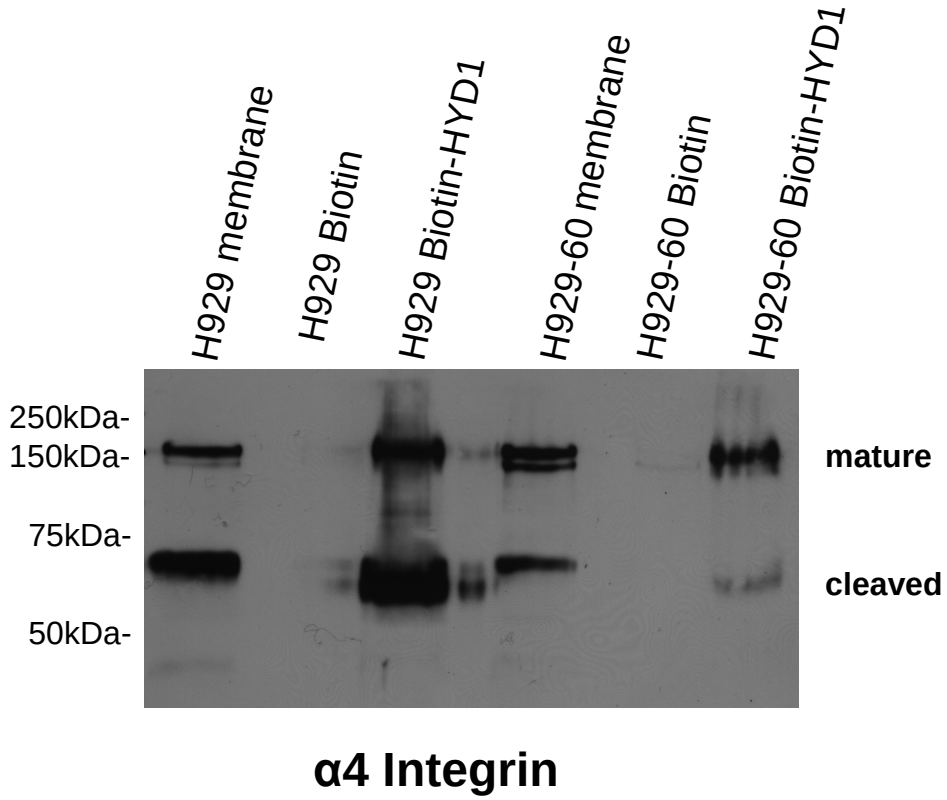

Figure 22: Biotin-HYD1 interacts with α4 integrin and binding to cleaved α4 integrin is attenuated in the resistant H929-60 cells. H929 and H929-60 membrane fractions were added to biotin or biotin-HYD1 bound NeutrAvidin beads for 18 hours as described in the methods and materials section. The experiment was repeated twice and a representative experiment is shown.

H929-60 cells displayed reduced binding to bone marrow stromal cells and demonstrate a compromised CAM-DR phenotype.

In addition to attenuated adhesion to FN and VCAM-1, H929-60 cells also exhibit a reduction in adhesion to the HS-5 stromal cell line and mesenchymal stroma cells (MSC) (Figure 21). We reasoned that acquisition of resistance towards HYD1, which correlated with reduced functional binding to fibronectin, VCAM-1, HS-5 stromal cells

and MSC, would likely result in a compromised CAM-DR phenotype. To test this premise, we utilized the HS-5 co-culture model of drug resistance. H929 and the HYD1 resistant variant H929-60 cells were treated with either melphalan or bortezomib in the presence or absence of HS-5/GFP bone marrow stromal cells. As shown in Figure 22, the HYD1 resistant cell line was not resistant in the co-culture bone marrow stromal model to melphalan or bortezomib, respectively. There is some controversy in the literature whether co-culturing myeloma cells with stroma cells causes resistance to bortezomib[174]. The apparent discrepancy may be the result of endpoints that measure growth compared to cell death, dose of bortezomib or the scheduling of how long myeloma cells interact with the stroma before exposure. Additionally, exposure to bortezomib for 24 hours was shown to downregulate α4 integrin levels and thus drug scheduling could also impact observed results [96]. However, our results are consistent with recent reports showing that myeloma cells are resistant to bortezomib in MSC co-culture models. [175]. Together, these data indicate that as myeloma cells are selected for resistance to HYD1 they are losing resistance to standard chemotherapy in the context of the bone marrow microenvironment due to reduced capacity to adhere to bone marrow stromal cells. Again these data support the premise that disrupting adhesive interactions are likely to improve the efficacy of standard chemotherapy in the context of the bone marrow microenvironment.

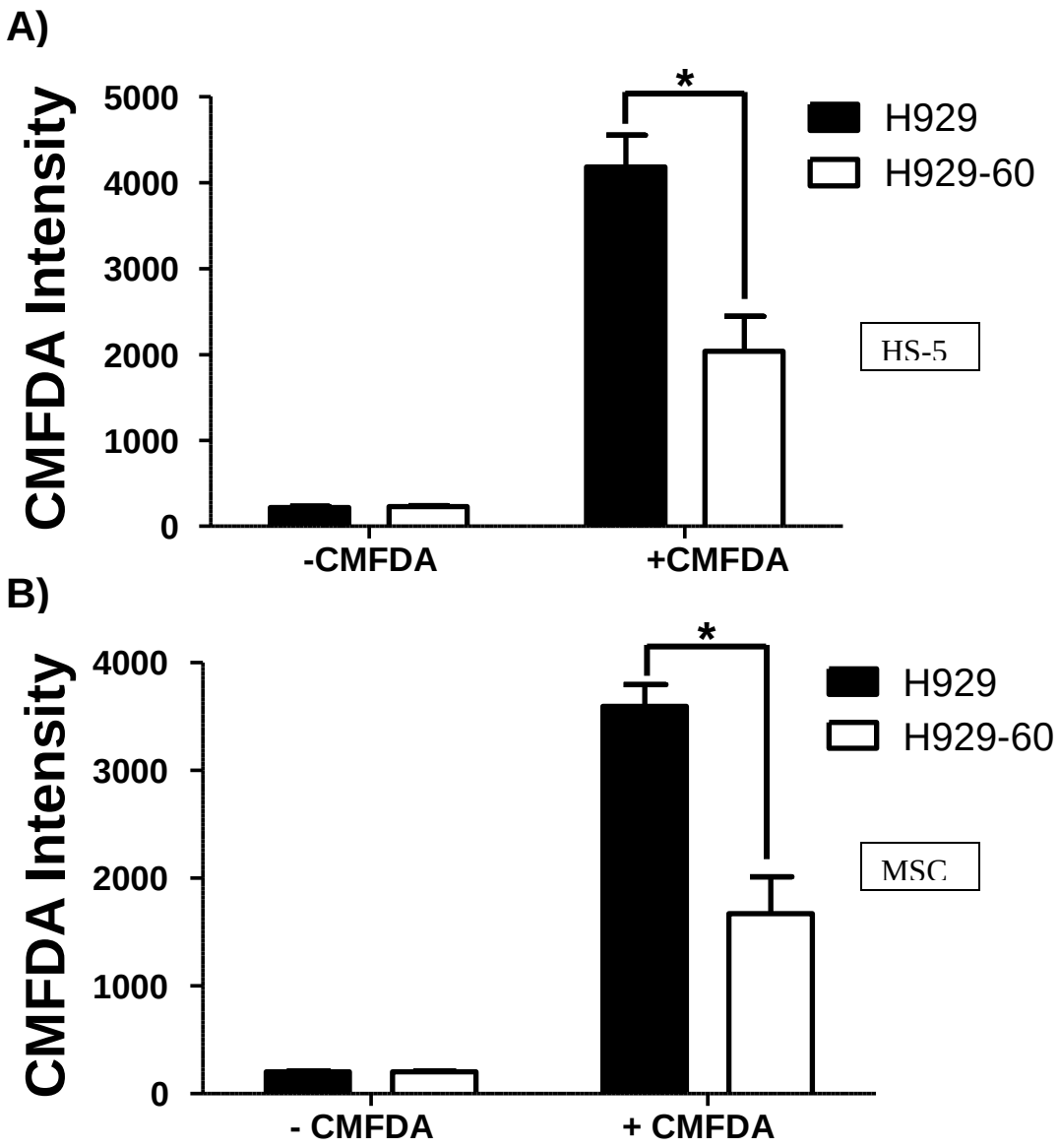

Figure 23: H929-60 cells display reduced binding to HS-5 and MSCs.
A-B) H929 and H929-60 cells pre-incubated with CMFDA dye were adhered to 10,000 A) HS-5 cells or B) MSC cells for 2 hours. After 2 hours, unadhered cells were removed and the fluorescence intensity was measured on a plate reader. A representative of three independent experiments was shown. (* =$p<0.05$, n=9 Students t-test).

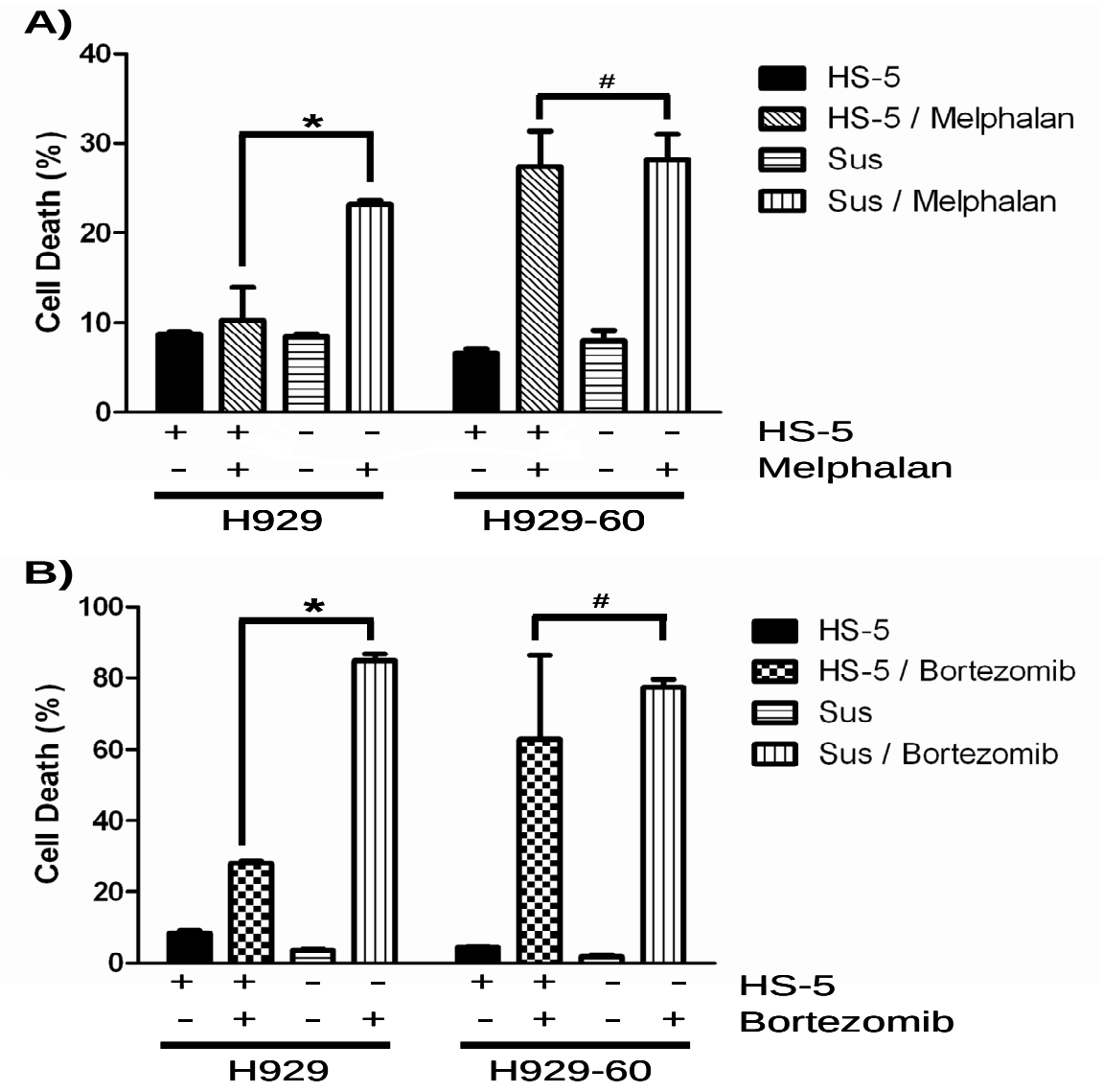

Figure 24: H929-60 cells are not resistant to melphalan or bortezomib in the stroma co culture model. A-B): H929 and H929-60 cells were adhered to HS-5 GFP cells for 24 hours. After 24 hours samples were treated with 15 μM melphalan or 16 nM bortezomib for 24 hours. Cell death was analyzed using To-PRO 3 intensity on a FACScalibur with the HS-5 GFP cells excluded from the analysis. A representative of three independent experiments was shown. (* =$p<0.05$, n=9 or# =$p>0.05$, n=9 Students t-test).

HYD1 induced cell death is increased in relapsed myeloma patient specimens compared to newly diagnosed specimens and correlates with α4 integrin expression.

In order to determine whether primary myeloma specimens are sensitive to HYD1 induced cell death, 7 newly diagnosed and 7 relapsed primary myeloma specimens were collected. Immunomagnetic beads were used to enrich for CD138 positive malignant plasma cell fractions. As shown in Figure 23A, the CD138 positive tumor population was more sensitive to HYD1 induced cell death compared to the CD138 negative population. In addition to measuring cell death, the levels of α4 integrin expression were determined in the CD138 positive cells by FACS analysis. As shown in Figure 23B, HYD1 induced cell death positively correlates with α4 integrin expression. Importantly, HYD1 was observed to be significantly ($p<0.05$, student's t-test) more active in relapsed refractory patients compared to newly diagnosed patients (Figure 24A). Finally as shown in Figure 24B, α4 integrin levels are increased in CD138 positive cells isolated from relapsed myeloma patients compared to newly diagnosed patients ($p<0.05$, student's t-test). Together, these data suggest that α4 integrin expression is selected for over the course of drug treatment and may contribute to the eventual failure to therapeutically manage multiple myeloma. Additionally, patients with high levels of α4 expression may benefit from combination strategies that include targeting this specific integrin complex such as Natalizumab[176] (humanized α4 antibody) or HYD1.

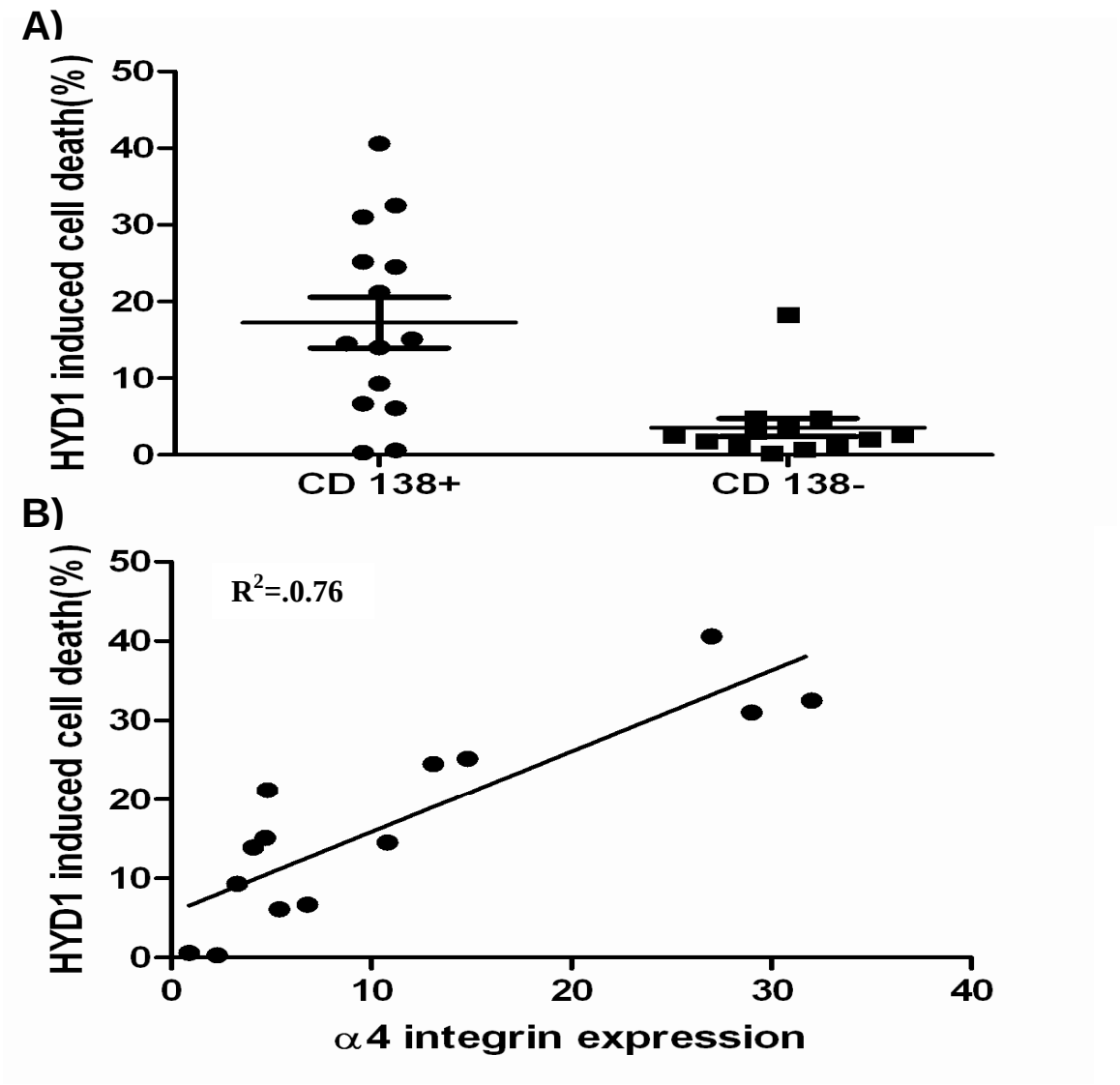

Figure 25: HYD1 induced cell death in CD138+ patient samples correlates with increased α4 integrin expression. A) CD138+ and CD138- cells were treated with 100 ug/ml HYD1 for 24 hours. After 24 hours cell death was measured by Topro-3 staining and FACS analysis. ($p<0.05$, Student's t-test) B) α4 integrin expression was compared to HYD1 induced cell death using a Pearson's correlation coefficient. The CD138+ population demonstrated a significant correlation between α4 integrin expression and HYD1 induced cell death ($p<0.05$).

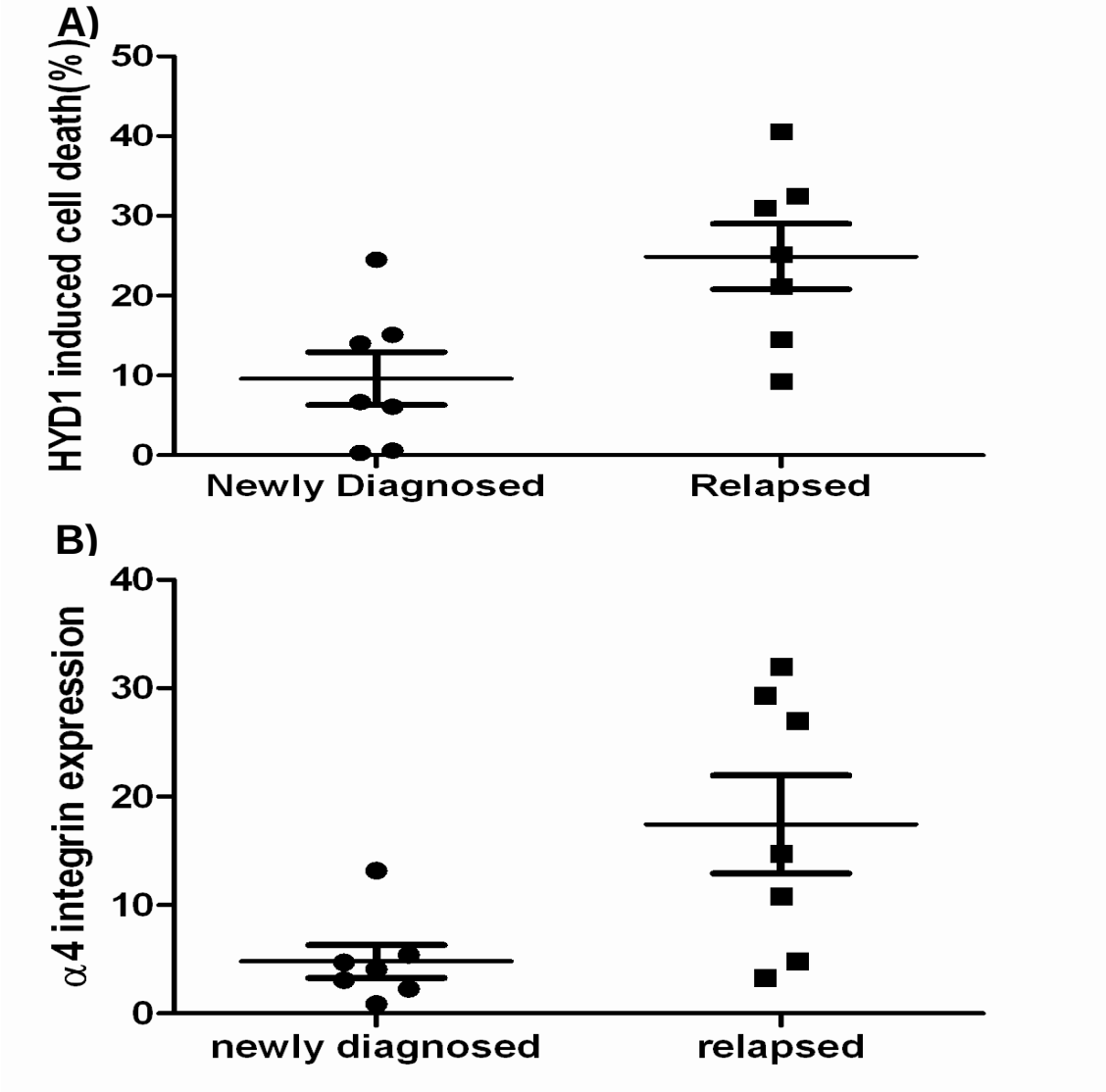

Figure 26: Relapsed specimens have increased HYD1 induced cell death and α4 integrin expression. A-B) Specimens were separated into two groups: newly diagnosed or relapsed patients. In A), CD138+ cells were treated with100 ug/ml HYD1 for 24 hours. After 24 hours cell death was measured by Topro-3 staining and FACS analysis (Student's t-test $p<0.05$) In B) CD138+ cells were used to analyze for α4 integrin expression by FACS analysis. (Student's t-test $p<0.05$

A cyclized form of the active region of HYD1, named HM-27, was developed in order to increase bioavailability and activity in MM cells.

One limitation to using peptidomimetics is that they have low bioavailability as they can be degraded by serum proteases. As almost all eukaryotic proteins are made up of L-amino acids, HYD1 was developed as a D-amino acid to make it more resistant to serum proteases. In addition to changing the chirality of the amino acids, peptidomimetics can also be pegylated or cyclized as a way to increase bioavailability. Before HYD1 was cyclized, the active region of HYD1 was determined by truncating the N and C terminus and testing for activity. Previous studies showed that the sequence of HYD1 necessary to support cell adhesion was kmvixw, the block to migration required xkmviswxx and activation of ERK signaling required ikmviswxx, with the shortest sequence active in all three assays being kmvisw [162]. As shown in figure 25, the shortest sequence of HYD1 that was also shown to have activity in MM cells was mvisw. By using alanine screens on the active region of HYD1 and constraining the sequence by cyclizing it, many compounds were tested for their ability to induce MM cell death. One compound tested was named HM-27 which contains the sequence Nleu-V-V-A-W. HM-27 was shown to be 30 fold more active in MM cells when compared to HYD1 (figure 26). H929-60 cells were also resistant to HM-27 when compared to H929 cells, indicating that HM-27 induces cell death in MM cells via the same mechanism of action as HYD1 (figure 27).

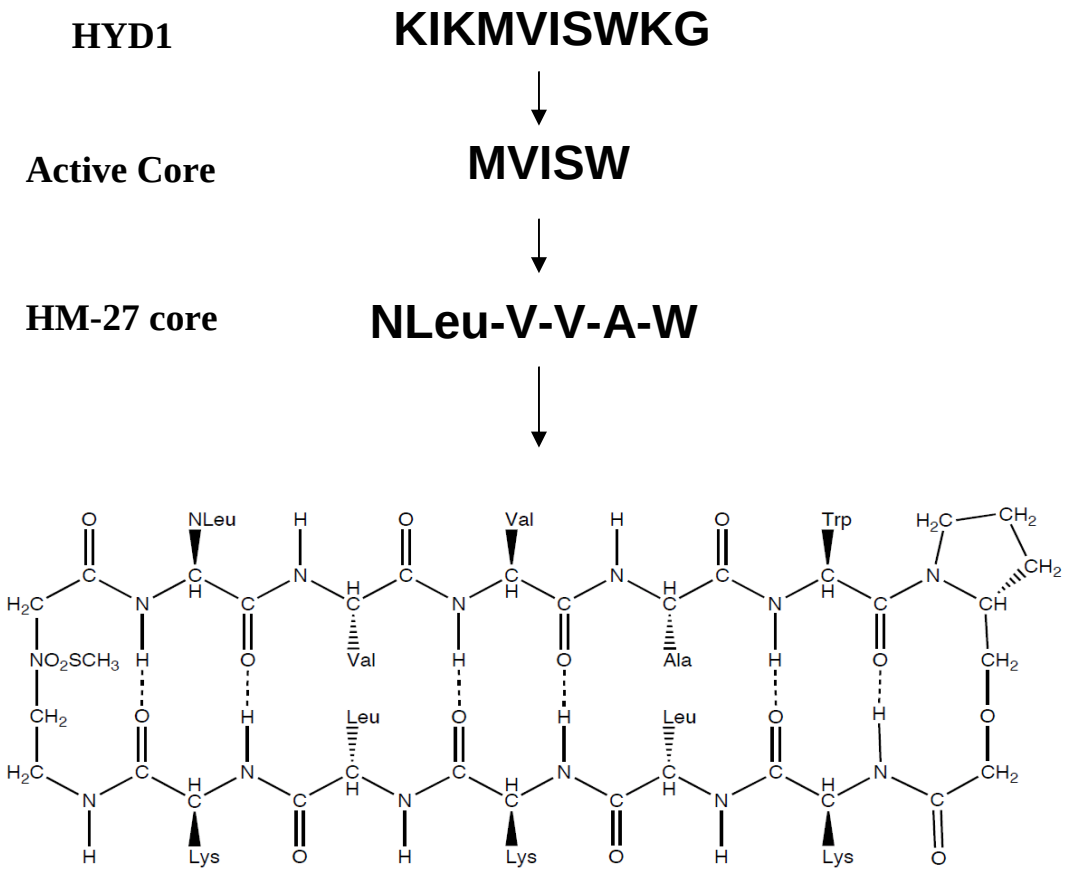

Figure 27: A cyclized variant of HYD1, HM-27, was developed using the active core of HYD1. Using truncation studies, the minimum sequence of HYD1 which still displays activity in MM cells is mvisw. Performing alanine substitutions on the active core and cyclizing the sequence to constrain the peptide produced the peptidomimetic, HM-27.

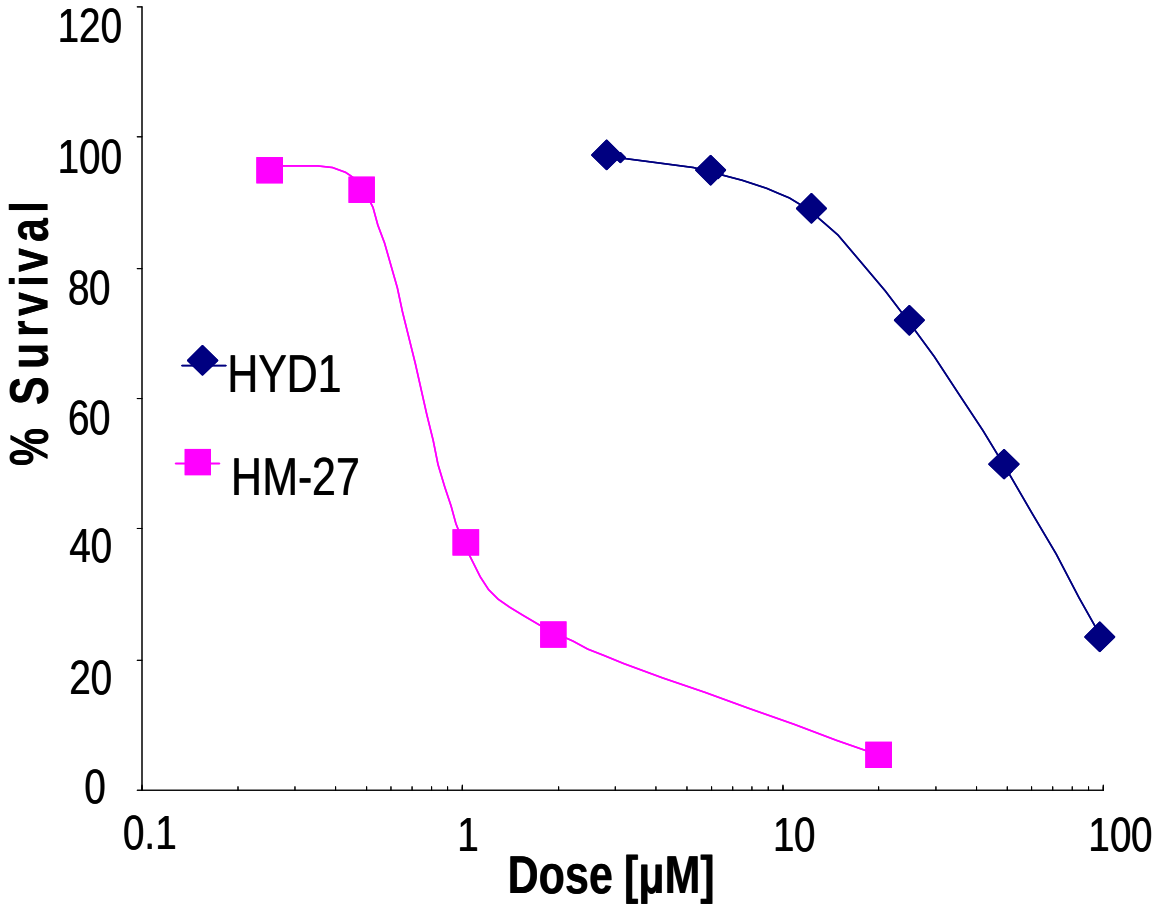

Figure 28: HM-27 displays increased activity in H929 cells when compared to HYD1. H929 cells were incubated with varying concentrations of HYD1 and HM-27 for 24 hours and drug induced cell death was determined by Topro-3 staining and FACS analysis. The experiment was repeated 3 independent times and shown is a representative experiment.

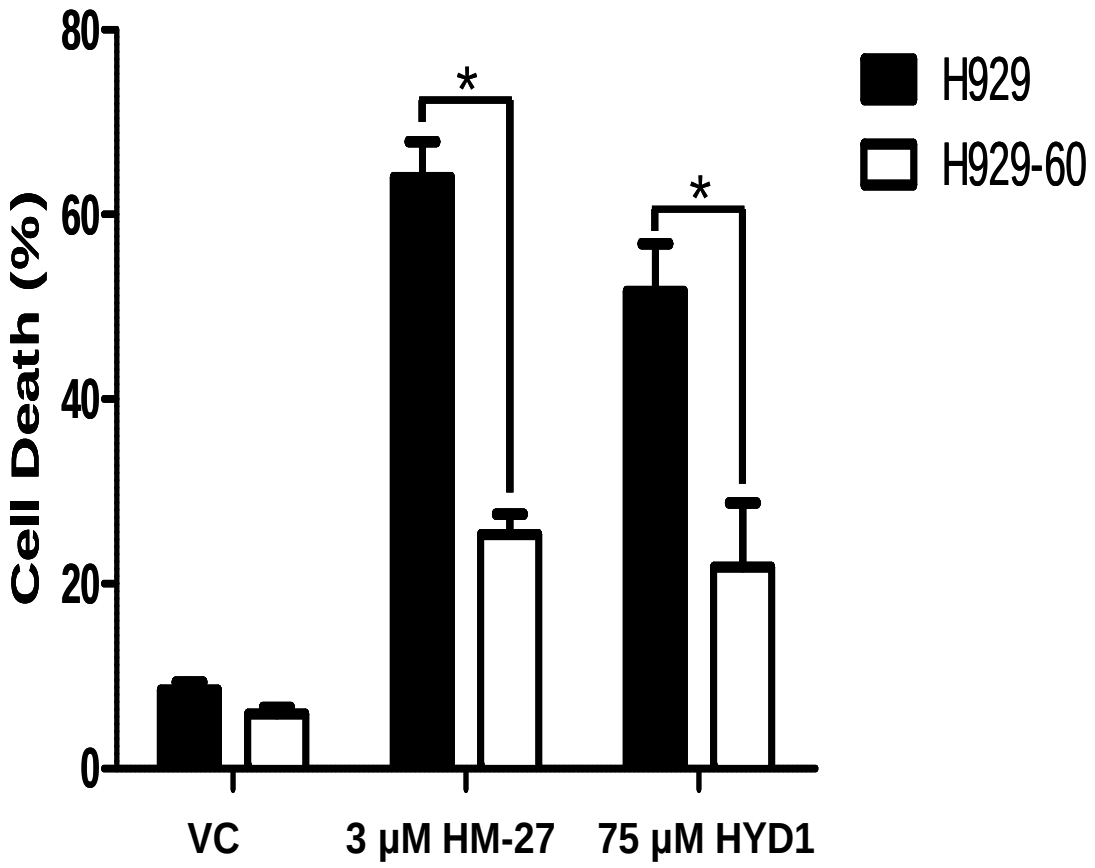

Figure 29: H929-60 cells are resistant to HM-27 induced cell death. H929 and H929-60 cells were incubated with varying concentrations of HYD1 and HM-27 for 6 hours and drug induced cell death was determined by Topro-3 staining and FACS analysis. The experiment was repeated 3 independent times and shown is a representative experiment. (∗= $p<0.05$, student's t-test)

HM-27 and HYD1 induce intracellular Ca^{2+} oscillations in MM cells.

Necrosis is predominantly described as an accidental or uncontrolled form of cellular death and is characterized by the activation of key bioenergetic events. These events that are usually implicated in necrosis are; increased mitochondrial dysfunction, ATP depletion, depletion of intracellular NAD^{+}, increased levels of intracellular Ca^{2+}, and increased generation of ROS. As was previously shown, HYD1 induced cell death in MM cells by depleting ATP, inducing loss of the mitochondria membrane potential and generation of ROS. HYD1 was also shown to deplete intracellular NAD^{+} levels in MM cells (data not shown). Levels of intracellular Ca^{2+} are also an important in mediating necrotic cell death. If the concentration of intracellular Ca^{2+} is at too high a level (>1μM), the mitochondria can become overloaded with Ca^{2+}, leading to the opening of the mPT pore and ATP depletion, which in turn leads to necrosis [130]. In order to test if HYD1 treatment induced an increase in intracellular Ca^{2+}, H929 and H929-60 cells were incubated with Fura-2 dye and time lapse images were taken for either 60 minutes after treatment with HYD1 or 30 minutes for HM-27. Both HYD1 (75 μM) and HM-27 (3 μM) were shown to elevate levels of intracellular Ca^{2+} in H929 and H929-60 cells. HYD1 and HM-27 induced intracellular Ca^{2+} oscillations were also reduced in H929-60 cells when compared to H929 cells (figure 28). Individual H929 cells were examined to determine if there were differences between the total levels or temporal differences in Ca^{2+} levels after HYD1 or HM-27 treatment. As seen in figure 29, Ca^{2+} levels were increased and occur earlier (10 minutes) after treated with HM-27 when compared to HYD1 (30 minutes). These data suggest that HM-27 is more efficient in eliciting a Ca^{2+} response in MM cells when compared to HYD1.

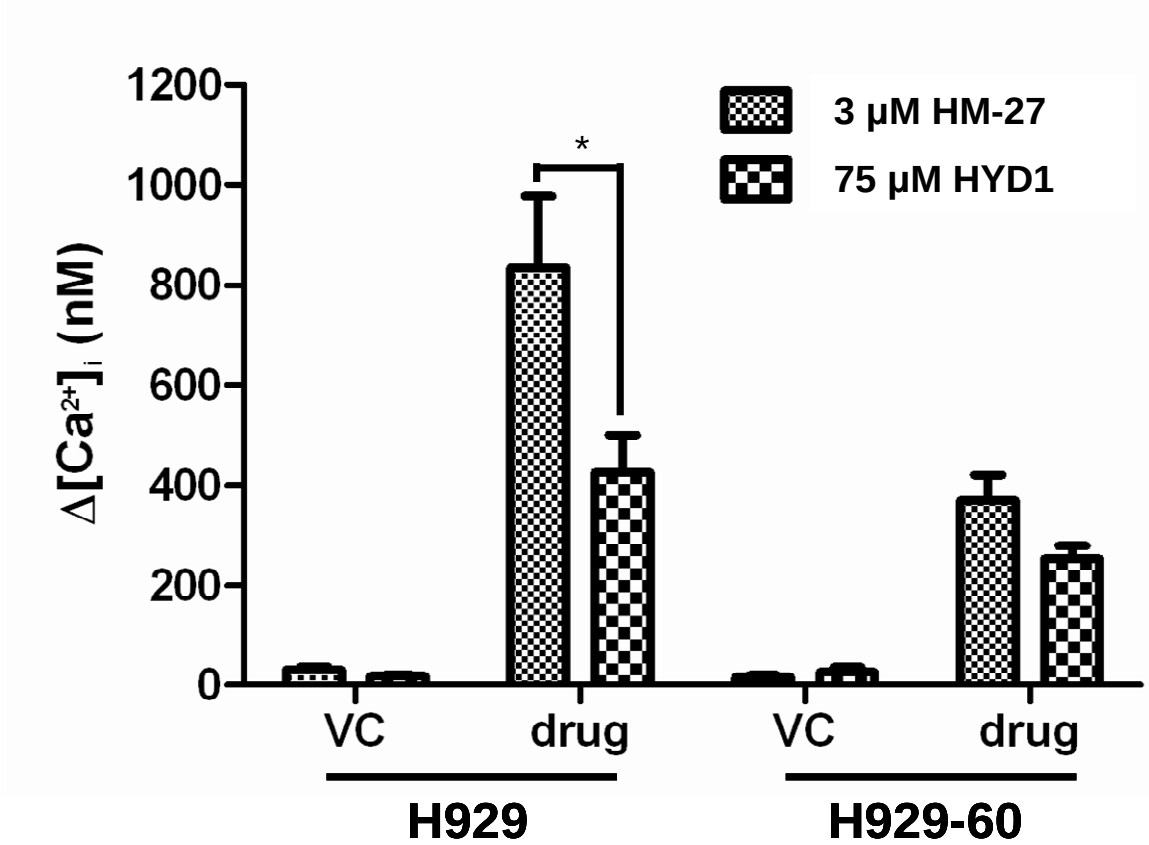

Figure 30: Intracellular Ca^{2+} levels are increased after treatment with HYD1 and HM-27. H929 and H929-60 cells were adhered to cell-tak coated plates for 15 minutes and then incubated with Fura-2 dye for 30 minutes. Time lapse images were taken for either 60 minutes after treatment with 75 μM HYD1 or 30 minutes after treatment with 3 μM HM-27. A representative of three independent experiments was shown. (* =$p<0.05$, Students t-test).

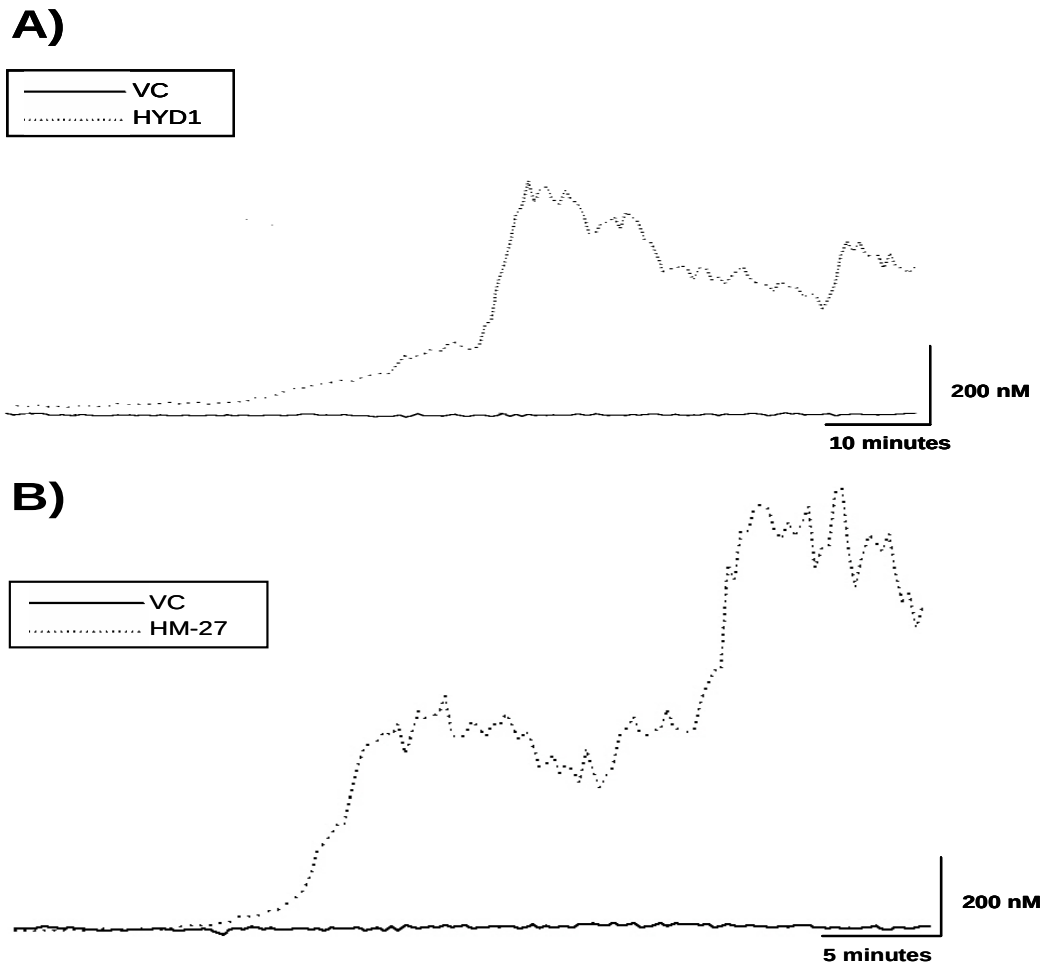

Figure 31: There were differences in total levels of Ca^{2+} and differences in the time needed to induce a Ca^{2+} response after treatment with HYD1 and HM-27. H929 and H929-60 cells were adhered to cell-tak coated plates and were incubated with Fura-2 dye for 30 minutes. Time lapse images were taken for either 60 minutes after treatment with 75 μM HYD1 or 30 minutes after treatment with 3 μM HM-27. A representative cell closest to the median Ca^{2+} response of the whole population was shown.

HM-27 induced increases in intracellular Ca^{2+} are a result of release from ER stores and blocking this release resulted in increased HM-27 induced cell death.

Increases in intracellular Ca^{2+} occur either by influx via plasma membrane channels or by release from internal stores in the ER or mitochondria. In order to determine the source of HM-27 induced intracellular Ca^{2+} oscillations, H929 cells were pretreated with the PLC inhibitor, U73122, in order to block Ca^{2+} release from the ER or placed in a PSS buffer that did not contain $CaCl_2$ in order to block Ca^{2+} influx through plasma membrane channels. As shown in figures 30 and 31, inhibiting Ca^{2+} influx through plasma membrane channels by depleting extracellular Ca^{2+} stores did not decrease the levels of Ca^{2+} induced by HM-27 treatment. However, blocking the release of Ca^{2+} from ER stores using U73122 decreased HYD1 induced Ca^{2+} oscillations. In addition, inhibiting both the release of Ca^{2+} from ER stores and Ca^{2+} influx through plasma membrane channels completely blocked the HM-27 induced Ca^{2+} response. These data suggest that the increase in intracellular Ca^{2+} seen after treatment with HM-27 were a result of the release of Ca^{2+} from ER stores and not from influx via plasma membrane channels.

Next, it was determined if blocking the release of Ca^{2+} from ER stores would inhibit HM-27 induced cell death. Instead of inhibiting HM-27 induced cell death, pretreating with U73122 actually increased cell death (figure 32A). Next it was determined if there was a relationship between HYD1 induced Ca^{2+} oscillations and induction of autophagy. Previous reports have shown that beclin 1 and the ip3 receptor form a complex along with Bcl-2 on the ER membrane and disrupting this

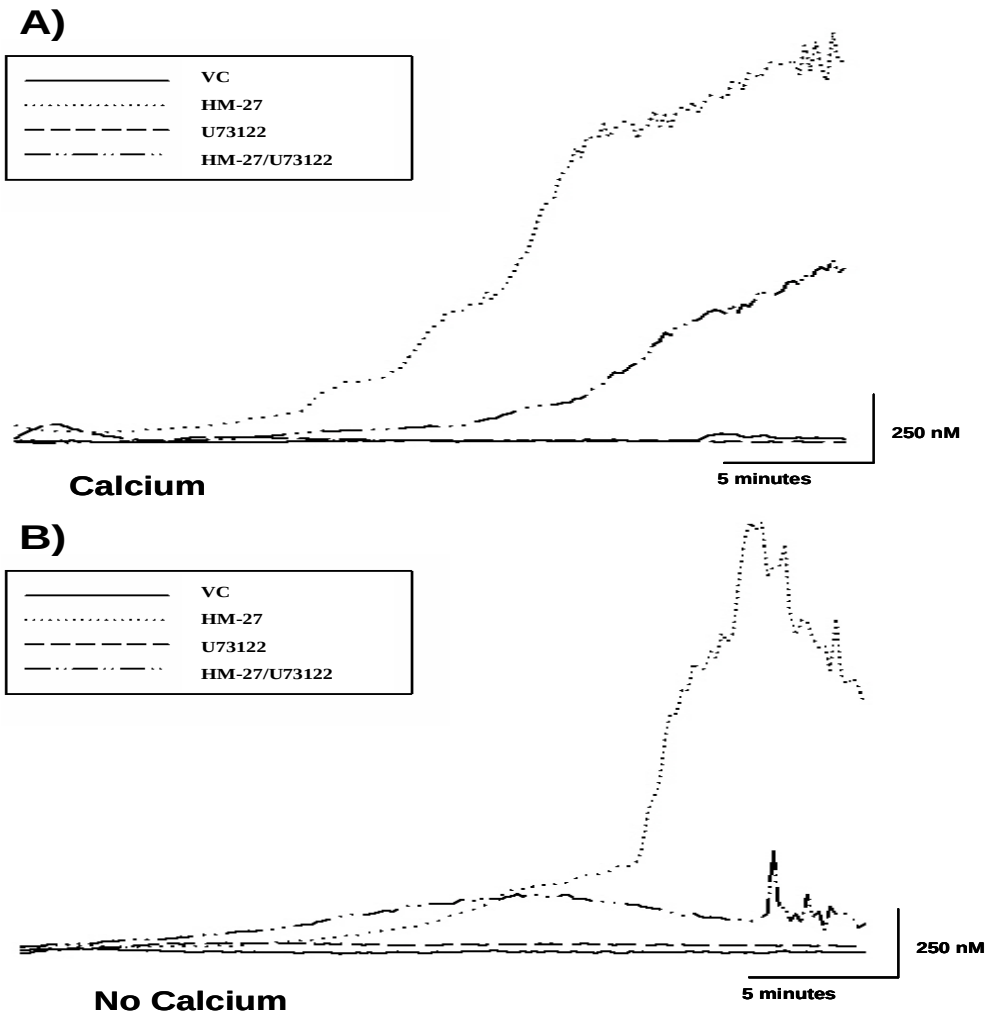

Figure 32. HYD1 induced Ca^{2+} oscillations occur via release from ER stores. H929 cells were adhered to cell-tak coated plates and then incubated with Fura-2 dye +/- U73122 for 30 minutes in PSS containing Ca^{2+} and PSS without Ca^{2+}. Time lapse images were taken for 30 minutes after treatment with 3 μM HM-27. A representative cell closest to the median Ca^{2+} response of the whole population was shown.

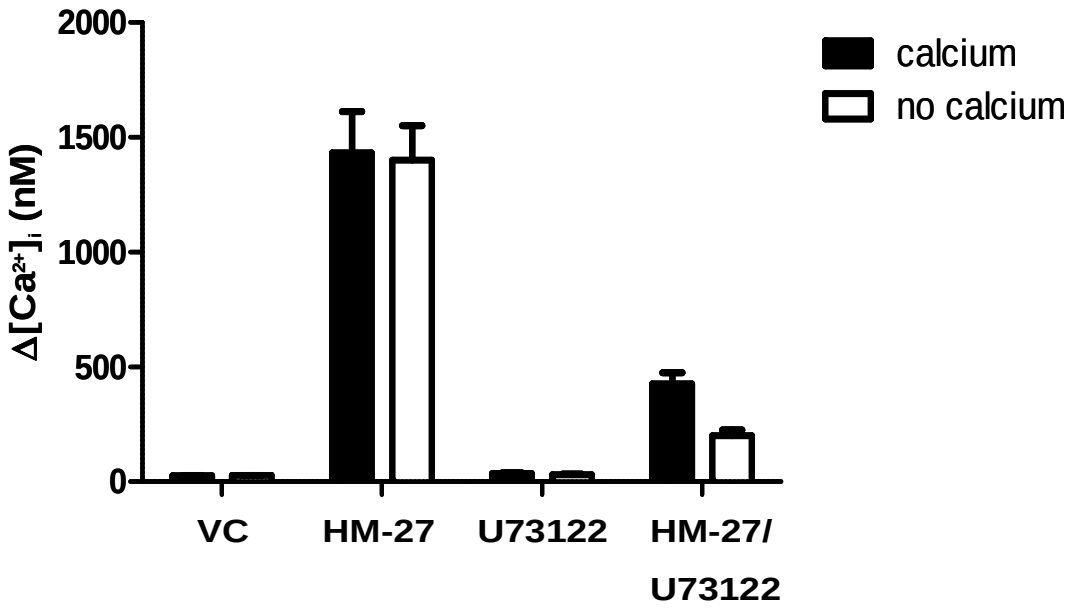

Figure 33. HYD1 induced Ca^{2+} oscillations occur via release from ER stores. H929 cells were adhered to cell-tak coated plates and then incubated with Fura-2 dye +/- U73122 for 30 minutes in PSS containing Ca^{2+} and PSS without Ca^{2+}. Time lapse images were taken for 30 minutes after treatment with 3 μM HM-27. A representative experiment is shown.

complex initiates the formation of autophagic vesicles. In order to determine if Ca^{2+} release from the ER causes an induction in autophagy, nucleoporin p62 degradation after HM-27 treatment was analyzed. As seen in figure 32B, HM-27 induced p62 degradation in H929 cells, indicating that HM-27 induced autophagy. Cells pretreated with U73122 partially blocked the degradation of p62, indicating that Ca^{2+} released from the ER causes the induction of autophagy seen after HM-27 treatment. As inhibiting autophagy or Ca^{2+}

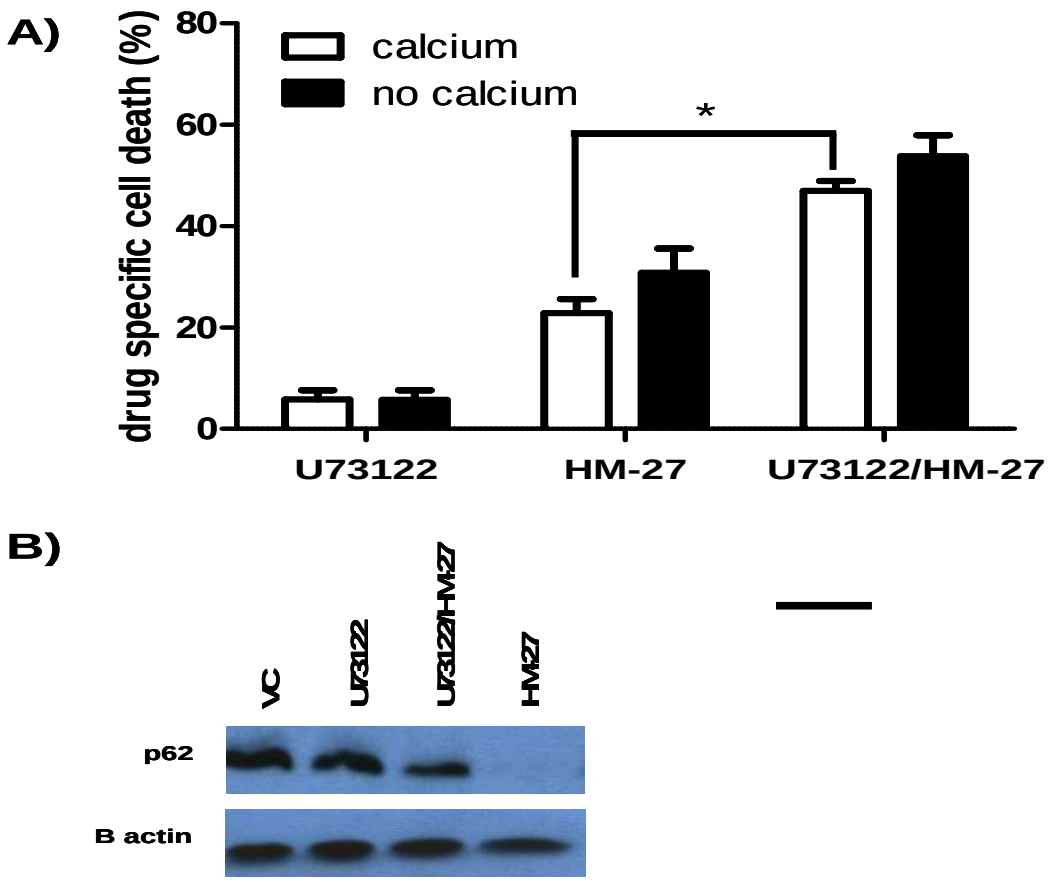

Figure 34. Inhibiting Ca^{2+} release from ER stores led to increased HM-27 induced cell death and blocked HM-27 induced autophagy. A) H929 were pretreated with 2 μM U73122 and treated with 3 μM HM-27 for 2 hours in PSS +/- Ca^{2+}. Drug induced cell death was determined by Topro-3 staining and FACS analysis. B) H929 were pretreated with 2 μM U73122 and treated with 3 μM HM-27 for 4 hours. Whole cell lysates of H929 cells were probed for p62 and beta actin by Western blot analysis. The experiments were repeated 3 independent times and shown is a representative experiment. (* = $p<0.05$, student's t-test

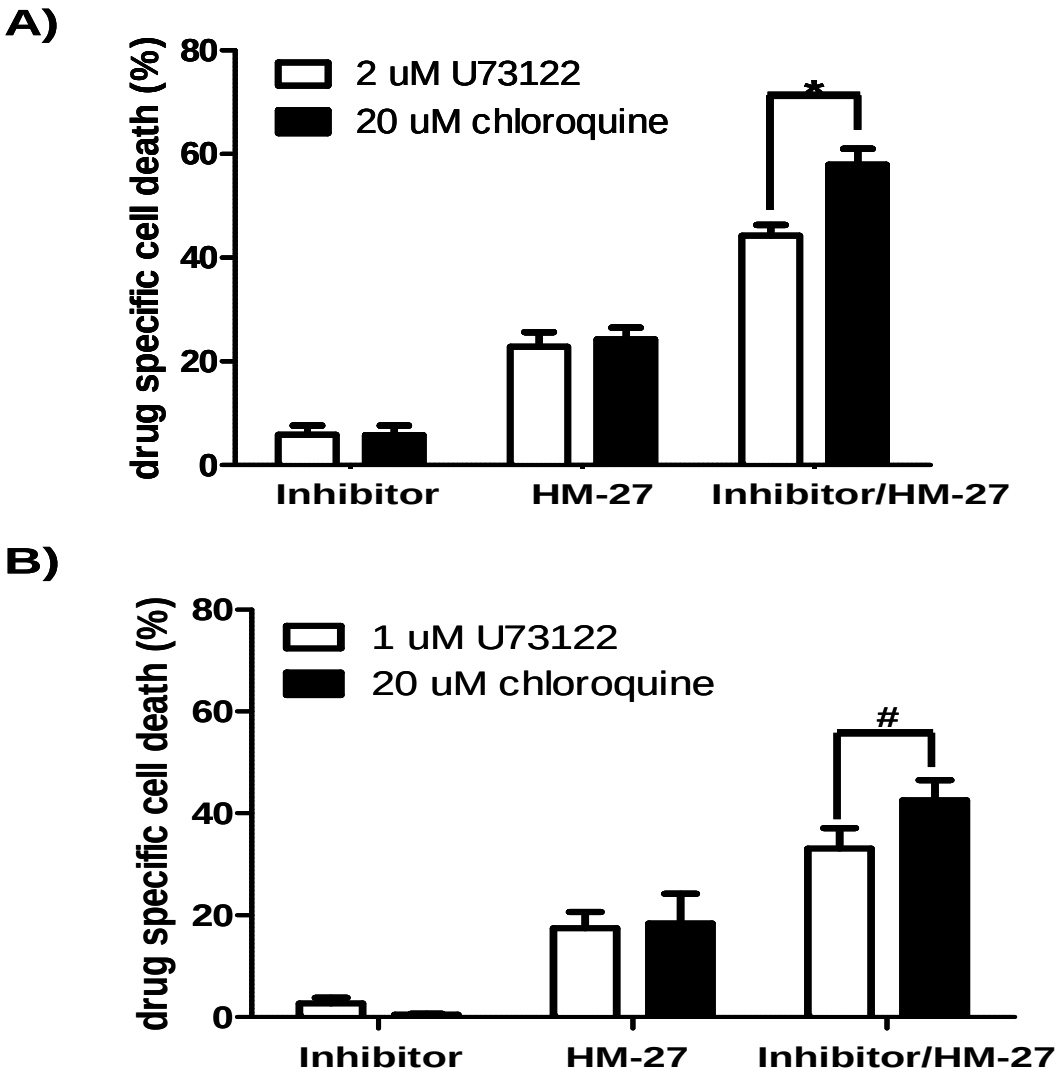

Figure 35. There is increased HM-27 induced cell death in MM cells pretreated with chloroquine when compared to cells pretreated with U73122. A) H929 and B) 8226 cells were pretreated with either U73122 or chloroquine for 30 minutes. Cells were then treated with 3 μM HM-27 for 2 hours. Drug induced cell death was determined by Topro-3 staining and FACS analysis. The experiments were repeated 3 independent times and shown is a representative experiment. (*= $p<0.05$, #=$p>0.05$, student's t-test)

release from the ER have both been shown to increase cell death after treatment with HM-27, H929 and U266 cells were pretreated with either the lysosomotropic agent chloroquine, which neutralizes lysosomal vesicles, or the plc inhibitor U73122 followed

by treatment with HM-27. As seen in figure 33 A and B, there was increased HM-27 induced cell death in MM cells pretreated with chloroquine when compared to cells pretreated with U73122. While more studies are needed to delineate the mechanism of how Ca^{2+} regulates autophagy after HM-27 treatment, these data do suggest that HM-27 cell death can be enhanced *in vitro* by inhibiting autophagy or Ca^{2+} release from the ER.

HM-27 induced cell death is increased in relapsed myeloma patient specimens with chloroquine pretreatment potentiating this effect.

In order to determine whether primary myeloma specimens are sensitive to HM-27 induced cell death, 6 newly diagnosed and 6 relapsed myeloma specimens were collected. Immunomagnetic beads were used to enrich for CD138 positive malignant plasma cell fractions. HM-27, like HYD1, was significantly more active in relapsed refractory patients compared to newly diagnosed patients. Patient samples were also treated with chloroquine to see if inhibiting autophagy would enhance HM-27 induced cell death *ex vivo*. As seen in figure 34, pretreatment with chloroquine potentiated HM-27 induced cell death in relapsed patient specimens but did not have any activity in newly diagnosed patients. Together, these data suggest that HM-27 like HYD1 has increased activity in relapsed patient samples compared to newly diagnosed specimens and pretreatment with agents that inhibit autophagy enhance HM-27 induced cell death *ex vivo*.

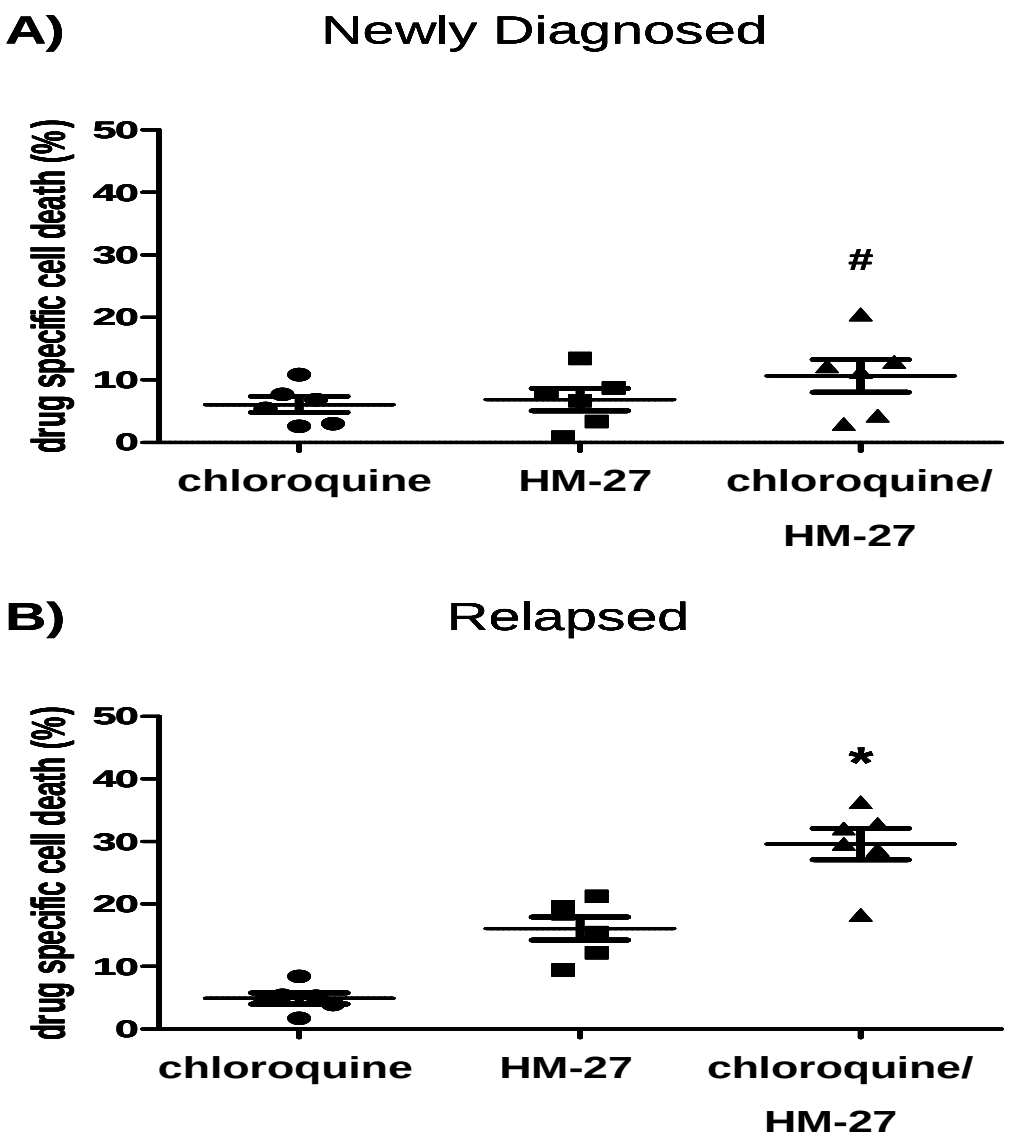

Figure 36. HM-27 induced cell death is increased in relapsed myeloma patient specimens with chloroquine pretreatment potentiating this effect. Specimens were separated into two groups depending on the clinical diagnosis; either A) newly diagnosed or B) relapsed patients. CD138+ cells were pretreated with 20 μM of chloroquine for 30 minutes followed by 6 μM of HM-27 for 24 hours. After 24 hours cell death was measured by Topro-3 staining and FACS analysis (Student's t-test * = $p<0.05$, # = $p>0.05$).

HM-27 has antitumor activity in an *in vivo* model.

C57BL/KaLwRijHsd mice were used to determine if HM-27 demonstrates anti-tumor activity *in vivo*. 6- to 8- week old mice were injected with 5TGM1 cells via their tail vein. At day 10 after injection, mice were treated with either 10 mg/kg HM-27, 25 mg/kg HM-27 or 0.5 mg/kg bortezomib. Mice were treated with drug 3 times a week for 3 weeks. An enzyme-linked immunosorbent assay (ELISA) was used to measure tumor burden by measuring IgG2B levels in serum each week for 4 weeks. On day 27, control mice had increased IgG2B levels when compared to drug treated mice with mice expressing levels over 1 mg/ml exhibiting hind leg paralysis (figure 35A). Survival was determined with mice being euthanized if they exhibited hind leg paralysis, an extended abdomen or the presence of a tumor over 2 cm in diameter or reached 100 days post inoculation. As seen in figure 35B, mice treated with 10 mg/kg of HM-27, 25 mg/kg HM-27 or 0.5 mg/kg of bortezomib displayed increased survival when compared to control mice. Since pretreatment with chloroquine potentiated HM-27 induced cell death *in vitro* and *ex vivo*, mice were treated with chloroquine and HM-27 to determine if there is increased *in vivo* activity when the drugs were given in combination compared to each drug alone. Mice were treated with 10 mg/kg chloroquine on days 9, 16, and 23 while mice were treated with 10 mg/kg HM-27 on days 10, 13, 15, 17, 20, 22, 24, 27 and 29. ELISA data indicated that there was increased tumor burden in control cells compared to cells treated with HM-27, chloroquine and combination treatment (figure 36A). However, there was no added survival benefit when chloroquine and HM-27 were

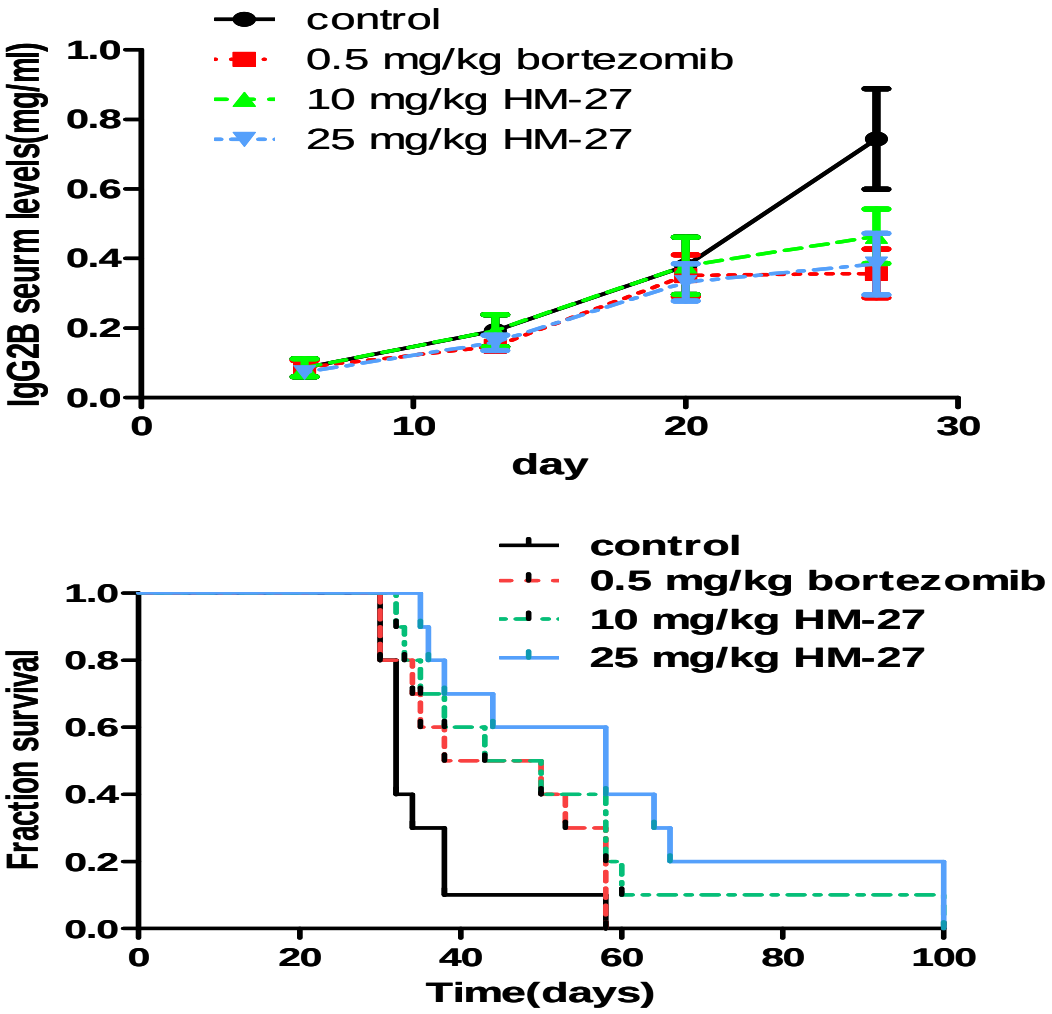

Figure 37: HM-27 has increased antitumor activity as a single agent *in vivo*. A) IgG2B serum levels were measured by ELISA once a week for 4 weeks per the manufacturer's instructions. B) $1x10^6$ 5TGM1 cells were injected into 6-8 week old C57BL/KaLwRijHsd mice via tail vein. At day 10, mice were treated with agents 3 times a week for 3 weeks. Mice were monitored daily for survival with all remaining mice euthanized at day 100 after treatment

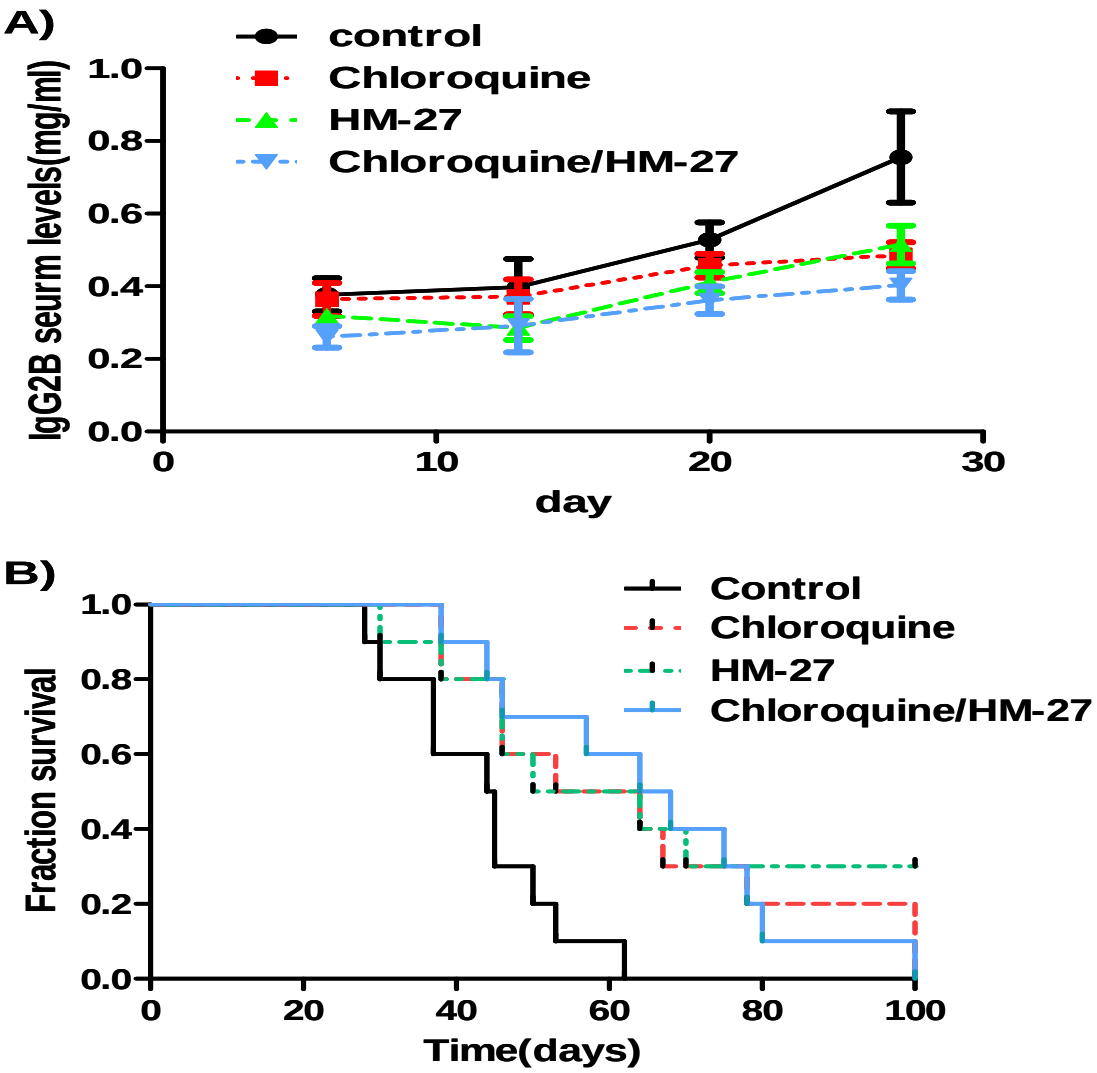

Figure 38: Combination treatment with HM-27 and chloroquine does not increases cell survival *in vivo*. . A) IgG2B serum levels were measured by ELISA once a week for 4 weeks per the manufacturer's instructions. B) $1x10^6$ 5TGM1 cells were injected into 6-8 week old C57BL/KaLwRijHsd mice via tail vein. Mice were treated with 10 mg/kg of chloroquine on days 9, 16, and 23. At day 10, mice were treated with 10 mg/kg of HM-27 3 times a week for 3 weeks. Mice were monitored daily for survival with all remaining mice euthanized at day 100 after treatment.

combined compared to chloroquine or HM-27 as a single agent (figure 36B). Combination studies were also done with bortezomib and HM-27 to determine if there is increased *in vivo* activity when the drugs were given in combination compared to each drug alone. Mice were treated with 0.5 mg/kg of bortezomib or 10 mg/kg HM-27 3 times a week for 3 weeks starting on day 10. ELISA data indicated that there was increased tumor burden in control cells compared to cells treated with HM-27, bortezomib and combination treatment (figure 37A). There also appears to be an increased survival in mice treated with both agents compared to mice treated with a single agent (figure 37B) These data indicate that HM-27, bortezomib and chloroquine each have *in vivo* activity as a single agent. Combination therapy utilizing bortezomib and HM-27 appears to have increased activity *in vivo* while combination therapy with chloroquine and HM-27 do not appear to have increased activity. More studies are needed to determine if there are ways to optimize the treatment schedule with chloroquine and HM-27 to see increased activity in combination.

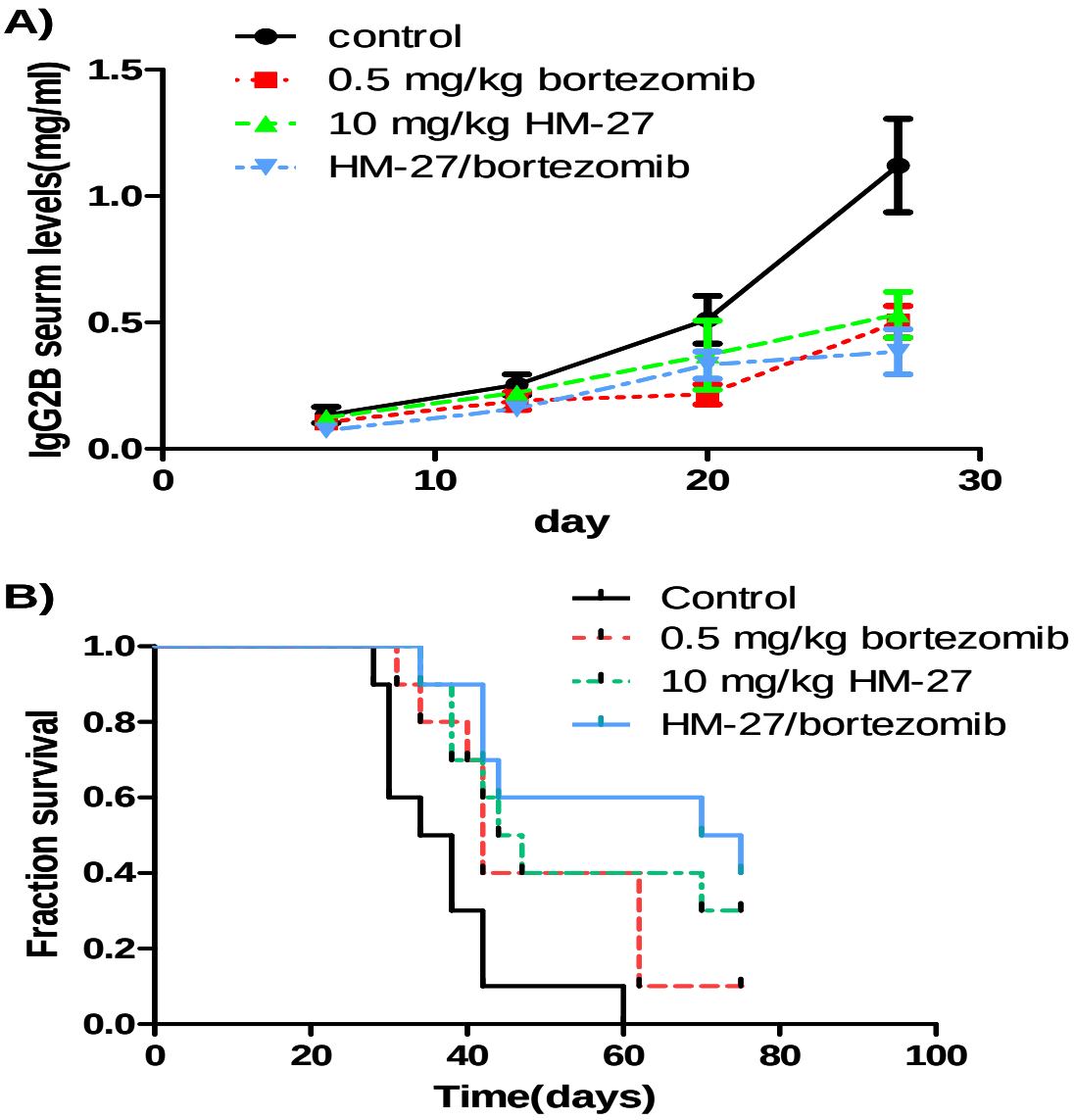

Figure 39: Combination treatment with HM-27 and bortezomib increases survival *in vivo*. A) IgG2B serum levels were measured by ELISA once a week for 4 weeks per the manufacturer's instructions. B) $1x10^6$ 5TGM1 cells were injected into 6-8 week old C57BL/KaLwRijHsd mice via tail vein. At day 10, mice were treated with 10 mg/kg of HM-27 and 0.5 mg/kg bortezomib 3 times a week for 3 weeks. Mice were monitored daily for survival.

Chapter 10: Discussion and Future Directions

Isogenic resistant cell lines have been used by many investigators as a model system for delineating important molecular determinants of response for novel as well as for developing and evaluating clinically approved agents [177-181]. Historically, some of these cell line models have allowed for the identification of targets associated with drug sensitivity and resistance[182]. Selection with HYD1 on H929 cells resulted in the formation of the resistant cell line, H929-60. By analyzing gene expression profiling data on both cell lines, it was determined that there were a significant number of integrin genes changed when H929 cells were selected with HYD1. Interestingly, even though H929-60 cells did not have reduced gene expression of α4 integrin, there was decreased protein surface expression of α4 integrin. Quantitative RT-PCR expression of α4 integrin validated the gene expression profiling data, indicating that the decrease in protein expression in α4 integrin is due to a post transcriptional modification. There are ways in which protein expression of α4 integrin are decreased even though gene expression was similar. H929-60 cells could have decreased rates of translation when compared to H929 cells. There could also be increased rates of α4 integrin mediated endocytosis and degradation by lysosomes or there could be increased rates of α4 integrin degradation by the proteasome in H929-60 cells. Fluorescein labeled transferrin could be used to determine if there is increased endocytosis in H929-60 cells. Blocking the proteasome in

H929-60 cells can also be used to see if there is restoration of α4 integrin levels after proteasome inhibition.

HYD1 was previously characterized as a β1 inhibitory peptide as it inhibited adhesion to laminin by binding to α3 and α6 integrins. HYD1 was not shown to inhibit the ability of the α6β4 integrin to adhere to laminin however. Therefore most of the studies done on the HYD1 resistant cells focused on the α4β1 heterodimer. Using this logic, we determined that knocking down surface expression of α4 and β1 integrins was sufficient to decrease HYD1 induced cell death in MM cell lines. However, α4 integrin has been shown to heterodimerize with either β1 integrin or β7 integrin. β7 integrin, like α4 integrin, displayed no change in gene expression but exhibited decreased surface protein expression in H929-60 cells. A previous study has shown that increased β7 integrin expression correlated with poor survival in MM cell lines and patient samples [95]. More studies are needed to determine if HYD1 also targets the α4β7 heterodimer as well as VLA-4. The surface expression of β7 integrins can also be knocked down as a way to determine if the α4β7 heterodimer is also implicated in HYD1 induced cell death.

Previous data showed that HYD1 was able to block adhesion of MM cells to FN after 2 hours but was not able to block adhesion of MM cells to HS-5 cells. However, selection with HYD1 resulted in a cell line with compromised adhesive interactions towards extracellular matrices and HS-5 bone marrow stroma cells and MSCs. Since MM cell adhesion to stromal cells occurs by a multitude of receptors, it would be interesting to determine if any of the other adhesion mediated receptors besides VLA-4 and α4β7 integrins are changed as cells are selected for HYD1 resistance. One explanation could be that MM cells bind to stromal cells through both α4β1 and α4β7

integrins but HYD1 is only able to target α4β1 integrin therefore not inhibiting the adhesive capabilities of α4β7 integrin. However, as H929-60 cells are selected for resistance, they lose surface expression of α4 integrins thereby downregulating both the α4β1 and α4β7 heterodimers thereby decreasing adhesion to stromal cells. Another explanation is that other receptors that mediate adhesion of MM cells to BMSCs are downregulated. Subsequent studies have also shown that there is also decreased surface protein expression of CD44 in the resistant cell line, which has been shown to mediate MM adhesion to bone marrow stromal cells and contribute to CAM-DR [14]. Conversely, gene expression profiling data showed that there was an 8 fold increase in αL integrin in H929-60 cells compared to H929 cells. Alpha L integrin dimerizes with β2 integrin to form LFA-1, a protein that adheres to ICAM receptors on BMSCs and has been shown to contribute to CAM-DR [66]. It can be speculated that HYD1 resistant cells compensate for decreased α4 integrin levels by upregulating the expression of other proteins responsible for adhesion to stroma cells. Future studies would be aimed at determining the surface expression levels of proteins such as LFA-1, notch-1 and CD138 which mediate adhesion to stromal cells and contribute to CAM-DR.

It was reasoned that a reduction in functional binding to the HS-5 bone marrow stroma cell line may render the HYD1 resistant cell line sensitive to standard therapy in the co-culture model of drug resistance. Indeed this was found to be true, as the HYD1 resistant cell line was not resistant to melphalan or bortezomib induced cell death in the co-culture model of drug resistance. Moreover, it was demonstrated that α4 integrin expression and sensitivity towards HYD1 was increased in specimens obtained from relapsed patients compared to newly diagnosed patients, suggesting that α4 expression is

selected either as a consequence of standard drug exposure or disease progression. Previous studies have shown that α4 integrin is increased in relapsed patient samples, when compared to newly diagnosed patients [93]. This observation in patient specimens is also in agreement with acquisition of resistance towards melphalan and doxorubicin in myeloma cell lines as expression of α4 integrin increased with selection for drug resistance[69]. It is attractive to speculate that agents which disrupt cell adhesion may indeed be a good strategy for compromising the overall fitness of cells in the context of the BME. Agents that disrupt cell adhesion may be critical to test the development of evolutionary based double bind strategies, where resistance to a drug is predicted to occur at the cost of fitness within the niche. The utilization of double bind strategies is a unique concept recently proposed by Gatenby and colleagues for delaying the emergence of resistant variants in the treatment of cancer and indeed HYD1 may fit the criteria for an agent to test this unique therapeutic strategy [183].

Our data indicate that reducing α4β1 integrin expression was sufficient to confer partial drug resistance to HYD1. However, since only partial resistance was observed, additional components contained within the HYD1 binding complex may contribute to HYD1 induced cell death. An unbiased approach was used in order to determine other surface proteins that are found in the complex with which HYD1 interacts. We incubated membrane fractions with biotin conjugated HYD1 in order to identify other proteins that bind to HYD1 by mass spectrometry. Other proteins that bound to biotin HYD1 besides α4 integrin were CD44, CD147 and CD138. Previous studies have shown that CD44 and VLA-4 interact on the surface of malignant B cells but not normal B cells [184]. CD147 has been shown to induce metalloproteinases as well as interact with CD44 on metastatic

prostate cancer cells. CD138 also mediates MM cell adhesion to BMSCs. Further studies with CD44 have shown that overexpression of CD44 on 8226 cells sensitizes these cells to HM-27, implicating CD44 as another key protein in the complex with more studies to be done on CD147 and CD138. It would be interesting to speculate that HYD1 and HM-27 disrupt a complex that contains these proteins that have been shown to be of vital importance to CAM-DR and metastasis in MM and cancer in general. However HYD1 and HM-27 could be interacting with each surface protein individually and is not disrupting a specific complex. Future studies are aimed at determining the primary binding targets for HYD1 and HM-27 and if direct binding to the target or disruption of a binding complex induces cell death in MM cells.

We were able to show that expression of α4 integrin in primary patient specimens correlated with sensitivity towards HYD1 induced cell death *ex-vivo,* a finding that correlated well with our cell line observations. We propose that to ensure adequate designs of trials it is essential to define biomarkers of response using patient specimens in early phases of drug development, as response markers can take time to validate and often lag behind the design of early clinical trials[185]. Additionally, our studies indicate that a larger study determining the prognostic value of VLA-4 integrin is warranted in multiple myeloma. In the drug resistant cell line, we observed a predominant reduction in the cleavage of α4 integrin compared to the mature form. Interestingly, α4 integrin is the only integrin that has been shown to exist in a cleaved and mature form on the plasma membrane. While there is no definitive answer as to why the α4 integrin is cleaved, previous studies comparing the cleaved form and mature form have showed that as T cells are activated they shift expression from the mature form to the cleaved form [186].

However, functional studies have shown that there is no difference in integrin mediated adhesion to FN when the two isoforms are compared in chronic myelogenous leukemia cells [92]. It is intriguing to speculate whether the cleaved fragment of α4 integrin is required for HYD1 induced cell death and whether the cleaved form has any significance with respect to disease progression in multiple myeloma.

Recent data demonstrate that targeting α4 integrin in a syngeneic mouse 5TGM1 model via monoclonal antibody treatment reduced the tumor burden in the bone marrow, spleen and liver[187]. Moreover, the VCAM-1/VLA-4 axis increases MIP-1 alpha and beta levels and increases the ability of myeloma cells to support osteoclastogenesis[188]. Based on these findings, it will be important to determine whether HYD1 inhibits the ability of myeloma cells to disrupt bone homeostasis by either inhibiting the activation of osteoclasts or disrupting the ability of myeloma cells to inhibit the differentiation of osteoblasts[189-191]. Another strategy for targeting integrins is to inhibit pathways required for inside-out activation of VLA-4 integrins. Thus VLA-4 can be modulated by regulating the affinity for ligand as well as clustering or avidity of the integrin heterodimer[192, 193]. A potential strategy could include targeting Rap1, which is known to be required for inside out activation of VLA-4[194]. Another approach is inhibition of CXCR4, where recently, Azab et al. showed that AMD3100 inhibits adhesion of myeloma cells to stroma and sensitized myeloma cells to chemotherapy in co-culture models of drug resistance[175]. However, HYD1 is unique to our knowledge, as in addition to blocking cell adhesion, HYD1 induces necrotic cell death directly in the myeloma cell, a finding that was not observed with α4 blocking antibody or RGD containing peptides (data not shown).

HYD1 induced necrotic cell death was characterized by increased mitochondrial dysfunction and an increase in ROS. In order to determine pathways that may lead to increased mitochondrial dysfunction, we analyzed the gene expression profiling data for changes in expression between H929-60 and H929 cells. One pathway that was determined to be significant changed using GeneGO software was the intracellular Ca^{2+} signaling pathway, specifically the release of Ca^{2+} from ER stores. Guanine nucleotide-binding protein G(q) subunit alpha (GNAQ) is the G protein subunit responsible for the activation of plc-β and was decreased by 2.5 fold in H929-60 cells. Plc-β is responsible for the cleavage of PIP2 into DAG and ip3 and was decreased by 2 fold in H929-60 cells. The ip3 receptor is located on the ER membrane and when bound by ip3 releases Ca^{2+} from ER stores. There are 3 isoforms of the ip3r but only the 3rd isoform was shown to be expressed in H929 cells with a 1.9 fold decrease in expression in H929-60 cells. Previous studies have shown that when Ca^{2+} is released into the cytosol via release from ER stores, or when extracellular Ca^{2+} crosses the plasma membrane, cell death can be initiated due to mitochondrial Ca^{2+} overload. Decreased levels of HYD1 and HM-27 induced Ca^{2+} oscillations in H929-60 cells were observed when compared to H929 cells. However when these oscillations were inhibited by U73122, there was an increase in HM-27 induced cell death instead of a decrease in cell death. These data suggest that the release of Ca^{2+} after HYD1 and HM-27 treatment contribute to cell survival instead of cell death. In addition to studies showing that increases in intracellular Ca^{2+} can cause mitochondrial overload and increases in ROS, other studies have shown that superoxides can enhance ip3 induced Ca^{2+} release from the ER [195]. Preliminary data from our lab also showed that preincubation with NAC was able to inhibit HYD1 induced Ca^{2+}

oscillations in H929 and 8226 cells suggesting that an increase in ROS caused the release of Ca^{2+} from ER stores after HYD1 treatment. More studies are needed to determine the association between mitochondrial dysfunction, increases in ROS and Ca^{2+} release from the ER after treatment with HYD1.

Our data shows that HM-27 is more efficient at eliciting a Ca^{2+} response in MM cells when compared to HYD1. On closer examination of the Ca^{2+} response after treatment with HM-27, there appears that there could be a biphasic response. It is known that depleting Ca^{2+} from ER stores can cause the influx of Ca^{2+} from the extracellular compartment via store operated channels. A Ca^{2+} sensor that spans the ER membrane, STIM1, is able to detect when ER stores of Ca^{2+} are depleted. When this happens, STIM1 interacts with ORAI1 on store operated channels which causes influx of Ca^{2+} into the cell. The STIM1/ORAI1 pathway supports the data that there appears to be an initial smaller Ca^{2+} response after treatment with HM-27 with a greater response occurring later. However, depleting extracellular levels of Ca^{2+} did not decrease the increases in Ca^{2+} seen after treatment with HM-27 while blocking release of Ca^{2+} from ER stores did decrease HM-27 induced Ca^{2+} levels, indicating that the Ca^{2+} response seen is through release of ER stores. It could be argued that the initial increase in Ca^{2+} is a result of influx from plasma membrane channels and the subsequent increase in Ca^{2+} occurs because of release from ER stores. Pretreatment with U73122 decreased the levels of intracellular Ca^{2+} seen after HM-27 treatment to around the levels that are seen during the primary Ca^{2+} response after HM-27 treatment. Removing extracellular Ca^{2+} did not decrease the overall levels of Ca^{2+} seen after HM-27 treatment but removing extracellular Ca^{2+} and pretreating with U73122 completely blocked the Ca^{2+} response. Subsequent

studies are needed to determine the exact mechanism of Ca^{2+} response after HM-27 treatment.

If increases in intracellular Ca^{2+} are not causing mitochondrial overload and necrotic cell death, the next question becomes what is causing these events. Recent evidence is suggests that necrosis is not just an accidental form of cell death but instead can be regulated like apoptosis. One such form of regulated necrosis has been termed necroptosis. Necroptosis has been shown to be activated by ligation of cell death receptors such as FAS, TNFR and TRAILR. Upon binding of ligands, these receptors recruit several death domain-containing proteins such as RIP1, RIP3, and caspase 8 [134]. If caspase 8 is not inhibited, caspase 8 cleaves RIP1 and RIP3 and induces caspase dependent apoptosis. If caspase 8 is inhibited, RIP1 and RIP3 become phosphorylated and induce necroptosis [135]. Phosphorylated RIP1 causes PARP activation, ATP depletion, activation of ROS and an increase in intracellular calcium, all considered to be hallmarks of necrosis. Data generated in our lab showed that inhibiting RIP1 with necrostatin was able to partially block HM-27 induced cell death, indicating that HM-27 induced cell death may result from necroptosis. One way in which RIP1 causes mitochondrial dysfunction is through translocation of the mitochondrial fissure protein DRP1 from the actin cytoskeleton to the mitochondria [196]. Previous studies have also shown that ligation of the membrane protein CD47, or integrin associated protein, caused translocation of DRP1 from the cytoskeleton to the mitochondria and caused subsequent necrotic cell death in B-cell leukemia [197]. It would be intriguing to examine why HYD1 and HM-27 are causing necrotic cell death in MM cells by either associating with

death cell receptors on the plasma membrane or by causing translocation of DRP1 from the cytoskeleton to the mitochondria.

The studies in C57BL/KaLwRijHsd mice show that HM-27 has activity in an *in vivo* model and combination treatment of bortezomib and HM-27 seemed to increase mouse survival while combination treatment with chloroquine and HM-27 did not. The results with chloroquine and HM-27 were surprising as pretreatment with chloroquine was shown to potentiate HM-27 induced cell death *in vitro* and *ex vivo*. One issue could be the treatment schedule in mice. As chloroquine has an extremely long half life in *in vivo* systems, we decreased the amount of times the mice were treated from 9 days to 3 days. Maybe there would be increased survival after combination treatment if the amount of treatments were increased to 9. Interestingly, it was also shown that chloroquine had activity as a single agent. This result is consistent with previous reports that chloroquine has activity in breast cancer and colon cancer mouse models [198, 199]. Previous data from our lab has shown that HYD1 potentiated melphalan activity in the SCID-hu model. Since selection of resistance to melphalan in MM cells results in cells that express higher levels of α4 integrin, it would be interesting to see if there is increased survival when these agents are combined in the 5TGM1 mouse model.

Based on the data generated, it is interesting to speculate how HYD1 and HM-27 are inducing cell death in MM myeloma cells. CD44 and VLA-4 have been shown to localize together on the plasma membrane and have both been shown to mediate cell adhesion to the ECM protein FN. Adhesion to FN by integrins promotes both the formation and growth of focal adhesions. One kinase that gets recruited to the focal adhesion and activates downstream pathways, such as the AKT and ERK pathways, is

FAK/pyk2. In addition to activating these pathways, FAK/pyk2 has also been shown to interact with proteins and inhibit death signals when cells are adhered to ecm proteins. FAK has been shown to interact with the death domain of RIP1, therefore inhibiting the formation of the death complex and RIP1 mediated cell death [200]. Src has also been shown to interact with FAK and phosphorylate procaspase-8 on procaspase-8's Tyr380 residue, resulting in a loss of caspase-8 proapoptotic function [201, 202]. As shown in figure 40, HYD1/HM-27 could function to mimic a region of FN that binds to CD44. By mimicking FN and binding to CD44 but not VLA-4, the peptides are causing disappropriate downstream signaling. Incubation with HYD1/HM-27 has been shown to cause transient activation of pyk2 and ERK, indicating that HYD1/HM-27 is causing the formation of focal adhesions and subsequent downstream signaling. However, since HM-27 is not binding to VLA-4 or other proteins that mediate adhesion to FN, FAK/pyk2 does not associate with RIP1 and inhibit RIP1's ability to cause cell death. However, HYD1/HM-27 binding to CD44 is still causing Src mediated phosphorylation of procaspase-8 and inhibiting apoptosis induced by caspase-8. This disassociation would cause RIP1 to generate a death complex resulting in cell death induced by necrosis and cell survival signals including release of Ca^{2+} from the ER and induction of autophagy. One way to test this hypothesis would be to do immunoprecipitation assays in the presence or absence of FN and compare to immunoprecipitation assays in the presence and absence of HM-27 to determine if RIP1 associates with pyk2 in the presence of FN and if this association is disturbed upon treatment with HM-27.

Historically, drug development has focused on aberrations in signaling intrinsic to the tumor cells using unicellular models. However, it has been argued that tumors evolve

in the context of the microenvironment, and thus it is feasible that some phenotypes observed in tumors such as drug resistance and metastasis will only be expressed in the context of cues derived from the microenvironment [174, 203-205]. In summary, our data continue to support the premise that targeting survival signals that occur between tumor cells and the microenvironment is an attractive strategy for increasing the therapeutic potential of combination regimens and may lead to better clinical management of cancers such as multiple myeloma considered to be intrinsically resistant to standard therapy with no currently available curative therapies.

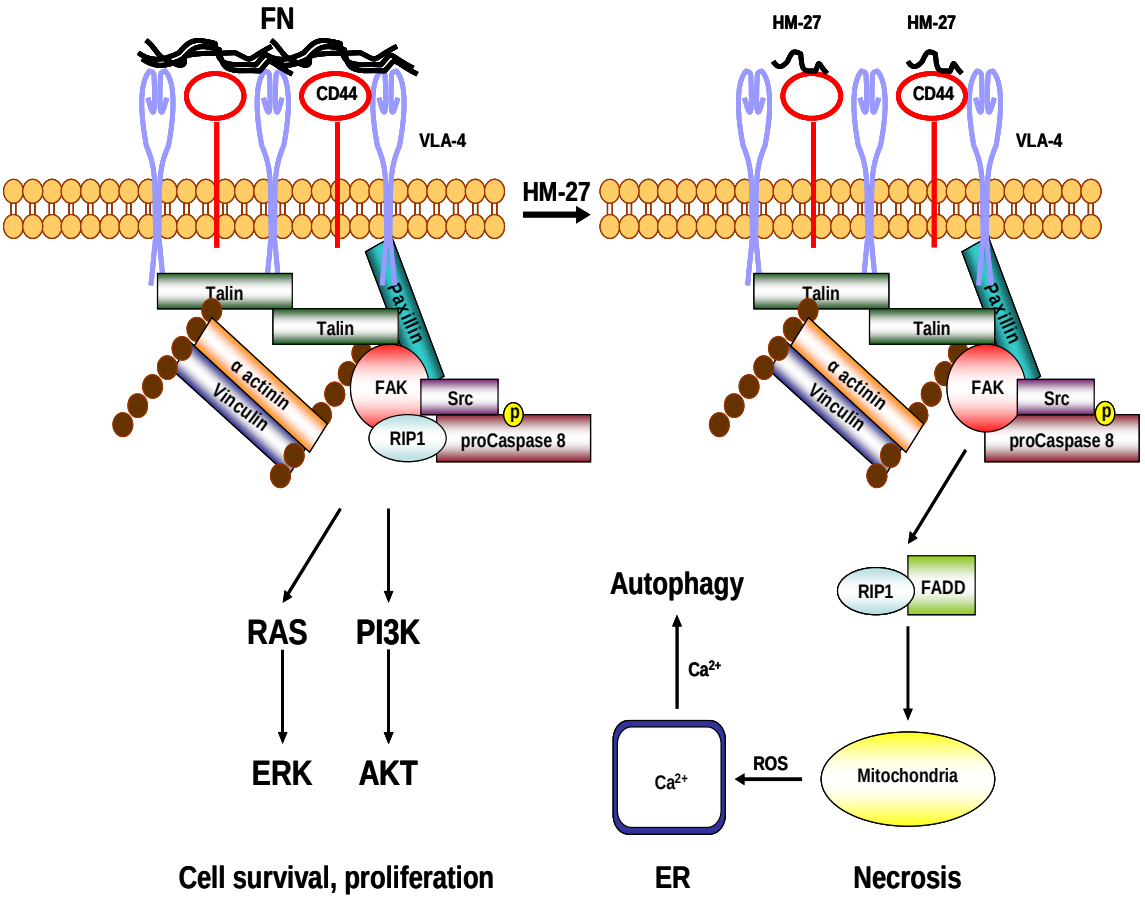

Figure 40: Proposed mechanism of HM-27 induced cell death. HYD1/HM-27 functions by binding to CD44 and leading to disappropriate signaling. One way that HYD1/HM-27 could be causing inappropriate signaling is by causing a disassociation of RIP1 from FAK which enables RIP1 to form a death complex. Formation of the death complex results in cell death induced by necrosis and cell survival signals including the release of Ca^{2+} from the ER and induction of autophagy.

Literature Cited

1. Galloway, J.L. and L.I. Zon, *Ontogeny of hematopoiesis: examining the emergence of hematopoietic cells in the vertebrate embryo.* Current topics in developmental biology, 2003. **53**: p. 139-58.

2. Orkin, S.H. and L.I. Zon, *Hematopoiesis: an evolving paradigm for stem cell biology.* Cell, 2008. **132**(4): p. 631-44.

3. Medina, K.L., et al., *Identification of very early lymphoid precursors in bone marrow and their regulation by estrogen.* Nature immunology, 2001. **2**(8): p. 718-24.

4. Allman, D. and J.P. Miller, *Common lymphoid progenitors, early B-lineage precursors, and IL-7: characterizing the trophic and instructive signals underlying early B cell development.* Immunologic research, 2003. **27**(2-3): p. 131-40.

5. Schlissel, M., *How pre-B cells know when they have it right.* Nature immunology, 2003. **4**(9): p. 817-9.

6. Johnson, K., et al., *Regulatory events in early and late B-cell differentiation.* Molecular immunology, 2005. **42**(7): p. 749-61.

7. Nemazee, D., et al., *B-cell-receptor-dependent positive and negative selection in immature B cells.* Current topics in microbiology and immunology, 2000. **245**(2): p. 57-71.

8. Allen, C.D., T. Okada, and J.G. Cyster, *Germinal-center organization and cellular dynamics.* Immunity, 2007. **27**(2): p. 190-202.

9. Tuscano, J.M., et al., *Bcl-x rather than Bcl-2 mediates CD40-dependent centrocyte survival in the germinal center.* Blood, 1996. **88**(4): p. 1359-64.

10. Sze, D.M., et al., *Intrinsic constraint on plasmablast growth and extrinsic limits of plasma cell survival.* The Journal of experimental medicine, 2000. **192**(6): p. 813-21.

11. Odendahl, M., et al., *Generation of migratory antigen-specific plasma blasts and mobilization of resident plasma cells in a secondary immune response.* Blood, 2005. **105**(4): p. 1614-21.

12. Ridley, R.C., et al., *Expression of syndecan regulates human myeloma plasma cell adhesion to type I collagen.* Blood, 1993. **81**(3): p. 767-74.

13. Ellyard, J.I., et al., *Antigen-selected, immunoglobulin-secreting cells persist in human spleen and bone marrow.* Blood, 2004. **103**(10): p. 3805-12.

14. Van Driel, M., et al., *CD44 variant isoforms are involved in plasma cell adhesion to bone marrow stromal cells.* Leukemia : official journal of the Leukemia Society of America, Leukemia Research Fund, U.K, 2002. **16**(1): p. 135-43.

15. Terstappen, L.W., et al., *Identification and characterization of plasma cells in normal human bone marrow by high-resolution flow cytometry.* Blood, 1990. **76**(9): p. 1739-47.

16. Manz, R.A., A. Thiel, and A. Radbruch, *Lifetime of plasma cells in the bone marrow.* Nature, 1997. **388**(6638): p. 133-4.

17. Moser, K., et al., *Long-lived plasma cells in immunity and immunopathology.* Immunology letters, 2006. **103**(2): p. 83-5.

18. Kyle, R.A. and S.V. Rajkumar, *Multiple myeloma.* The New England journal of medicine, 2004. **351**(18): p. 1860-73.

19. Kyle, R.A., et al., *Prevalence of monoclonal gammopathy of undetermined significance.* The New England journal of medicine, 2006. **354**(13): p. 1362-9.

20. Landgren, O., et al., *Risk of monoclonal gammopathy of undetermined significance (MGUS) and subsequent multiple myeloma among African American and white veterans in the United States.* Blood, 2006. **107**(3): p. 904-6.

21. Landgren, O., et al., *Monoclonal gammopathy of undetermined significance (MGUS) consistently precedes multiple myeloma: a prospective study.* Blood, 2009. **113**(22): p. 5412-7.

22. Kyle, R.A., et al., *Clinical course and prognosis of smoldering (asymptomatic) multiple myeloma.* The New England journal of medicine, 2007. **356**(25): p. 2582-90.

23. Chiecchio, L., et al., *Loss of 1p and rearrangement of MYC are associated with progression of smouldering myeloma to myeloma: sequential analysis of a single case.* Haematologica, 2009. **94**(7): p. 1024-8.

24. Dewald, G.W., et al., *The clinical significance of cytogenetic studies in 100 patients with multiple myeloma, plasma cell leukemia, or amyloidosis.* Blood, 1985. **66**(2): p. 380-90.

25. Fonseca, R., et al., *International Myeloma Working Group molecular classification of multiple myeloma: spotlight review*. Leukemia : official journal of the Leukemia Society of America, Leukemia Research Fund, U.K, 2009. **23**(12): p. 2210-21.

26. Brenner, H., A. Gondos, and D. Pulte, *Recent major improvement in long-term survival of younger patients with multiple myeloma.* Blood, 2008. **111**(5): p. 2521-6.

27. Bergsagel, P.L. and W.M. Kuehl, *Chromosome translocations in multiple myeloma.* Oncogene, 2001. **20**(40): p. 5611-22.

28. Avet-Loiseau, H., et al., *Rearrangements of the c-myc oncogene are present in 15% of primary human multiple myeloma tumors.* Blood, 2001. **98**(10): p. 3082-6.

29. Tricot, G., et al., *Poor prognosis in multiple myeloma is associated only with partial or complete deletions of chromosome 13 or abnormalities involving 11q and not with other karyotype abnormalities.* Blood, 1995. **86**(11): p. 4250-6.

30. Qazilbash, M.H., et al., *Deletion of the short arm of chromosome 1 (del 1p) is a strong predictor of poor outcome in myeloma patients undergoing an autotransplant.* Biology of blood and marrow transplantation : journal of the American Society for Blood and Marrow Transplantation, 2007. **13**(9): p. 1066-72.

31. Fonseca, R., et al., *Clinical and biologic implications of recurrent genomic aberrations in myeloma.* Blood, 2003. **101**(11): p. 4569-75.

32. Gabrea, A., et al., *Secondary genomic rearrangements involving immunoglobulin or MYC loci show similar prevalences in hyperdiploid and nonhyperdiploid myeloma tumors.* Genes, chromosomes & cancer, 2008. **47**(7): p. 573-90.

33. Bergsagel, P.L. and W.M. Kuehl, *Molecular pathogenesis and a consequent classification of multiple myeloma.* Journal of clinical oncology : official journal of the American Society of Clinical Oncology, 2005. **23**(26): p. 6333-8.

34. Harada, H., et al., *Phenotypic difference of normal plasma cells from mature myeloma cells.* Blood, 1993. **81**(10): p. 2658-63.

35. Robillard, N., et al., *CD28, a marker associated with tumoral expansion in multiple myeloma.* Clinical cancer research : an official journal of the American Association for Cancer Research, 1998. **4**(6): p. 1521-6.

36. Kyle, R.A., et al., *Monoclonal gammopathy of undetermined significance (MGUS) and smoldering (asymptomatic) multiple myeloma: IMWG consensus perspectives risk factors for progression and guidelines for monitoring and management.* Leukemia : official journal of the Leukemia Society of America, Leukemia Research Fund, U.K, 2010. **24**(6): p. 1121-7.

37. Birgegard, G., P. Gascon, and H. Ludwig, *Evaluation of anaemia in patients with multiple myeloma and lymphoma: findings of the European CANCER ANAEMIA SURVEY.* European journal of haematology, 2006. **77**(5): p. 378-86.

38. Greipp, P.R., et al., *International staging system for multiple myeloma.* Journal of clinical oncology : official journal of the American Society of Clinical Oncology, 2005. **23**(15): p. 3412-20.

39. Stewart, A.K., P.G. Richardson, and J.F. San-Miguel, *How I treat multiple myeloma in younger patients.* Blood, 2009. **114**(27): p. 5436-43.

40. San Miguel, J.F., et al., *Bortezomib plus melphalan and prednisone for initial treatment of multiple myeloma.* The New England journal of medicine, 2008. **359**(9): p. 906-17.

41. Rajkumar, S.V., et al., *Combination therapy with lenalidomide plus dexamethasone (Rev/Dex) for newly diagnosed myeloma.* Blood, 2005. **106**(13): p. 4050-3.

42. Anderson, K.C., et al., *Clinically relevant end points and new drug approvals for myeloma.* Leukemia : official journal of the Leukemia Society of America, Leukemia Research Fund, U.K, 2008. **22**(2): p. 231-9.

43. Richardson, P.G., et al., *Bortezomib or high-dose dexamethasone for relapsed multiple myeloma.* The New England journal of medicine, 2005. **352**(24): p. 2487-98.

44. Barlogie, B., et al., *High-dose chemoradiotherapy and autologous bone marrow transplantation for resistant multiple myeloma.* Blood, 1987. **70**(3): p. 869-72.

45. Alexanian, R., B. Barlogie, and D. Dixon, *High-dose glucocorticoid treatment of resistant myeloma.* Annals of internal medicine, 1986. **105**(1): p. 8-11.

46. Glasmacher, A., et al., *A systematic review of phase-II trials of thalidomide monotherapy in patients with relapsed or refractory multiple myeloma.* British journal of haematology, 2006. **132**(5): p. 584-93.

47. Lonial, S., C.S. Mitsiades, and P.G. Richardson, *Treatment options for relapsed and refractory multiple myeloma.* Clinical cancer research : an official journal of the American Association for Cancer Research, 2011. **17**(6): p. 1264-77.

48. Dimopoulos, M., et al., *Lenalidomide plus dexamethasone for relapsed or refractory multiple myeloma.* The New England journal of medicine, 2007. **357**(21): p. 2123-32.

49. Reece, D.E., et al., *Phase I-II trial of bortezomib plus oral cyclophosphamide and prednisone in relapsed and refractory multiple myeloma.* Journal of clinical oncology : official journal of the American Society of Clinical Oncology, 2008. **26**(29): p. 4777-83.

50. Durie, B.G., et al., *International uniform response criteria for multiple myeloma.* Leukemia : official journal of the Leukemia Society of America, Leukemia Research Fund, U.K, 2006. **20**(9): p. 1467-73.

51. Bakkus, M.H., et al., *Post-transplantation tumour load in bone marrow, as assessed by quantitative ASO-PCR, is a prognostic parameter in multiple myeloma.* British journal of haematology, 2004. **126**(5): p. 665-74.

52. Alsayed, Y., et al., *Mechanisms of regulation of CXCR4/SDF-1 (CXCL12)-dependent migration and homing in multiple myeloma.* Blood, 2007. **109**(7): p. 2708-17.

53. Burns, J.M., et al., *A novel chemokine receptor for SDF-1 and I-TAC involved in cell survival, cell adhesion, and tumor development.* The Journal of experimental medicine, 2006. **203**(9): p. 2201-13.

54. Lu, D.Y., et al., *SDF-1alpha up-regulates interleukin-6 through CXCR4, PI3K/Akt, ERK, and NF-kappaB-dependent pathway in microglia.* European journal of pharmacology, 2009. **613**(1-3): p. 146-54.

55. Murakami, M., et al., *IL-6-induced homodimerization of gp130 and associated activation of a tyrosine kinase.* Science, 1993. **260**(5115): p. 1808-10.

56. Corradini, P., et al., *Mutational activation of N- and K-ras oncogenes in plasma cell dyscrasias.* Blood, 1993. **81**(10): p. 2708-13.

57. Neumann, C., et al., *Interleukin-6 induces tyrosine phosphorylation of the Ras activating protein Shc, and its complex formation with Grb2 in the human multiple myeloma cell line LP-1.* European journal of immunology, 1996. **26**(2): p. 379-84.

58. Ogata, A., et al., *IL-6 triggers cell growth via the Ras-dependent mitogen-activated protein kinase cascade.* Journal of immunology, 1997. **159**(5): p. 2212-21.

59. Hsu, J.H., et al., *Role of the AKT kinase in expansion of multiple myeloma clones: effects on cytokine-dependent proliferative and survival responses.* Oncogene, 2002. **21**(9): p. 1391-400.

60. Puthier, D., et al., *Mcl-1 and Bcl-xL are co-regulated by IL-6 in human myeloma cells.* British journal of haematology, 1999. **107**(2): p. 392-5.

61. Hideshima, T., et al., *The role of tumor necrosis factor alpha in the pathophysiology of human multiple myeloma: therapeutic applications.* Oncogene, 2001. **20**(33): p. 4519-27.

62. De Bruyne, E., et al., *IGF-1 suppresses Bim expression in multiple myeloma via epigenetic and posttranslational mechanisms.* Blood, 2010. **115**(12): p. 2430-40.

63. Le Gouill, S., et al., *VEGF induces Mcl-1 up-regulation and protects multiple myeloma cells against apoptosis.* Blood, 2004. **104**(9): p. 2886-92.

64. Liu, P., M. Oken, and B. Van Ness, *Interferon-alpha protects myeloma cell lines from dexamethasone-induced apoptosis.* Leukemia : official journal of the Leukemia Society of America, Leukemia Research Fund, U.K, 1999. **13**(3): p. 473-80.

65. Ohwada, C., et al., *CD44 and hyaluronan engagement promotes dexamethasone resistance in human myeloma cells.* European journal of haematology, 2008. **80**(3): p. 245-50.

66. Schmidmaier, R., et al., *The HMG-CoA reductase inhibitor simvastatin overcomes cell adhesion-mediated drug resistance in multiple myeloma by geranylgeranylation of Rho protein and activation of Rho kinase.* Blood, 2004. **104**(6): p. 1825-32.

67. Nefedova, Y., et al., *Inhibition of Notch signaling induces apoptosis of myeloma cells and enhances sensitivity to chemotherapy.* Blood, 2008. **111**(4): p. 2220-9.

68. Lauring, J., et al., *The multiple myeloma associated MMSET gene contributes to cellular adhesion, clonogenic growth, and tumorigenicity.* Blood, 2008. **111**(2): p. 856-64.

69. Damiano, J.S., et al., *Cell adhesion mediated drug resistance (CAM-DR): role of integrins and resistance to apoptosis in human myeloma cell lines.* Blood, 1999. **93**(5): p. 1658-67.

70. Hazlehurst, L.A., et al., *Adhesion to fibronectin via beta1 integrins regulates p27kip1 levels and contributes to cell adhesion mediated drug resistance (CAM-DR).* Oncogene, 2000. **19**(38): p. 4319-27.

71. Shain, K.H., T.H. Landowski, and W.S. Dalton, *Adhesion-mediated intracellular redistribution of c-Fas-associated death domain-like IL-1-converting enzyme-like inhibitory protein-long confers resistance to CD95-induced apoptosis in hematopoietic cancer cell lines.* Journal of immunology, 2002. **168**(5): p. 2544-53.

72. Hazlehurst, L.A., R.F. Argilagos, and W.S. Dalton, *Beta1 integrin mediated adhesion increases Bim protein degradation and contributes to drug resistance in leukaemia cells.* British journal of haematology, 2007. **136**(2): p. 269-75.

73. Hazlehurst, L.A., et al., *Genotypic and phenotypic comparisons of de novo and acquired melphalan resistance in an isogenic multiple myeloma cell line model.* Cancer research, 2003. **63**(22): p. 7900-6.

74. Knobloch, J., et al., *Thalidomide resistance is based on the capacity of the glutathione-dependent antioxidant defense.* Molecular pharmaceutics, 2008. **5**(6): p. 1138-44.

75. Sanchez-Vega, B. and V. Gandhi, *Glucocorticoid resistance in a multiple myeloma cell line is regulated by a transcription elongation block in the glucocorticoid receptor gene (NR3C1).* British journal of haematology, 2009. **144**(6): p. 856-64.

76. Oerlemans, R., et al., *Molecular basis of bortezomib resistance: proteasome subunit beta5 (PSMB5) gene mutation and overexpression of PSMB5 protein.* Blood, 2008. **112**(6): p. 2489-99.

77. Liu, Q. and Y. Gazitt, *Potentiation of dexamethasone-, paclitaxel-, and Ad-p53-induced apoptosis by Bcl-2 antisense oligodeoxynucleotides in drug-resistant multiple myeloma cells.* Blood, 2003. **101**(10): p. 4105-14.

78. Nakagawa, Y., et al., *IAP family protein expression correlates with poor outcome of multiple myeloma patients in association with chemotherapy-induced overexpression of multidrug resistance genes.* American journal of hematology, 2006. **81**(11): p. 824-31.

79. Chen, Q., et al., *The FA/BRCA pathway is involved in melphalan-induced DNA interstrand cross-link repair and accounts for melphalan resistance in multiple myeloma cells.* Blood, 2005. **106**(2): p. 698-705.

80. Hynes, R.O., *Integrins: bidirectional, allosteric signaling machines.* Cell, 2002. **110**(6): p. 673-87.

81. Michishita, M., V. Videm, and M.A. Arnaout, *A novel divalent cation-binding site in the A domain of the beta 2 integrin CR3 (CD11b/CD18) is essential for ligand binding.* Cell, 1993. **72**(6): p. 857-67.

82. Xiong, J.P., et al., *Crystal structure of the extracellular segment of integrin alpha Vbeta3 in complex with an Arg-Gly-Asp ligand.* Science, 2002. **296**(5565): p. 151-5.

83. Komoriya, A., et al., *The minimal essential sequence for a major cell type-specific adhesion site (CS1) within the alternatively spliced type III connecting segment domain of fibronectin is leucine-aspartic acid-valine.* The Journal of biological chemistry, 1991. **266**(23): p. 15075-9.

84. Beglova, N., et al., *Cysteine-rich module structure reveals a fulcrum for integrin rearrangement upon activation.* Nature structural biology, 2002. **9**(4): p. 282-7.

85. Arnaout, M.A., B. Mahalingam, and J.P. Xiong, *Integrin structure, allostery, and bidirectional signaling.* Annual review of cell and developmental biology, 2005. **21**: p. 381-410.

86. Calderwood, D.A., et al., *The phosphotyrosine binding-like domain of talin activates integrins.* The Journal of biological chemistry, 2002. **277**(24): p. 21749-58.

87. Mitra, S.K., D.A. Hanson, and D.D. Schlaepfer, *Focal adhesion kinase: in command and control of cell motility.* Nature reviews. Molecular cell biology, 2005. **6**(1): p. 56-68.

88. Astier, A., et al., *The related adhesion focal tyrosine kinase is tyrosine-phosphorylated after beta1-integrin stimulation in B cells and binds to p130cas.* The Journal of biological chemistry, 1997. **272**(1): p. 228-32.

89. Jensen, G.S., et al., *Expression of multiple beta 1 integrins on circulating monoclonal B cells in patients with multiple myeloma.* American journal of hematology, 1993. **43**(1): p. 29-36.

90. Uchiyama, H., et al., *Characterization of adhesion molecules on human myeloma cell lines.* Blood, 1992. **80**(9): p. 2306-14.

91. Pulido, R., et al., *Functional evidence for three distinct and independently inhibitable adhesion activities mediated by the human integrin VLA-4. Correlation with distinct alpha 4 epitopes.* The Journal of biological chemistry, 1991. **266**(16): p. 10241-5.

92. Teixido, J., et al., *Functional and structural analysis of VLA-4 integrin alpha 4 subunit cleavage.* The Journal of biological chemistry, 1992. **267**(3): p. 1786-91.

93. Schmidmaier, R., et al., *Evidence for cell adhesion-mediated drug resistance of multiple myeloma cells in vivo.* The International journal of biological markers, 2006. **21**(4): p. 218-22.

94. Damiano, J.S. and W.S. Dalton, *Integrin-mediated drug resistance in multiple myeloma.* Leukemia & lymphoma, 2000. **38**(1-2): p. 71-81.

95. Neri, P., et al., *Integrin beta7-mediated regulation of multiple myeloma cell adhesion, migration, and invasion.* Blood, 2011. **117**(23): p. 6202-13.

96. Noborio-Hatano, K., et al., *Bortezomib overcomes cell-adhesion-mediated drug resistance through downregulation of VLA-4 expression in multiple myeloma.* Oncogene, 2009. **28**(2): p. 231-42.

97. Olson, D.L., et al., *Anti-alpha4 integrin monoclonal antibody inhibits multiple myeloma growth in a murine model.* Molecular cancer therapeutics, 2005. **4**(1): p. 91-9.

98. Podar, K., et al., *The selective adhesion molecule inhibitor Natalizumab decreases multiple myeloma cell growth in the bone marrow microenvironment: therapeutic implications.* British journal of haematology, 2011. **155**(4): p. 438-48.

99. Kiziltepe, T., et al., *Rationally engineered nanoparticles target multiple myeloma cells, overcome cell-adhesion-mediated drug resistance, and show enhanced efficacy in vivo.* Blood cancer journal, 2012. **2**(4): p. e64.

100. Kuwada, S.K., *Drug evaluation: Volociximab, an angiogenesis-inhibiting chimeric monoclonal antibody.* Current opinion in molecular therapeutics, 2007. **9**(1): p. 92-8.

101. Mullamitha, S.A., et al., *Phase I evaluation of a fully human anti-alphav integrin monoclonal antibody (CNTO 95) in patients with advanced solid tumors.* Clinical cancer research : an official journal of the American Association for Cancer Research, 2007. **13**(7): p. 2128-35.

102. Buckley, C.D., et al., *RGD peptides induce apoptosis by direct caspase-3 activation.* Nature, 1999. **397**(6719): p. 534-9.

103. Smith, J.W., et al., *Interaction of integrins alpha v beta 3 and glycoprotein IIb-IIIa with fibrinogen. Differential peptide recognition accounts for distinct binding sites.* The Journal of biological chemistry, 1990. **265**(21): p. 12267-71.

104. Reardon, D.A., et al., *Randomized phase II study of cilengitide, an integrin-targeting arginine-glycine-aspartic acid peptide, in recurrent glioblastoma multiforme.* Journal of clinical oncology : official journal of the American Society of Clinical Oncology, 2008. **26**(34): p. 5610-7.

105. Khalili, P., et al., *A non-RGD-based integrin binding peptide (ATN-161) blocks breast cancer growth and metastasis in vivo.* Molecular cancer therapeutics, 2006. **5**(9): p. 2271-80.

106. Cianfrocca, M.E., et al., *Phase 1 trial of the antiangiogenic peptide ATN-161 (Ac-PHSCN-NH(2)), a beta integrin antagonist, in patients with solid tumours.* British journal of cancer, 2006. **94**(11): p. 1621-6.

107. Barkan, D. and A.F. Chambers, *beta1-integrin: a potential therapeutic target in the battle against cancer recurrence.* Clinical cancer research : an official journal of the American Association for Cancer Research, 2011. **17**(23): p. 7219-23.

108. Reinmuth, N., et al., *Alphavbeta3 integrin antagonist S247 decreases colon cancer metastasis and angiogenesis and improves survival in mice.* Cancer research, 2003. **63**(9): p. 2079-87.

109. Zhao, Y., et al., *Tumor alphavbeta3 integrin is a therapeutic target for breast cancer bone metastases.* Cancer research, 2007. **67**(12): p. 5821-30.

110. Chinnaiyan, A.M., *The apoptosome: heart and soul of the cell death machine.* Neoplasia, 1999. **1**(1): p. 5-15.

111. van Loo, G., et al., *The serine protease Omi/HtrA2 is released from mitochondria during apoptosis. Omi interacts with caspase-inhibitor XIAP and induces enhanced caspase activity.* Cell death and differentiation, 2002. **9**(1): p. 20-6.

112. Hsu, H., J. Xiong, and D.V. Goeddel, *The TNF receptor 1-associated protein TRADD signals cell death and NF-kappa B activation.* Cell, 1995. **81**(4): p. 495-504.

113. Kataoka, T., et al., *FLIP prevents apoptosis induced by death receptors but not by perforin/granzyme B, chemotherapeutic drugs, and gamma irradiation.* Journal of immunology, 1998. **161**(8): p. 3936-42.

114. Gomez-Bougie, P., et al., *Melphalan-induced apoptosis in multiple myeloma cells is associated with a cleavage of Mcl-1 and Bim and a decrease in the Mcl-1/Bim complex.* Oncogene, 2005. **24**(54): p. 8076-9.

115. Sharma, S. and A. Lichtenstein, *Dexamethasone-induced apoptotic mechanisms in myeloma cells investigated by analysis of mutant glucocorticoid receptors.* Blood, 2008. **112**(4): p. 1338-45.

116. Mitsiades, N., et al., *The proteasome inhibitor PS-341 potentiates sensitivity of multiple myeloma cells to conventional chemotherapeutic agents: therapeutic applications.* Blood, 2003. **101**(6): p. 2377-80.

117. Perez, L.E., et al., *Bortezomib restores stroma-mediated APO2L/TRAIL apoptosis resistance in multiple myeloma.* European journal of haematology, 2010. **84**(3): p. 212-22.

118. McCafferty-Grad, J., et al., *Arsenic trioxide uses caspase-dependent and caspase-independent death pathways in myeloma cells.* Molecular cancer therapeutics, 2003. **2**(11): p. 1155-64.

119. Wei, Y., et al., *JNK1-mediated phosphorylation of Bcl-2 regulates starvation-induced autophagy.* Molecular cell, 2008. **30**(6): p. 678-88.

120. Wirawan, E., et al., *Caspase-mediated cleavage of Beclin-1 inactivates Beclin-1-induced autophagy and enhances apoptosis by promoting the release of proapoptotic factors from mitochondria.* Cell death & disease, 2010. **1**: p. e18.

121. Bell, B.D., et al., *FADD and caspase-8 control the outcome of autophagic signaling in proliferating T cells.* Proceedings of the National Academy of Sciences of the United States of America, 2008. **105**(43): p. 16677-82.

122. Lum, J.J., et al., *Growth factor regulation of autophagy and cell survival in the absence of apoptosis.* Cell, 2005. **120**(2): p. 237-48.

123. Pan, Y., et al., *Targeting autophagy augments in vitro and in vivo antimyeloma activity of DNA-damaging chemotherapy.* Clinical cancer research : an official journal of the American Association for Cancer Research, 2011. **17**(10): p. 3248-58.

124. Hoang, B., et al., *Effect of autophagy on multiple myeloma cell viability.* Molecular cancer therapeutics, 2009. **8**(7): p. 1974-84.

125. David, E., et al., *Tipifarnib sensitizes cells to proteasome inhibition by blocking degradation of bortezomib-induced aggresomes.* Blood, 2010. **116**(24): p. 5285-8.

126. Narita, M., et al., *Bax interacts with the permeability transition pore to induce permeability transition and cytochrome c release in isolated mitochondria.* Proceedings of the National Academy of Sciences of the United States of America, 1998. **95**(25): p. 14681-6.

127. Nicolli, A., et al., *Interactions of cyclophilin with the mitochondrial inner membrane and regulation of the permeability transition pore, and cyclosporin A-sensitive channel.* The Journal of biological chemistry, 1996. **271**(4): p. 2185-92.

128. Ha, H.C. and S.H. Snyder, *Poly(ADP-ribose) polymerase is a mediator of necrotic cell death by ATP depletion.* Proceedings of the National Academy of Sciences of the United States of America, 1999. **96**(24): p. 13978-82.

129. McConkey, D.J. and S. Orrenius, *The role of calcium in the regulation of apoptosis.* Journal of leukocyte biology, 1996. **59**(6): p. 775-83.

130. Qian, T., B. Herman, and J.J. Lemasters, *The mitochondrial permeability transition mediates both necrotic and apoptotic death of hepatocytes exposed to Br-A23187.* Toxicology and applied pharmacology, 1999. **154**(2): p. 117-25.

131. Yamashima, T., *Ca2+-dependent proteases in ischemic neuronal death: a conserved 'calpain-cathepsin cascade' from nematodes to primates.* Cell calcium, 2004. **36**(3-4): p. 285-93.

132. Nordberg, J. and E.S. Arner, *Reactive oxygen species, antioxidants, and the mammalian thioredoxin system.* Free radical biology & medicine, 2001. **31**(11): p. 1287-312.

133. Schulze-Osthoff, K., et al., *Cytotoxic activity of tumor necrosis factor is mediated by early damage of mitochondrial functions. Evidence for the involvement of mitochondrial radical generation.* The Journal of biological chemistry, 1992. **267**(8): p. 5317-23.

134. Micheau, O. and J. Tschopp, *Induction of TNF receptor I-mediated apoptosis via two sequential signaling complexes.* Cell, 2003. **114**(2): p. 181-90.

135. Hitomi, J., et al., *Identification of a molecular signaling network that regulates a cellular necrotic cell death pathway.* Cell, 2008. **135**(7): p. 1311-23.

136. Sugimoto, K., et al., *Low-dose doxorubicin-induced necrosis in Jurkat cells and its acceleration and conversion to apoptosis by antioxidants.* British journal of haematology, 2002. **118**(1): p. 229-38.

137. Nakamura, M., et al., *Induction of necrosis in human myeloma cells by kigamicin.* Anticancer research, 2008. **28**(1A): p. 37-43.

138. Long, S.B., E.B. Campbell, and R. Mackinnon, *Voltage sensor of Kv1.2: structural basis of electromechanical coupling.* Science, 2005. **309**(5736): p. 903-8.

139. Putney, J.W., Jr., *Capacitative calcium entry: sensing the calcium stores.* The Journal of cell biology, 2005. **169**(3): p. 381-2.

140. Prakriya, M., et al., *Orai1 is an essential pore subunit of the CRAC channel.* Nature, 2006. **443**(7108): p. 230-3.

141. Prince, W.T., H. Rasmussen, and M.J. Berridge, *The role of calcium in fly salivary gland secretion analyzed with the ionophore A-23187.* Biochimica et biophysica acta, 1973. **329**(1): p. 98-107.

142. Chen, R., et al., *Bcl-2 functionally interacts with inositol 1,4,5-trisphosphate receptors to regulate calcium release from the ER in response to inositol 1,4,5-trisphosphate.* The Journal of cell biology, 2004. **166**(2): p. 193-203.

143. Rong, Y.P., et al., *Targeting Bcl-2-IP3 receptor interaction to reverse Bcl-2's inhibition of apoptotic calcium signals.* Molecular cell, 2008. **31**(2): p. 255-65.

144. Annis, M.G., et al., *Endoplasmic reticulum localized Bcl-2 prevents apoptosis when redistribution of cytochrome c is a late event.* Oncogene, 2001. **20**(16): p. 1939-52.

145. White, C., et al., *The endoplasmic reticulum gateway to apoptosis by Bcl-X(L) modulation of the InsP3R.* Nature cell biology, 2005. **7**(10): p. 1021-8.

146. Oakes, S.A., et al., *Proapoptotic BAX and BAK regulate the type 1 inositol trisphosphate receptor and calcium leak from the endoplasmic reticulum.* Proceedings of the National Academy of Sciences of the United States of America, 2005. **102**(1): p. 105-10.

147. Kim, H.R., et al., *Bax Inhibitor-1 Is a pH-dependent regulator of Ca2+ channel activity in the endoplasmic reticulum.* The Journal of biological chemistry, 2008. **283**(23): p. 15946-55.

148. Nutt, L.K., et al., *Bax and Bak promote apoptosis by modulating endoplasmic reticular and mitochondrial Ca2+ stores.* The Journal of biological chemistry, 2002. **277**(11): p. 9219-25.

149. Ludwinski, M.W., et al., *Critical roles of Bim in T cell activation and T cell-mediated autoimmune inflammation in mice.* The Journal of clinical investigation, 2009. **119**(6): p. 1706-13.

150. Seo, Y.W., et al., *The cell death-inducing activity of the peptide containing Noxa mitochondrial-targeting domain is associated with calcium release.* Cancer research, 2009. **69**(21): p. 8356-65.

151. Hoyer-Hansen, M., et al., *Control of macroautophagy by calcium, calmodulin-dependent kinase kinase-beta, and Bcl-2.* Molecular cell, 2007. **25**(2): p. 193-205.

152. Vicencio, J.M., et al., *The inositol 1,4,5-trisphosphate receptor regulates autophagy through its interaction with Beclin 1.* Cell death and differentiation, 2009. **16**(7): p. 1006-17.

153. Criollo, A., et al., *Regulation of autophagy by the inositol trisphosphate receptor.* Cell death and differentiation, 2007. **14**(5): p. 1029-39.

154. Sarkar, S. and D.C. Rubinsztein, *Inositol and IP3 levels regulate autophagy: biology and therapeutic speculations.* Autophagy, 2006. **2**(2): p. 132-4.

155. Tsunoda, T., et al., *Inositol 1,4,5-trisphosphate (IP3) receptor type1 (IP3R1) modulates the acquisition of cisplatin resistance in bladder cancer cell lines.* Oncogene, 2005. **24**(8): p. 1396-402.

156. Verbert, L., et al., *Caspase-3-truncated type 1 inositol 1,4,5-trisphosphate receptor enhances intracellular Ca2+ leak and disturbs Ca2+ signalling.* Biology of the cell / under the auspices of the European Cell Biology Organization, 2008. **100**(1): p. 39-49.

157. Nawrocki, S.T., et al., *Bortezomib sensitizes pancreatic cancer cells to endoplasmic reticulum stress-mediated apoptosis.* Cancer research, 2005. **65**(24): p. 11658-66.

158. Lam, K.S., et al., *A new type of synthetic peptide library for identifying ligand-binding activity.* Nature, 1991. **354**(6348): p. 82-4.

159. Pennington, M.E., K.S. Lam, and A.E. Cress, *The use of a combinatorial library method to isolate human tumor cell adhesion peptides.* Molecular diversity, 1996. **2**(1-2): p. 19-28.

160. DeRoock, I.B., et al., *Synthetic peptides inhibit adhesion of human tumor cells to extracellular matrix proteins.* Cancer research, 2001. **61**(8): p. 3308-13.

161. Sroka, T.C., M.E. Pennington, and A.E. Cress, *Synthetic D-amino acid peptide inhibits tumor cell motility on laminin-5.* Carcinogenesis, 2006. **27**(9): p. 1748-57.

162. Sroka, T.C., et al., *The minimum element of a synthetic peptide required to block prostate tumor cell migration.* Cancer biology & therapy, 2006. **5**(11): p. 1556-62.

163. Nair, R.R., et al., *HYD1-induced increase in reactive oxygen species leads to autophagy and necrotic cell death in multiple myeloma cells.* Molecular cancer therapeutics, 2009. **8**(8): p. 2441-51.

164. Wang, X., et al., *Mechanisms of AIF-mediated apoptotic DNA degradation in Caenorhabditis elegans.* Science, 2002. **298**(5598): p. 1587-92.

165. Enari, M., et al., *A caspase-activated DNase that degrades DNA during apoptosis, and its inhibitor ICAD.* Nature, 1998. **391**(6662): p. 43-50.

166. Mizushima, N. and T. Yoshimori, *How to interpret LC3 immunoblotting.* Autophagy, 2007. **3**(6): p. 542-5.

167. Boya, P., et al., *Inhibition of macroautophagy triggers apoptosis.* Molecular and cellular biology, 2005. **25**(3): p. 1025-40.

168. Hazlehurst, L.A., et al., *Reduction in drug-induced DNA double-strand breaks associated with beta1 integrin-mediated adhesion correlates with drug resistance in U937 cells.* Blood, 2001. **98**(6): p. 1897-903.

169. Nefedova, Y., T.H. Landowski, and W.S. Dalton, *Bone marrow stromal-derived soluble factors and direct cell contact contribute to de novo drug resistance of myeloma cells by distinct mechanisms.* Leukemia, 2003. **17**(6): p. 1175-82.

170. Sroka, T.C., M.E. Pennington, and A.E. Cress, *Synthetic D-amino acid peptide inhibits tumor cell motility on laminin-5.* Carcinogenesis, 2006.

171. Hazlehurst, L.A., et al., *Multiple mechanisms confer drug resistance to mitoxantrone in the human 8226 myeloma cell line.* Cancer Res, 1999. **59**(5): p. 1021-8.

172. Bednarczyk, J.L., M.C. Szabo, and B.W. McIntyre, *Post-translational processing of the leukocyte integrin alpha 4 beta 1.* J Biol Chem, 1992. **267**(35): p. 25274-81.

173. Teixido, J., et al., *Functional and structural analysis of VLA-4 integrin alpha 4 subunit cleavage.* J Biol Chem, 1992. **267**(3): p. 1786-91.

174. McMillin, D.W., et al., *Tumor cell-specific bioluminescence platform to identify stroma-induced changes to anticancer drug activity.* Nat Med, 2009. **16**(4): p. 483-9.

175. Azab, A.K., et al., *The CXCR4 inhibitor AMD3100 disrupts the interaction of multiple myeloma cells with the bone marrow microenvironment and enhances their sensitivity to therapy.* Blood, 2009.

176. Baker, D.E., *Natalizumab: overview of its pharmacology and safety.* Rev Gastroenterol Disord, 2007. **7**(1): p. 38-46.

177. Gutman, D., A.A. Morales, and L.H. Boise, *Acquisition of a multidrug-resistant phenotype with a proteasome inhibitor in multiple myeloma.* Leukemia, 2009. **23**(11): p. 2181-3.

178. Banerjee, D., et al., *Novel aspects of resistance to drugs targeted to dihydrofolate reductase and thymidylate synthase.* Biochim Biophys Acta, 2002. **1587**(2-3): p. 164-73.

179. Mahon, F.X., et al., *Selection and characterization of BCR-ABL positive cell lines with differential sensitivity to the tyrosine kinase inhibitor STI571: diverse mechanisms of resistance.* Blood, 2000. **96**(3): p. 1070-9.

180. Morgan, S.E., et al., *Differences in mutant p53 protein stability and functional activity in teniposide-sensitive and -resistant human leukemic CEM cells.* Oncogene, 2000. **19**(43): p. 5010-9.

181. Robey, R.W., et al., *ABCG2: determining its relevance in clinical drug resistance.* Cancer Metastasis Rev, 2007. **26**(1): p. 39-57.

182. Gottesman, M.M. and V. Ling, *The molecular basis of multidrug resistance in cancer: the early years of P-glycoprotein research.* FEBS Lett, 2006. **580**(4): p. 998-1009.

183. Gatenby, R.A., et al., *Adaptive therapy.* Cancer Res, 2009. **69**(11): p. 4894-903.

184. Redondo-Munoz, J., et al., *Alpha4beta1 integrin and 190-kDa CD44v constitute a cell surface docking complex for gelatinase B/MMP-9 in chronic leukemic but not in normal B cells.* Blood, 2008. **112**(1): p. 169-78.

185. Khleif, S.N., J.H. Doroshow, and W.N. Hait, *AACR-FDA-NCI Cancer Biomarkers Collaborative consensus report: advancing the use of biomarkers in cancer drug development.* Clin Cancer Res. **16**(13): p. 3299-318.

186. Blue, M.L., et al., *Specific cleavage of the alpha 4 integrin associated with activation of peripheral T lymphocytes.* Immunology, 1993. **78**(1): p. 80-5.

187. Olson, D.L., et al., *Anti-alpha4 integrin monoclonal antibody inhibits multiple myeloma growth in a murine model.* Mol Cancer Ther, 2005. **4**(1): p. 91-9.

188. Abe, M., et al., *Vicious cycle between myeloma cell binding to bone marrow stromal cells via VLA-4-VCAM-1 adhesion and macrophage inflammatory protein-1alpha and MIP-1beta production.* J Bone Miner Metab, 2009. **27**(1): p. 16-23.

189. Epstein, J. and S. Yaccoby, *Consequences of interactions between the bone marrow stroma and myeloma.* Hematol J, 2003. **4**(5): p. 310-4.

190. Tian, E., et al., *The role of the Wnt-signaling antagonist DKK1 in the development of osteolytic lesions in multiple myeloma.* N Engl J Med, 2003. **349**(26): p. 2483-94.

191. Yaccoby, S., et al., *Cancer and the microenvironment: myeloma-osteoclast interactions as a model.* Cancer Res, 2004. **64**(6): p. 2016-23.

192. Abram, C.L. and C.A. Lowell, *The ins and outs of leukocyte integrin signaling.* Annu Rev Immunol, 2009. **27**: p. 339-62.

193. Luo, B.H., C.V. Carman, and T.A. Springer, *Structural basis of integrin regulation and signaling.* Annu Rev Immunol, 2007. **25**: p. 619-47.

194. de Bruyn, K.M., et al., *The small GTPase Rap1 is required for Mn(2+)- and antibody-induced LFA-1- and VLA-4-mediated cell adhesion.* J Biol Chem, 2002. **277**(33): p. 29468-76.

195. Suzuki, Y.J. and G.D. Ford, *Superoxide stimulates IP3-induced Ca2+ release from vascular smooth muscle sarcoplasmic reticulum.* The American journal of physiology, 1992. **262**(1 Pt 2): p. H114-6.

196. Wang, Z., et al., *The mitochondrial phosphatase PGAM5 functions at the convergence point of multiple necrotic death pathways.* Cell, 2012. **148**(1-2): p. 228-43.

197. Bras, M., et al., *Drp1 mediates caspase-independent type III cell death in normal and leukemic cells.* Molecular and cellular biology, 2007. **27**(20): p. 7073-88.

198. Maycotte, P., et al., *Chloroquine sensitizes breast cancer cells to chemotherapy independent of autophagy.* Autophagy, 2012. **8**(2): p. 200-12.

199. Zheng, Y., et al., *Chloroquine inhibits colon cancer cell growth in vitro and tumor growth in vivo via induction of apoptosis.* Cancer investigation, 2009. **27**(3): p. 286-92.

200. Kurenova, E., et al., *Focal adhesion kinase suppresses apoptosis by binding to the death domain of receptor-interacting protein.* Molecular and cellular biology, 2004. **24**(10): p. 4361-71.

201. Cursi, S., et al., *Src kinase phosphorylates Caspase-8 on Tyr380: a novel mechanism of apoptosis suppression.* The EMBO journal, 2006. **25**(9): p. 1895-905.

202. Finlay, D. and K. Vuori, *Novel noncatalytic role for caspase-8 in promoting SRC-mediated adhesion and Erk signaling in neuroblastoma cells.* Cancer research, 2007. **67**(24): p. 11704-11.

203. Bissell, M.J. and D. Radisky, *Putting tumours in context.* Nat Rev Cancer, 2001. **1**(1): p. 46-54.

204. Hazlehurst, L.A., T.H. Landowski, and W.S. Dalton, *Role of the tumor microenvironment in mediating de novo resistance to drugs and physiological mediators of cell death.* Oncogene, 2003. **22**(47): p. 7396-402.

205. Nair, R.R., J. Tolentino, and L.A. Hazlehurst, *The bone marrow microenvironment as a sanctuary for minimal residual disease in CML*. Biochem Pharmacol. **80**(5): p. 602-12.